Olefin Insertion and β-Elimination Reactions of

Permethylniobocene Olefin Hydride and Permethylscandocene Alkyl Complexes

Thesis by

Barbara J. Burger

In Partial Fulfillment of the Requirements

for the Degree of

Doctor of Philosophy

California Institute of Technology

Pasadena, California

1987

(submitted May 4, 1987)

to heroes

ACKNOWLDGEMENTS

At this point my thesis is just about done and I am beginning to get a little sentimental about all the people that have made the last four years very special for me. First of all I would like to thank all the members of the Bercaw group that I have had the good fortune to interact with over the past four years. In particular, a special thanks goes to the two graduate students with whom I shared a vacuum line over the years. Tippy and Ray, you taught me an awful lot about science and at the same time kept me laughing and wondering which piece of glassware you were going to "borrow" next. Naturally, the Bercaw group wouldn't be what it is without the "Big Cheese" himself (I wonder what it would be called). John, thanks for all of the support and advice and especially for laughing at my stupid little jokes and childhood anecdotes.

There are a number of people who have made the last few months an awful lot easier for me. A great deal of thanks go to Leigh, Nancy, Jim and Brew for all of their friendship through "these crazy times," and to Lark for dragging me out on Friday and Saturday evenings when I *thought* that I would be content being a Caltech geek.

Much appreciation is extended toward Doug Meinhart, Eric Anslyn and Dave Wheeler for all of their *cheerful* assistance on the NMR and to Bernie Santarsiero for all of his help in doing the two crystal structures contained in this thesis. The Shell Oil Company is gratefully acknowledged for a graduate fellowship (1986-87).

Finally, I would like to thank my family, especially my parents, for their continued support and encouragement throughout this time. And, yes, Dad, I am finally going to take a job and *work* for a living!

ABSTRACT

Permethylniobocene styrene hydride complexes, $Cp^*_2Nb(CH_2=CHC_6H_4$-*m*-X)H (Cp^* = C_5Me_5, X = CH_3, NMe_2, CF_3) have been prepared and their rates of olefin insertion measured by coalescence techniques. The rates compare favorably with those measured for the analogous *para*-substituted complexes, suggesting that electronic effects in the transition state are largely inductive in nature. The crystal structure of $Cp^*_2Nb(CH_2=CHC_6H_5)H$ was determined. The phenyl ring of the styrene is twisted out of resonance with the olefin to avoid unfavorable steric interactions with the bulky Cp^* rings.

The rates of ethylene insertion in the Sc-C bond for Cp^*_2ScR (R = CH_3, CH_2CH_3, $CH_2CH_2CH_3$) have been measured at low temperature by ^{13}C NMR; the second order rate constants (M^{-1} sec^{-1}, -80 °C) are R = CH_3, 8.1(2) x 10^{-4}; R = CH_2CH_3, 4.4(2) x 10^{-4}; R = $CH_2CH_2CH_3$, 6.1(2) x 10^{-3}. The slow rate for the $ScCH_2CH_3$ complex is attributed to a ground state stabilization by a β-C-H interaction.

The β-hydrogen elimination rates for a series of permethylscandocene alkyl complexes $Cp^*_2ScCH_2CH_2R$ (R = H, CH_3, CH_2CH_3, $SiMe_3$, C_6H_5, C_6H_4-*p*-CH_3, C_6H_4-*p*-CF_3, and C_6H_4-*p*-NMe_2) were measured by trapping kinetics. A transition state for the β-hydrogen elimination was proposed where there is a partial positive charge on the β-carbon and the hydrogen is transferred to the scandium center as H^-.

[Cp^*_2ScH] catalyses the ring opening of methylenecyclopropane and methylenecyclobutane. The ring opening (β-alkyl elimination) is reversible in the case of methylenecyclobutane. Addition of one equivalent of methylenecyclopentane to [Cp^*_2ScH] results in the formation of the scandium cyclopentylmethyl complex. This complex undergoes preferential β-alkyl (reversibly) over β-hydrogen elimination due to the unfavorable steric congestion encountered in the transition state of the latter.

[Cp^*_2ScH] reacts rapidly at -80 °C with ethyl vinyl ether and vinylfluoride to generate an equimolar mixture of the Cp^*_2ScX (X = OEt, F, respectively) and $Cp^*_2ScCH_2CH_3$. No intermediates are seen in these reactions and two mechanisms, one involving a β-X ethyl intermediate and one invoking direct σ-bond metathesis are proposed to account for the products. With vinyldiphenylphosphine, the initial product of insertion, $Cp^*_2ScCH_2CH_2PPh_2$ is stable at low temperature; upon warming, this complex undergoes β-PPh_2 elimination.

TABLE OF CONTENTS

INTRODUCTION

The processes of olefin insertion into metal hydrogen and metal carbon bonds and the reverse reactions, that of β-hydrogen and β-alkyl elimination, are fundamental transformations that occur in a variety of organometallic systems (see Scheme I).[1,2]

OLEFIN INSERTION / β-HYDROGEN ELIMINATION

$$L_nM\text{-}H + CH_2{=}CHR \rightleftharpoons L_nM\text{-}CH_2CH_2R$$

OLEFIN INSERTION / β-ALKYL ELIMINATION

$$L_nM\text{-}R + CH_2{=}CHR' \rightleftharpoons L_nM\text{-}CH_2CHRR'$$

Scheme I.

Indeed, at least one of these reactions is involved in virtually all catalytic cycles involving olefins. For example, in olefin polymerization, chain propagation occurs by olefin insertion into a metal-carbon bond[3] while β-hydrogen elimination serves as a chain termination step. It is the relative rates of these two steps that determine the chain length of the polymer.[4]

Despite the importance of these elementary steps, the detailed mechanisms by which they occur have yet to be understood. This is due primarily to the difficulty in isolating these simple transformations from other reactions that the metal complex undergoes. In general, these steps are implicated, but, because of the ease with which they occur, they cannot be observed directly. Experimental and theoretical studies performed to date[5] indicate that these

processes occur on a single metal center. A cyclic four centered transition state (shown below) has been proposed for both elimination and insertion reactions.

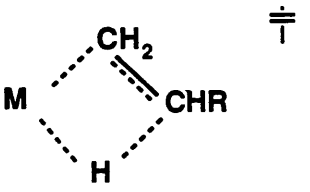

For the elimination reactions, a vacant coordination site adjacent to the alkyl group is required. An olefin adduct is generally assumed for the insertion reactions;[6] the hydrogen or alkyl group and the olefin must have a *cis* arrangement. In general, alkyl migrations have been found to be less rapid than analogous hydrogen migrations.[7] The origin for this observation is considered to be kinetic in nature; that is, hydrogen, with a non-directional s valence orbital, is better able to adopt a bridging structure in the transition state than an alkyl group. Similar reasoning might also be operative in elimination reactions; the more favorable hydrogen bridge (over alkyl) may explain why the β-hydrogen elimination reaction is ubiquitous while there are few examples of β-alkyl elimination.

Previous efforts in our research group have focused on elucidating the mechanism of olefin insertion into a metal hydrogen bond.[8] The permethylniobocene olefin hydride complexes, $Cp^*_2Nb(CH_2=CHR)H$ were chosen as suitable candidates for such a mechanistic study principally because, for these complexes, the olefin insertion step could be isolated from all other reactions and observed by dynamic NMR techniques. In addition, a variety of olefin complexes could be prepared allowing steric and electronic effects on the insertion reaction to be probed.

Chapter I describes our efforts to address the effect of sterics on the olefin insertion reaction in the permethylniobocene olefin hydride system. A series of *meta*-substituted styrene

hydride complexes, $Cp^*_2Nb(CH=CHPh\text{-}m\text{-}X)H$, have been synthesized and their rates of olefin insertion measured by coalescence techniques. The ground state structure of the parent complex, $Cp^*_2Nb(CH=CHPh)H$ was determined by single crystal x-ray diffraction.

Attempts to extend our studies in the permethylniobocene (and its third row analog, permethyltantalocene) system to olefin insertion into a metal-carbon bond proved fruitless. That is, olefin alkyl complexes of permethylniobocene and permethyltantalocene were prepared and were found to be resistant to olefin insertion under a variety of reaction conditions.[9] Subsequently, we turned our attention to the permethylscandocene alkyl complexes, Cp^*_2ScR, which had been shown to be active ethylene polymerization catalysts.[10] Since these complexes are stable as base-free monomers and react with olefins in the absence of any Lewis acid cocatalyst, they appeared to be well suited to an examination of the olefin alkyl insertion reaction. Specifically, the effect of the migrating alkyl group on the olefin insertion rate was probed by measuring the ethylene insertion rate for a series of permethylscandocene alkyl complexes by ^{13}C NMR. In addition, the stoichiometric reaction of scandium alkyl complexes with internal alkynes was investigated as a model for a single insertion in the ethylene polymerization reaction. The results of the ethylene and alkyne reactions of permethylscandocene alkyl complexes are described in Chapter II.

Finally, in Chapter III, the focus is shifted from insertion reactions to β-elimination reactions. A series of permethylscandocene alkyl complexes, $Cp^*_2ScCH_2CH_2R$ (R = H, CH_3, CH_2CH_3, $SiMe_3$, Ph, Ph-*p*-CF_3, Ph-*p*-NMe_2 and Ph-*p*-CH_3) have been synthesized to probe the steric and electronic effects on the β-hydrogen elimination. In addition, complexes of the general types $Cp^*_2ScCH_2\overline{CH(CH_2)_nCH_2}$ and $Cp^*_2ScCH_2CH_2X$ (X = halogen, OR, PR_2, SiR_3) have been prepared and used to investigate the processes of β-alkyl and β-X elimination.

In summary, the synthesis of permethylniobocene olefin hydride complexes and permethylscandocene alkyl complexes has been carried out. These complexes have been used as models to examine in detail the processes of olefin insertion and β-elimination.

REFERENCES

1. Parshall, G. W. *Homogeneous Catalysis*; John Wiley & Sons: New York; 1980, Ch. 3.

2. For a general review of β-elimination reactions see: Cross, R. J.; in *The Chemistry of the Metal-Carbon Bond*; Hartley, F. R.; Patia, S., Eds.; John Wiley and Sons: New York; 1985, Vol. 2, Ch. 8.

3. See Chapter II of this thesis for examples supporting this statement.

4. Collman, J. P.; Hegedus, L. S.; Norton, J. R.; Finke, R. G. *Principles and Applications of Organometallic Chemistry*; University Science Books: Mill Valley, California, 1987, p. 567.

5. (a) Halpern, J.; Okamoto, T.; Zakchariev, A. *J. Mol. Catal.* **1976**, *2*, 65-68. (b) Byrne, J. W.; Blaser, H. U.; Osborn, J. A. *J. Am. Chem. Soc.* **1975**, *97*, 3871-3873. (c) Chaudret, B. N.; Cole-Hamilton, D. J.; Wilkinson, G. *Acta Chem. Scand., Ser. A* **1978**, A32, 763-769. (d) Pardy, R. A.; Taylor, M. J.; Constable, E. C.; Mersh, J. D.; Sanders, J. K. M. *J. Organomet. Chem.* **1982**, *231*, C25-C30. (e) Roe, D. C. XIth International Conference on Organometallic Chemistry, Callaway Gardens, Pine Mountain, Georgia, Oct. 10-14, 1983, Abstracts, p. 133. (f) Roe, D. C. *J. Am. Chem. Soc.* **1983**, *105*, 7771-7772. (g) Halpern, J.; Okamoto, T. *Inorg. Chim. Acta* **1984**, *89*, L53-L54. (h) White, J. F.; Whitesides, G. M. *J. Am. Chem. Soc.* **1976**, *98*, 6521. (i) Evans, J.; Schwartz, J.. Urquhart, P. W. *J. Organomet. Chem.* **1976**, *120*, 257. (j) Reger, D. L.; Culbertson, E. C. *J. Am. Chem. Soc.* **1976**, *98*, 2789. (k) Ikariya, T.; Yamamoto, A. *J. Organomet. Chem.* **1976**, *120*, 257. (l) Bruno, J. W.; Kaina, D. G.; Mintz, E. A.; Marks, T. *J. Am. Chem. Soc.* **1982**, *104*, 1860. (m) Thorn, D. L.; Hoffman, R. *J. Am. Chem. Soc.* **1978**, *100*, 2079.

6. Reference 1, page 30.

7. Threlkel, R. S.; Bercaw, J. E. *J. Am. Chem. Soc.* **1981**, *103*, 2650-2659 and references therein.

8. (a) McGrady, N. D.; McDade, C.; Bercaw, J. E. In *Organometallic Compounds: Synthesis, Structure, and Theory*; Shapiro, B. L., Ed.; Texas A&M University Press; College Station, TX, 1983, pp 46-85. (b) Doherty, N. M. Ph. D. Thesis, California Institute of Technology, **1984**. (c) Doherty, N. M.; Bercaw, J. E. *J. Am. Chem. Soc.* **1985**, *107*, 2670-2682.

9. $Cp^*_2M(CH_2{=}CH_2)R$ (M = Ta: R = CH_3, CH_2CH_3, Ph; M = Nb: R = CH_3) were prepared by treatment of $Cp^*_2M(CH_2{=}CH_2)Cl$ with the appropriate alkyl (aryl) grignard reagent in diethyl ether. The synthesis of $Cp^*_2Nb(CH_2{=}CH_2)Cl$ has been previously reported (see Reference 7b); the synthesis of $Cp^*_2Ta(CH_2{=}CH_2)Cl$ is described in Appendix 2. Reaction of these complexes with CO led to simple ligand substitution, forming $Cp^*_2M(CO)R$. There was no reaction with MeCN at room temperature; heating to 80°C led to decomposition. Thermolysis in d_6-benzene (140°C, days) produced a myriad of products suggesting involvement of the Cp^* rings. In none of these reactions was there any evidence for olefin insertion.

10. (a) Thompson, M. E.; Bercaw, J. E. *Pure Appl. Chem.* **1984**, *56*, 1; (b) Thompson, J. E.; Baxter, S. M.; Bulls, A. R.; Burger, B. J.; Nolan, M. C.; Santarsiero, B. D.; Schaefer, W. P.; Bercaw, J. E. *J. Am. Chem. Soc.* **1987**, *109*, 203-219.

CHAPTER I

Mechanistic and Structural Studies of the Insertion Reactions of Styrene Hydride Complexes of Permethylniobocene

INTRODUCTION

Although olefin insertion into metal hydrogen bonds and its microscopic reverse β–H elimination are very common in organometallic chemistry and are elementary steps in a number of catalytic processes, few mechanistic studies of these fundamental transformations have been carried out.[1] Previous efforts in our research group have focused on the first of these transformations.[2] The first system that our group examined was a series of olefin hydride complexes of permethylniobocene, $Cp^*_2Nb(CH_2{=}CHR)H$ ($Cp^* = \eta^5$–C_5Me_5, R = H, Me, Ph, C_6H_4–*p*–X (X = CF_3, Me, OMe, NMe_2)). Even where R ≠ H, a single isomer is formed, which from NMR data[2b] and steric considerations is presumed to be that with the carbon bearing the substituent R located at the *endo* (central, less crowded) position of the equatorial plane of the bent sandwich structure.

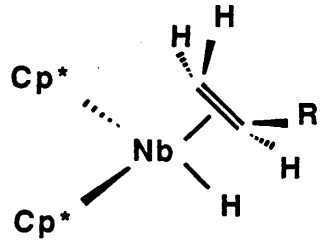

endo

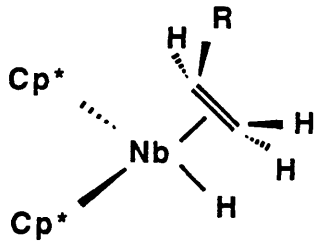

exo

The rate of insertion of the olefin into the Nb–H bond (k_1) was determined by magnetization transfer and coalescence techniques (^{1}H NMR) (equation 1).

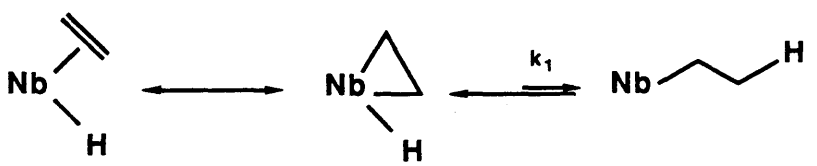

(1)

Nb^{III} Nb^{V} Nb^{III}

A lower limit of k_{-1} (>100 k_1) can be estimated from the undetectably small concentrations (^{1}H NMR) of the alkyl tautomer. Interception of the coordinatively unsaturated intermediate by an external ligand (L = CO, $CNCH_3$) is much slower than β–H elimination, so that the rate of formation of $Cp^*_2Nb(CH_2CH_2R)L$ follows second order kinetics, being first order in both [$Cp^*_2Nb(CH_2{=}CHR)H$] and [L], even at the highest practical concentrations of incoming ligand.

From the k_1's measured for the series of olefin complexes, a model for the insertion process was developed. It was proposed that this insertion reaction proceeds *via* a four center transition state with partial positive charge development at the β–carbon.

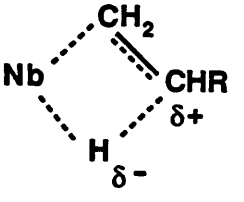

Figure I. Transition state proposed for olefin insertion reaction.[2c]

Electronic effects were found to exert a modest effect on the relative transition states, as evidenced by the differing rates of olefin insertion as one varied the *para*–substituent of the coordinated styrenes. Electronic effects can be transmitted either through the σ framework (induction) or the styrene π system (resonance). An approximate measure of the relative contributions of these two independent modes of transmission can be gained through a comparative study of the rates of insertion as the *meta*– and *para*–substituents are varied. *meta*–Substituent effects on the reaction rate are transmitted principally through induction, whereas a combined resonant and inductive effect is seen on the reaction rate of a *para*–substituted arene.[3] Therefore, comparing the rates of *meta*- *vs. para*-substitution should reveal the relative importance of induction and resonance in the overall electronic effect. Toward

this end, a series of *meta*–substituted styrene hydride complexes of permethylniobocene were synthesized. The rates of olefin insertion for these complexes were measured by coalescence techniques (^{1}H NMR).

The ground state equilibrium binding constants (relative to ethylene) were determined for the *para*-substituted styrenes included in the initial study and were found to be essentially identical. This apparent insensitivity was attributed to a supposition that the phenyl ring of the styrene, due to steric interactions with the pentamethylcyclopentadienyl rings, was twisted out of resonance with the olefin π cloud thereby diminishing the substituent's resonant electronic effects. A crystal structure of the parent styrene hydride complex, $Cp^*_2Nb(CH_2=CHC_6H_5)H$, was determined to examine the ground state structure of this complex and thereby test the validity of this assumption.

Herein are reported the results of our study of the kinetics of $Cp^*_2Nb(CH_2=CHC_6H_4$-*m*-X)H and the crystal structure of $Cp^*_2Nb(CH_2=CHC_6H_5)H$.

RESULTS AND DISCUSSION

Synthesis and Characterization of *meta*-Substituted Styrene Hydride Complexes of Permethylniobocene.

Treatment of $Cp^*_2NbH_3$ (1) with excess *meta*–substituted styrene (5 to 6 equivalents) in toluene at 80 °C for one day affords the styrene hydride complexes, **2-4**.

$$Cp^*_2NbH_3 + m\text{-}X\text{-}C_6H_4CH{=}CH_2 \longrightarrow Cp^*_2Nb(CH_2{=}CHC_6H_4\text{-}m\text{-}X)H$$

X = CF_3, CH_3, NMe_2

(2) X = CF_3

(3) X = CH_3

(4) X = NMe_2

One equivalent of the hydrogenated product, *m*–X–$C_6H_4CH_2CH_3$, is formed concomitantly. The desired compounds are isolated by extraction and crystallization from petroleum ether. The yields for this reaction vary with styrene, but typically range from 50–80%.

The ^1H NMR spectra of the complexes (see Table I) are all similar and are analogous to the *para*–styrene complexes.[2b] At 25 °C the Cp^* rings are nonequivalent, giving rise to two singlets. The olefinic protons exist as three sets of doublet of doublets. The coupling constants of the olefin protons are essentially invariant to *meta*–substitution: $^3J_{trans}$ = 14, $^3J_{cis}$ = 10, $^2J_{gem}$ = 6 Hz. The hydride resonance for all of these complexes is a broad singlet (coupled to the quadrupolar Nb nucleus (I = 9/2, 100% natural abundance [4]) about 2 ppm upfield from TMS. Any coupling of the hydride to the olefinic protons is not resolved and must therefore be less than 0.5 Hz.

The ^{13}C–^1H coupling constants, measured in the gated (^1H NOE enhanced) ^{13}C NMR spectra for **2** and **3**, are in the range 140–146 Hz (see Table II). These values are indicative of

substantial metallocyclopropane character (Nb^{V}) in these formally Nb^{III} olefin adducts, and are similar to other complexes of d^2 bent metallocenes.[5]

The IR spectral data for **2** and **3** are given in the Experimental Section. The most prominent feature of each spectrum is the strong ν_{Nb-H} centered at about 1750 cm^{-1}, which varies little for the complexes.

Determination of the Olefin Insertion Rate by Coalescence Techniques.

The rate of olefin insertion (k_1) was determined for the complexes **3–5** by coalescence techniques (^1H NMR, 90 MHz). At 25 °C, the complexes all have inequivalent Cp^* rings due to the unsymmetrical substitution of the olefin. The two rings can be exchanged by olefin insertion, rapid rotation about the C–C bond and β–hydrogen elimination (see Scheme I).[6] The rate of insertion, k_1, at the coalescence temperature, can be calculated from the frequency separation of the two Cp^* resonances in the room temperature (slow exchange limit) spectrum.[7]

$$k_1(T_c) = 2k_{exchange} = (\sqrt{2}\pi)\Delta\nu$$

From the Eyring equation,[8] the free energy of activation, $\Delta G^{\ddagger}(T_c)$, can be obtained. Values of $\Delta G^{\ddagger}(50\,°C)$ were calculated for complexes **2-4** using an average value of +7 (±5) e.u. for $\Delta S^{\ddagger}$.[9] The values of T_c, $k_1(T_c)$, $\Delta G^{\ddagger}(T_c)$ and $\Delta G^{\ddagger}(50\,°C)$ for complexes **3–5** are given in Table III. A Hammett plot (log k_1 vs. σ_{meta}) is shown in Figure II.

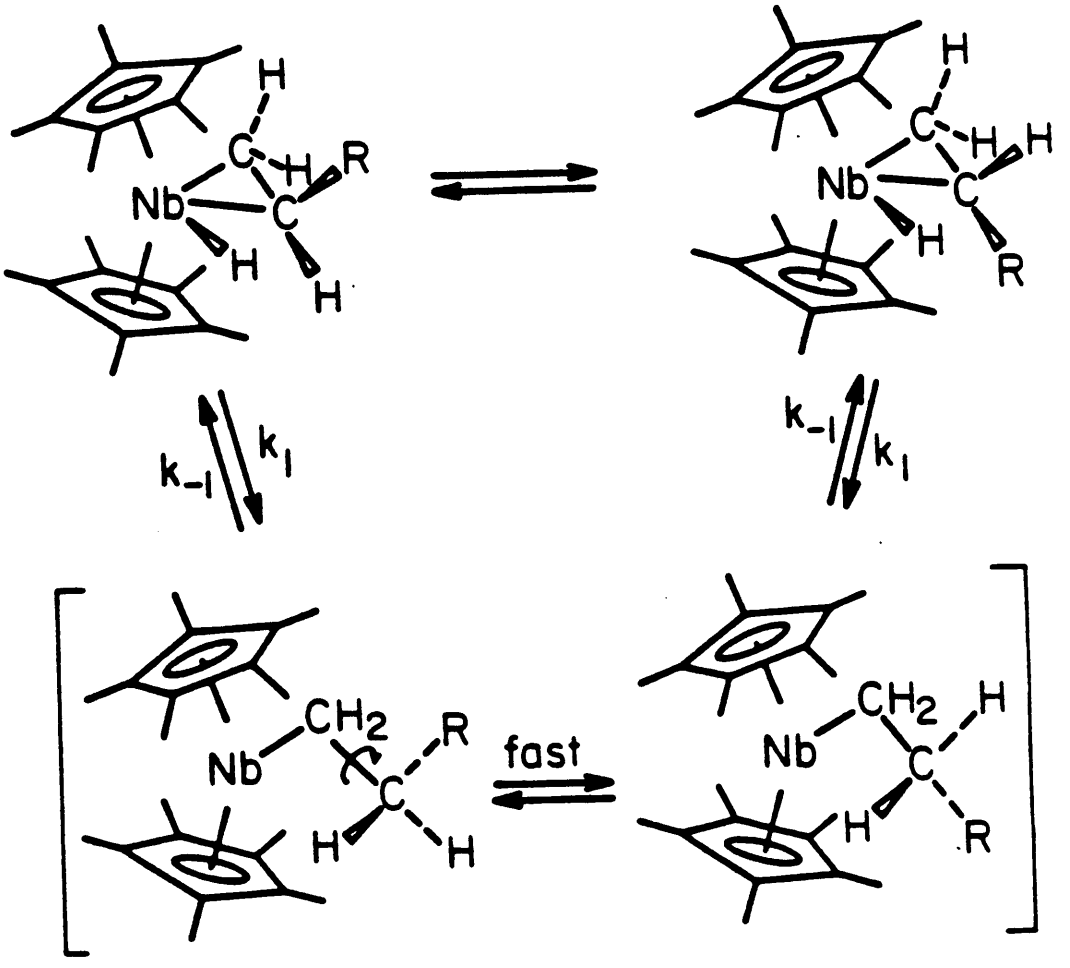

Scheme I. Mechanism for Exchange of Pentamethycyclopentadienyl rings in $Cp^*_2Nb(CH_2=CHR)H$.

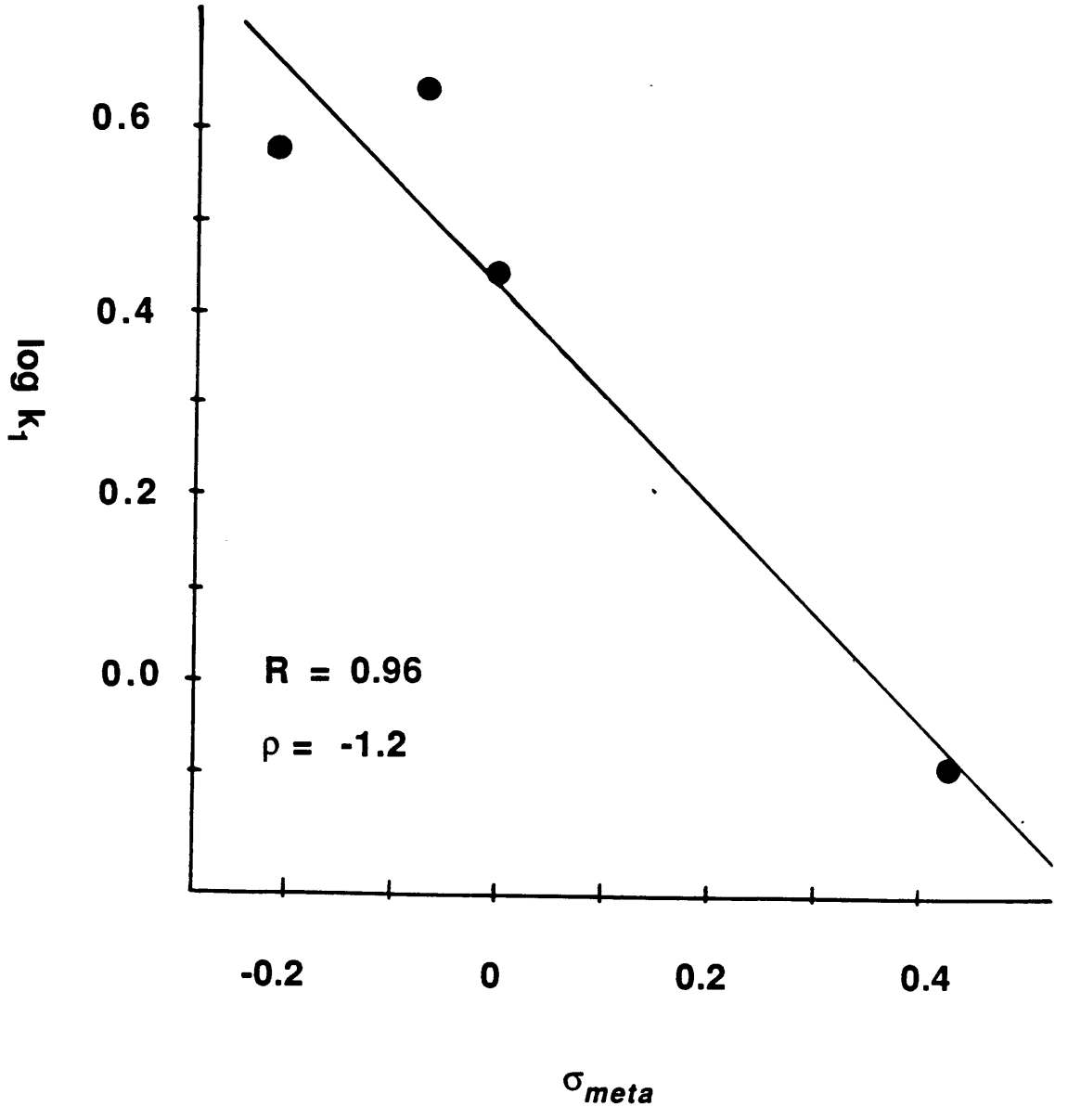

Figure II. Hammett Plot for Olefin Insertion Rates for $Cp^*_2Nb(CH_2=CHC_6H_4$-*m*-X)H.

Discussion of Styrene Hydride Insertion Rates.

The values of $\Delta G^{\ddagger}$(50 °C) for the *meta*– and *para*–substituted styrene hydride complexes are compared in Table IV. Data for the *meta*–substituted styrenes appear to support the model suggested before; that is, the transition state for the olefin insertion reaction is four center, essentially non–polar, with a small positive charge developed at the β–carbon. The small value for ρ_{meta} (–1.2), as shown in Figure II, is characteristic of a four–centered transition state.[10] Thus electron donating groups (CH_3) stabilize the transition state and facilitate the insertion process (relative to H); electron withdrawing groups (CF_3) retard the insertion process. The value of $\Delta G^{\ddagger}$(50 °C) for the *m*–CF_3 and *p*–CF_3 are essentially the same. This is not at all surprising since CF_3 is strongly electron withdrawing by induction and transmits very little electronic effect through the π–cloud.[11] Since the inductive effect of a substituent is, to a first approximation, the same at the *meta* and *para* positions,[3] this result was just what we had anticipated. The effect of the CF_3 group on the rate of insertion through resonance effects was less than the experimental error. Similarly, the *m*– and *p*–CH_3 styrenes react at the same rate. Thus, for substituents which exhibit electronic effects primarily through induction, the insertion rates for *meta*– and *para*–substituted styrenes are the same.

The relative importance of resonant and inductive electronic effects is evident from comparison of the data for the *m*– and *p*–NMe_2 complexes. The NMe_2 group is electron withdrawing by induction, yet strongly electron releasing by resonance. Since a substituent at the *meta* position transmits electronic effects primarily through induction,[12] the difference between the two $\Delta G^{\ddagger}$ values (kcal · mol^{-1} at 50 °C) (18.1 and 17.6 for *m*–NMe_2 and *p*–NMe_2, respectively) can be attributed to resonance transmission of electronic effects. Since the difference between the two activation barriers is quite small, the electronic effects can be defined as primarily inductive in nature. The significance of this result, that there is little difference in the insertion rates for *meta*– and *para*–NMe_2 styrene complexes, stems from the very nature of the

resonance interaction. In order to transfer electronic effects from the π cloud of the phenyl ring to the β–carbon, the olefinic carbons must achieve some degree of coplanarity with the aromatic ring during the transition state. Thus, this result is consistent with the fact that the analogous *para*–substituted styrene insertion rates correlate better with σ_p with σ_+[2c] and lends credence to the supposition that, due to unfavorable steric interactions, the phenyl ring of the styrene is not completely in resonance with the olefin in the transition state.

Structure Determination of $Cp^*_2Nb(CH_2{=}CHC_6H_5)H$ (5).

A yellow crystal of 5, suitable for x–ray diffraction, was grown from a slowly cooled petroleum ether/benzene solution. The molecular structure of $Cp^*_2Nb(CH_2{=}CHC_6H_5)H$ is shown in Figure III; a skeletal view of the niobium coordination sphere with notable bond lengths and angles is shown in Figure IV. The Cp^* ligands are coordinated in the conventional η^5 fashion; the Nb–C and C–C bond lengths (Table IX) are similar to those reported for other Group V pentamethylcyclopentadienyl complexes.[13] The structure confirms the *endo* arrangement of the olefin as assigned from NMR data.[2b]

The olefinic carbon–carbon bond length (C(1)–C(2)) of 1.431(6)Å) is larger than that of a free olefin (*eg.*, ethylene, 1.337(2)Å[14]), and representative of the C–C distances observed in olefin adducts of low-valent, electron-rich metal centers (*eg.*, $Cp^*_2Ti(CH_2{=}CH_2)$,[5c] 1.438(5)Å; $Cp^*Ta(CHCHMe_3)(\eta^2{-}C_2H_4)(PMe_3)$,[13c] 1.477(4)Å; $Cp_2Nb(CH_2{=}CH_2)CH_2CH_3$,[5a] 1.406(13)Å; $Cp^*_2Ta(CH_2{=}CH_2{\cdot}AlEt_3)H$,[13d] 1.44(2)Å. The lengthening of the olefin is considered indicative of electron back donation from the metal to the olefin.[15] Overlap of the filled b_2 orbital of the metallocene[16] with the empty olefin π^* orbital introduces metallocyclopropane, Nb(V), character into the formally Nb(III) olefin adduct. The slightly longer C–C bond length in 5 relative to that in $Cp_2Nb(CH_2{=}CH_2)CH_2CH_3$ undoubtedly reflects the greater donor ability of Cp^* over Cp.

The hydride was located in this structure. The Nb–H distance of 1.75(3)Å compares to other niobium complexes containing terminal hydride ligands (*eg.*, Cp_2NbH_3,[17] 1.65(6), 1.65(6), 1.76(7), all in Å; $[HNb(C_5H_5)(C_5H_4)]_2$,[18] 1.70(3) Å, and the Ta–H bond distances in Cp_2TaH_3,[20] 1.769(8), 1.775(9), 1.777(9), all in Å). A β-agostic interaction is ruled out by the C2–H distance of 2.59 Å.

Distortions in the crystal structure are consistent with the equilibrium binding studies. The phenyl ring of the styrene is indeed twisted away from coplanarity with the olefinic carbons. The dihedral angle between the olefin plane (plane defined by C(1), C(2), and C(3)) and the aromatic ring (C(3)–C(8)) is 32(9)°. Twisting of the phenyl ring decreases steric (repulsive) interactions with the Cp^* rings at the expense of a decrease in the resonance stabilization.

CONCLUSIONS

The model previously suggested (see Figure I) for the insertion of olefins into Nb–H bonds is supported by our study of the insertion rates of $Cp^*_2Nb(CH_2=CHC_6H_4\text{–}m\text{–}X)H$ complexes. Electronic effects are predominantly inductive in nature in the transition state, suggesting little coplanarity of the olefin and the aromatic ring of the styrene during the insertion process. The structure of $Cp^*_2Nb(CH_2=CHC_6H_5)H$ shows that the coordinated olefin has a large degree of metallocyclopropane character which is expected for this electron–rich Nb(III), d^2 center. Due to unfavorable steric interactions with the Cp^* rings, the phenyl ring of the styrene is twisted out of resonance with the olefinic carbons. These studies support our earlier supposition[2c] that the phenyl ring stays out of resonance with the olefin along the entire reaction coordinate to avoid unfavorable steric interactions with the Cp^* rings.

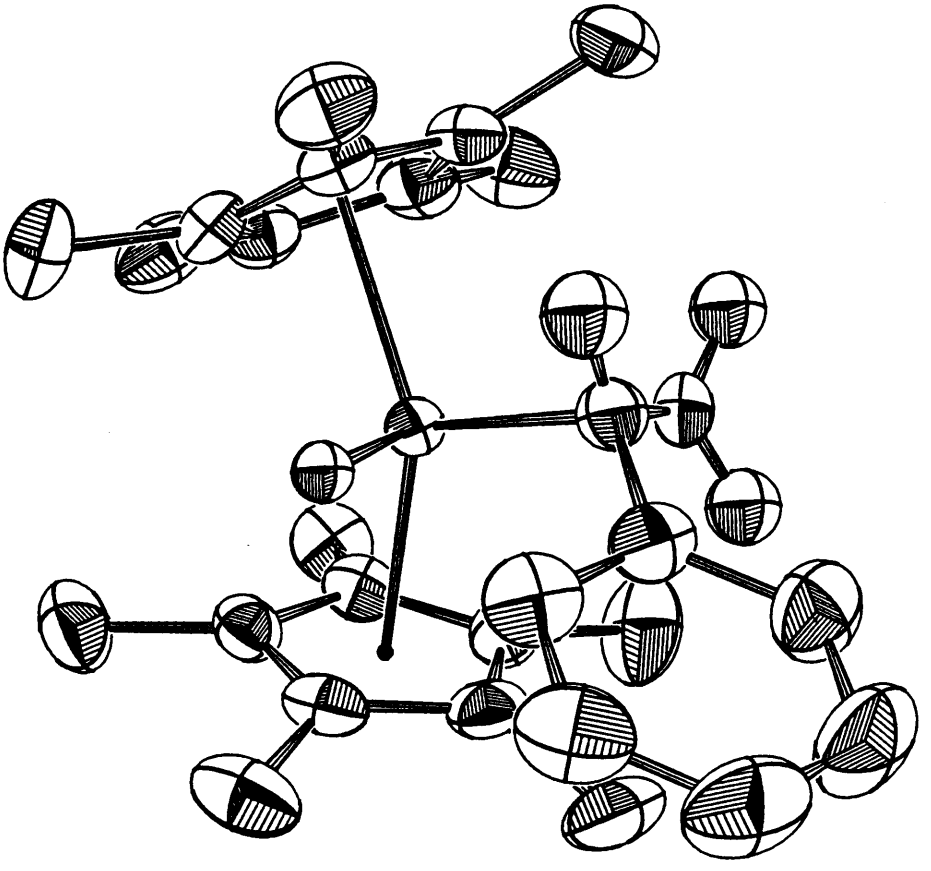

Figure III. Molecular Structure of $Cp^*_2Nb(CH_2=CHC_6H_5)H$.

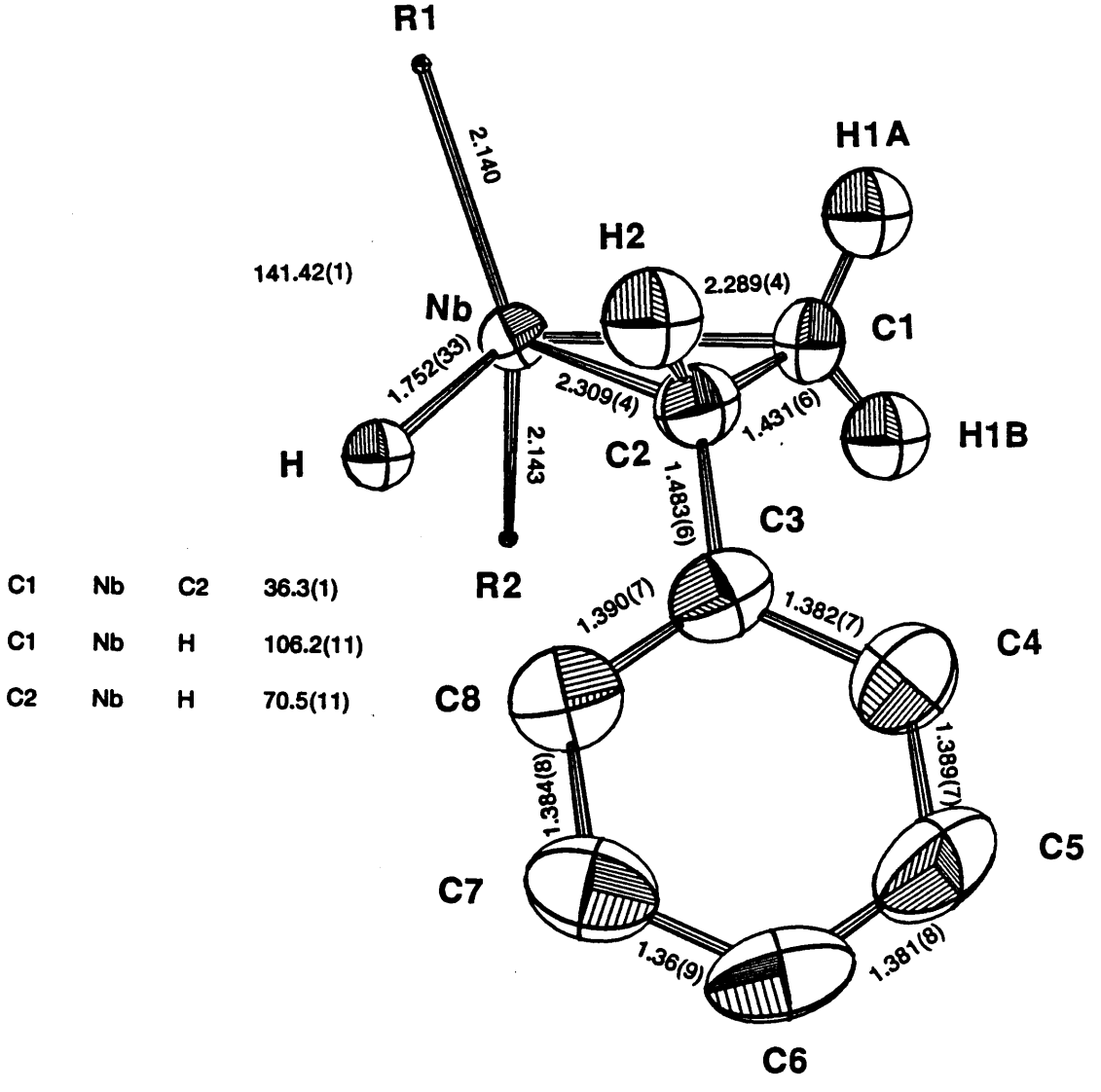

C1	Nb	C2	36.3(1)
C1	Nb	H	106.2(11)
C2	Nb	H	70.5(11)

Figure IV. Skeletal View of $Cp^*_2Nb(CH_2=CHC_6H_5)H$. [a]

[a]Bond distances are in Å. Bond angles are in degrees.

Table I. ^{1}H NMR Data for Cp^*_2Nb Complexes.[a]

Compound	Assignment	δ (ppm)	Coupling (Hz)
$Cp^*_2Nb(CH_2{=}CHC_6H_4\text{-}m\text{-}CF_3)H$ (**2**)	$[C_5(CH_3)_5]$	1.40 s	
	$[C_5(CH_3)_5]$	1.56 s	
	Nb-*H*	-2.27 br s[b]	
	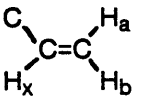	H_a 0.30 dd	J_{ax} = 6
		H_b 0.14 dd	J_{bx} = 10
		H_x 2.19 dd	J_{ab} = 13
	C_6H_4	6.82 d J = 8	
		7.04 t J = 8	
		7.58 d[c]	
		8.0 s	
$Cp^*_2Nb(CH_2{=}CHC_6H_4\text{-}m\text{-}CH_3)H$ (**3**)	$[C_5(CH_3)_5]$	1.55 s	
	$[C_5(CH_3)_5]$	1.72 s	
	Nb-*H*	-2.23 br s	
	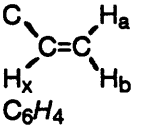	H_a 0.93 dd	J_{ax} = 6
		H_b 0.21 dd	J_{bx} = 10
		H_x 2.15 dd	J_{ab} = 14
	C_6H_4	7.60[c]	
		6.80[c]	
		7.21[c]	
	CH_3	2.38 s	
$Cp^*_2Nb(CH_2{=}CHC_6H_4\text{-}m\text{-}NMe_2)H$ (**4**)	$[C_5(CH_3)_5]$	1.54 s	
	$[C_5(CH_3)_5]$	1.65 s	
	Nb-*H*	-2.26 br s	
	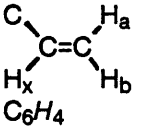	H_a 0.51 dd	J_{ax} = 6
		H_b 0.18 dd	J_{bx} = 10
		H_x 2.30 dd	J_{ab} = 14
	C_6H_4	7.56[c]	
		6.82[c]	
		7.15[c]	
	$N(CH_3)_2$	3.05 s	

[a] ^{1}H (90 and 400 MHz) NMR spectra were taken in benzene-d_6 at ambient temperature. Chemical shifts are reported in parts per million (δ) from tetramethylsilane added as an internal reference or to residual protons in the solvent. Coupling constants are reported in hertz.

[b]Broadening of all hydride signals reported is due to coupling to the quadrupolar Nb (I = 9/2, 100% abundance) nucleus.

[c]The linewidth of these signals precluded accurate measurement of the coupling constants.

Table II. ^{13}C NMR Data for Cp^*_2Nb Complexes.[a]

Compound	Assignment	δ (ppm)	Coupling (Hz)
$Cp^*_2Nb(CH_2{=}C_6H_4\text{-}m\text{-}CF_3)H$ (2)	$[C_5(CH_3)_5]$	105.84 s	
	$[C_5(CH_3)_5]$	105.26 s	
	$[C_5(CH_3)_5]$	11.54 q	J_{CH} = 120
	$[C_5(CH_3)_5]$	11.22 q	J_{CH} = 120
	$CH_2{=}CHC_6H_4X$	23.96 t	J_{CH} = 146
	$CH_2{=}CHC_6H_4X$	45.01 t	J_{CH} = 144
	$CH_2{=}CHC_6H_4X$	153.60 s	
		133.59 d	J_{CH} = 173
		118.51 d	J_{CH} = 177
		128.13 d[b]	
		127.48 d[b]	
		126.83 s	
	CF_3	(not found)	
$Cp^*_2Nb(CH_2{=}C_6H_4\text{-}m\text{-}CH_3)H$ (3)	$[C_5(CH_3)_5]$	105.32 s	
	$[C_5(CH_3)_5]$	104.67 s	
	$[C_5(CH_3)_5]$	11.41 q	J_{CH} = 126
	$[C_5(CH_3)_5]$	11.15 q	J_{CH} = 125
	$CH_2{=}CHC_6H_4X$	23.96 t	J_{CH} = 143
	$CH_2{=}CHC_6H_4X$	46.15 t	J_{CH} = 139
	$CH_2{=}CHC_6H_4X$	151.14 s	
		133.86 d	J_{CH} = 161
		131.05 d	J_{CH} = 160
		123.13 d	J_{CH} = 160
		128.26 d[b]	
		127.16 s	
	CH_3	21.81 q	J_{CH} = 125

[a] ^{13}C (100.25 MHz) NMR spectra were taken in benzene-d_6 at ambient temperature. Chemical shifts are reported in parts per million (δ) from tetramethylsilane referenced from solvent signal (C_6D_6, δ 128). Coupling constants ($J_{13C\text{-}1H}$) were obtained from a gated (^1H NOE enhanced) spectrum and are reported in hertz.

[b] Overlap with solvent resonance precluded accurate measurement of these coupling constants.

Table III. Rates for Olefin Insertion into the Niobium Hydride Bonds of $Cp^*_2Nb(CH_2{=}CHC_6H_4\text{-}m\text{-}X)H$. [a]

X	T_c(°C)	$k_c(s^{-1})$	$\Delta G^{\ddagger}(T_c)$[b] (kcalmol^{-1})	$\Delta G^{\ddagger}$(50°C) (kcalmol^{-1})
H[c]	83	59.0	18.1	18.3
m-CF_3	104	76.2	19.0	19.3
m-CH_3	76	53.4	17.8	18.0
m-NMe_2	75	44.2	17.9	18.1

[a]All data were measured at 90 MHz.

[b]Estimated error is ±0.1 (kcal · mol^{-1}).

[c]Data taken from Reference 2c.

Table IV. Comparison of $\Delta G^{\ddagger}$ (50 °C) for *meta*– and *para*–$Cp^*_2Nb(CH_2=CHC_6H_4\text{-}X)H$ Complexes.[a]

X	σ_{meta}[b]	$\Delta G^{\ddagger}{}_{meta}$[c] (kcalmol^{-1})	σ_{para}[b]	$\Delta G^{\ddagger}{}_{para}$[c,d] (kcalmol^{-1})
CF_3	0.43	19.3	0.54	19.1
CH_3	-0.07	18.0	-0.17	18.0
NMe_2	-0.21	18.1	-0.83	17.6

[a]For X = H, $\Delta G^{\ddagger}$(50 °C) = 18.3 kcal · mol^{-1}.

[b]Data are taken from Reference 10.

[c]$\Delta G^{\ddagger}$ is in kcal · mol^{-1} at 50 °C.

[d]Data taken from Reference 2c.

Table V. Summary of Crystal Data for $Cp^*_2Nb(CH_2CHC_6H_5)H$ (5).

formula: $C_{28}H_{39}Nb$	f.wt. 468.5
Space group Pbca	T = 21 °C
z = 8	V = 4813(1)Å^3
a = 14.626(3)	
b = 18.134(4)	
c = 18.147(4)	
λ MoKα = 0.71073 Å	
Scan Range 1.0° above Kα_1, 1.0° below Kα_2	
Reflections +h, +k, ±l	
Collected 8188 reflections	
Averaged 4124 reflections	
(3742 $I > 0$, 2644 $I > 3\sigma_I$)	

Table VI. Final Parameters.[a]

	x	y	z	U_{eq}[b]
Nb	7052(2)	18814(2)	14413(2)	273(1)
C1	19543(28)	18792(27)	22017(22)	402(10)
C2	11662(31)	17498(22)	26510(21)	369(10)
C3	10431(33)	10979(24)	31346(22)	442(11)
C4	1929(37)	8076(26)	32966(24)	526(13)
C5	1038(42)	1945(29)	37493(27)	633(15)
C6	8663(50)	-1297(29)	40601(30)	773(17)
C7	17031(46)	1667(33)	39233(32)	775(17)
C8	17985(37)	7735(28)	34674(27)	608(13)
C11	10378(30)	31508(24)	10348(24)	425(10)
C12	8717(30)	32129(21)	19327(21)	356(10)
C13	-448(29)	29903(21)	1932721)	356(10)
C14	-4503(28)	28141(23)	12553(21)	386(10)
C15	1978(31)	29274(21)	6950(22)	378(10)
C11M	19006(37)	33826(27)	6547(28)	629(14)
C12M	14952(35)	35671(23)	23447(28)	562(13)
C13M	-5419(32)	30523(25)	26632(23)	537(12)
C14M	-14579(33)	26742(29)	11456(27)	591(14)
C15M	-195(39)	30012(25)	-1135(24)	582(13)
C21	16817(30)	10159(24)	7787(24)	408(11)
C22	10412(30)	12891(23)	2611(22)	377(10)

C23	1556(30)	10431(23)	4861(23)	379(10)
C24	2726(32)	6034(23)	11265(24)	414(11)
C25	12109(33)	5813(22)	12982(23)	413(11)
C21M	27030(34)	10670(34)	6813(30)	714(17)
C22M	12953(35)	16230(26)	-4633(23)	508(12)
C23M	-7236(37)	10820(27)	628(25)	583(12)
C24M	-4486(36)	1420(26)	14894(29)	621(13)
C25M	16576(41)	474(26)	18273(27)	641(15)

[a] x, y, z $\times 10^5$; $U_{eq} \times 10^4$

[b] $U_{eq} = 1/3\ \Sigma_i\Sigma_i U_{ij}(a_i^* a_j^*) a_i^* \cdot a_j^*$; $\sigma U_{eq} = 6^{-1/2} <\sigma U_{ii}/U_{ii}> U_{eq}$

Table VII. Gaussian Amplitudes (x 10^4).

	U_{11}	U_{22}	U_{33}	U_{12}	U_{13}	U_{23}
Nb	268(2)	261(2)	290(2)	7(2)	-3(2)	-7(2)
C1	356(25)	396(23)	454(23)	4(25)	-133(19)	12(23)
C2	422(26)	357(25)	327(23)	10(21)	-49(20)	-10(19)
C3	589(32)	422(26)	314(23)	64(23)	-18(22)	-5(20)
C4	614(35)	540(31)	423(26)	17(27)	59(24)	6(23)
C5	749(40)	566(33)	584(34)	-105(30)	166(29)	40(26)
C6	1058(54)	542(32)	719(37)	30(37)	19(39)	306(28)
C7	866(47)	730(40)	729(38)	142(37)	-162(36)	308(33)
C8	658(340)	638(33)	529(30)	34(28)	-95(29)	109(27)
C11	473(27)	301(22)	500(25)	-53(23)	84(21)	80(23)
C12	449(29)	260(21)	449(23)	-3(21)	28(20)	-25(18)
C13	396(25)	293(23)	379(22)	66(19)	49(19)	6(18)
C14	352(26)	376(22)	430(26)	102(19)	-12(18)	42(18)
C15	465(28)	317(24)	353(29)	48(19)	-1(21)	56(18)
C11M	690(38)	550(31)	647(32)	-192(27)	246(30)	-3(26)
C12M	540(33)	408(25)	739(36)	-78(24)	-24(28)	-143(25)
C13M	536(32)	554(27)	522(27)	125(28)	174(23)	-76(24)
C14M	358(27)	720(36)	696(33)	121(26)	-99(26)	57(28)
C15M	767(36)	544(30)	435(25)	216(29)	26(26)	135(26)
C21	337(25)	430(25)	458(26)	77(21)	30(21)	-137(21)
C22	429(27)	389(24)	312(22)	-16(20)	58(19)	-49(19)
C23	367(27)	379(24)	392(24)	-27(21)	-8(20)	-88(20)
C24	497(30)	292(22)	454(25)	-63(22)	80(22)	-76(20)

C25	522(30)	282(22)	434(28)	102(21)	-4(22)	-82(20)
C21M	375(32)	1090(46)	678(34)	161(31)	-133(27)	-76(20)
C22M	545(32)	612(31)	366(24)	-25(25)	97(23)	-49(21)
C23M	482(29)	718(32)	549(28)	-60(31)	-111(28)	-133(25)
C24M	691(37)	480(28)	692(33)	-206(25)	171(31)	-97(28)
C25M	877(43)	388(27)	657(33)	222(29)	-36(32)	10(24)

Table VIII. Atom Coordinates (x 10^4) of Hydrogen Atoms.

	x	y	z
H	-210	1551	1970
H1A	2374	1448	2137
H1B	2291	2373	2187
H2	865	2147	2865
H4	-363	1039	3084
H5	-497	-29	3850
H6	804	-558	4373
H7	2241	-65	4156
H8	2404	978	3368
H111	1778	3397	140
H112	2134	3923	841
H113	2353	3022	752
H121	1569	3202	2727
H122	1174	3971	2534
H123	2035	3698	2194
H131	-185	3294	3058
H132	-668	2539	2829
H133	-1109	3280	2592
H141	-1617	2375	695
H142	-1741	3150	1099
H143	-1677	2438	1570

H151	515	3121	-374
H152	-458	3394	-169
H153	-334	2480	-357
H211	737	1762	-709
H212	2812	1542	486
H213	2966	746	400
H221	737	1762	-709
H222	1698	2065	-442
H223	1587	1253	-753
H231	-927	574	-174
H232	-640	1432	-320
H233	-1185	1245	389
H241	-214	-76	2023
H242	-585	-267	1177
H243	-976	428	1564
H251	2164	299	2048
H252	1900	-350	1532
H253	1174	-166	2251

Table IX. Distances and Angles.

Atom	Atom	Dist. (Å)	Atom	Atom	Atom	Angle
Nb	C1	2.289(4)	C1	C2	C3	124.4(4)
	C2	2.309(4)	C2	C3	C4	122.6(4)
	C11	2.466(4)	C3	C4	C5	121.0(5)
	C12	2.506(6)	C4	C5	C6	120.4(5)
	C13	2.458(4)	C5	C6	C7	119.0(6)
	C14	2.415(4)	C6	C7	C8	121.0(6)
	C15	2.446(4)	C2	C3	C8	119.9(4)
	C21	2.439(4)	C3	C8	C7	121.1(5)
	C22	2.446(4)	C3	C4	C8	117.5(4)
	C23	2.442(4)	C1	Nb	C2	36.3(1)
	C24	2.469(4)	C1	Nb	H	106.2(11)
	C25	2.484(4)	C2	Nb	H	70.5(11)
	H	1.752(33)	C11	C12	C13	107.9(4)
	R1	2.143	C12	C13	C14	108.3(3)
	R2	2.140	C13	C14	C15	108.4(4)
C1	C2	1.431(6)	C14	C15	C11	108.0(4)
	H1A	1.002(40)	C15	C11	C12	107.3(4)
	H1B	1.022(38)	C21	C22	C23	107.5(4)
C2	C3	1.483(6)	C22	C23	C24	107.5(4)
	H2	0.930(41)	C23	C24	C2	108.3(4)

C3	C4	1.382(7)
	C8	1.390(7)
C4	C5	1.389(7)
C5	C6	1.381(8)
C6	C7	1.36(9)
C7	C8	1.384(8)
C11	C12	1.411(6)
	C15	1.420(8)
	C11M	1.498(7)
C12	C13	1.421(6)
	C12M	1.492(6)
C13	C14	1.402(6)
	C13M	1.516(6)
C14	C15	1.405(6)
	C14M	1.509(6)
C15	C15M	1.507(6)
C21	C22	1.416(6)
	C25	1.403(9)
	C21M	1.507(7)
C22	C23	1.429(6)
	C22M	1.494(6)
C23	C24	1.420(6)
	C23M	1.500(6)
C24	C25	1.408(6)
	C24M	1.499(7)
C25	C25M	1.512(7)

C24	C25	C21	108.2(4)
C25	C21	C22	108.4(4)
R1	Nb	R2	141.42(1)

R1 and R2 are the centroid coordinates of C11 through C15 and C21 through C25 Cp* rings respectively.

EXPERIMENTAL SECTION

General Considerations.

All air sensitive manipulations were carried out using glove box or high vacuum line techniques. Solvents were dried over $LiAlH_4$ or sodium benzophenone and stored over titanocene. Benzene-d_6 and toluene-d_8 were dried over activated 4 Å molecular sieves and stored over titanocene.

Argon and hydrogen gases were purified by passage over MnO on vermiculite and activated molecular sieves. *meta*–Methylstyrene (Alfa) was used without further purification. *meta*-Trifluoromethylstyrene was prepared by the literature method for its *para*-substituted analog[19] except that the secondary alcohol, *m*-$CF_3C_6H_4CH(OH)CH_3$, was formed by the reaction of CH_3MgBr and *m*-$CF_3C_6H_4CHO$ (Marshallton). *meta*-Dimethylaminostyrene was prepared by this same procedure except that the secondary alcohol, *m*–NMe_2–C_6H_4CH–(OH)-CH_3, was prepared by alkylating *m*-$NMe_2C_6H_4CO_2H$ (Aldrich) with MeLi (Aldrich) and then reducing the resultant ketone, *m*-$NMe_2C_6H_4COCH_3$, with $NaBH_4$ in ethanol. *meta*-Dimethylaminostyrene and *meta*-trifluoromethylstyrene were purified by vacuum distillation and characterized by ^1H NMR.

NMR spectra were recorded on Varian EM-390 (^1H, 90 MHz), JEOL FX90Q (^1H, 89.56 MHz; ^{13}C, 22.50 MHz; ^{19}F, 84.26 MHz), and JEOL GX400Q (^1H, 399.78 MHz; ^{13}C, 100.38 MHz) spectrometers. Infrared spectra were recorded on a Beckman 4240 spectrometer and peak positions are reported in cm^{-1}. All elemental analyses were conducted by L. Henling of the Caltech Analytical Laboratory.

$Cp^*_2NbH_3$[20] and $Cp^*_2Nb(CH_2{=}CHC_6H_5)H$[2b] were prepared by literature methods.

$Cp^*_2Nb(CH_2=CHC_6H_4$-*m*-$CF_3)H$ (2). *meta*-Trifluoromethylstyrene (1.0 mL) was added to $Cp^*_2NbH_3$, **1**, (0.5 g, 1.36 mmol) in 10 mL toluene. The reaction mixture was heated at 80 °C for 20 hours. Toluene was removed under reduced pressure, leaving a dark brown oil. Addition of petroleum ether caused a yellow solid to precipitate from solution. Recrystallization from petroleum ether resulted in 360 mg of a yellow crystalline solid, **2**, (49%).

^{19}F NMR (benzene-d_6): δ-62.3 (relative to $CFCl_3$). IR (Nujol): 2715, 1745, 1668, 1594, 1578, 1470, 1378, 1348, 1320, 1212, 1167, 1128, 1108, 1063, 1020, 895, 797, 768, 738, 700, 656. Anal. Calcd. for $C_{29}H_{38}F_3Nb$: C, 64.92; H, 7.14. Found: C, 65.01; H, 7.06.

$Cp^*_2Nb(CH_2=CHC_6H_4$-*m*-$CH_3)H$ (3). The same procedure was used as described above except that *meta*-methylstyrene (0.7 mL) was added to $Cp^*_2NbH_3$, **1**, (0.5 g, 1.36 mmol) in 10 mL toluene. Yellow crystalline **3** (450 mg) was isolated after petroleum ether recrystallization, (68%).

IR (Nujol): 2708, 1752, 1688, 1594, 1572, 1486, 1478, 1377, 1280, 1243, 1176, 1152, 1089, 1061, 1022, 896, 880, 792, 768, 734, 698.

$Cp^*_2Nb(CH_2=CHC_6H_4$-$NMe_2)H$ (4). The same procedure was used as described above except that *meta*-dimethylaminostyrene (0.5 mL) was added to $Cp^*_2NbH_3$, **1** (0.367 g, 1.0 mmol) in 10 mL toluene. Yellow crystalline **4** (405 mg) was isolated after petroleum ether recrystallization, (80%).

Anal. Calcd. for $C_{30}H_{43}NNb$: C, 77.72; H, 9.57; N, 3.02.. Found: C, 77.09; H, 9.37; N, 3.49.

Measurement of Olefin Insertion Rates Using Coalescence Techniques.

Coalescence temperatures of the two Cp^* resonances for the olefin hydride complexes **2-4** were measured at 90 MHz on a JEOL FX90Q spectrometer. A typical sample was prepared in

a glove box by loading the olefin hydride complex (≈20 mg) and benzene-d_6 (0.4 mL) in a sealable NMR tube. Tubes were sealed either at −196 °C under an atmosphere of nitrogen or at −78 °C under 700 torr argon. The temperature at which coalescence occurs was measured by the peak separation of an ethylene glycol sample. The room temperature ^{1}H NMR spectrum was recorded before and after determination of the coalescence temperature; no decomposition was evident. The rate of insertion at the coalescence temperature was calculated using the Gutowsky-Holm Approximation, $k_1(T_c) = 2k_{exchange} = \sqrt{2}\pi\Delta\nu$,[8] where $\Delta\nu$ is the frequency separation between the Cp^* peaks in the room temperature spectrum. $\Delta G^{\ddagger}(T_c)$ can be calculated from the Eyring Equation, $\Delta G(T_c) = RT_c\ln(\kappa kT_c/k_ch)$,[21] assuming a transmission coefficient, κ, of 1.

Structure Determination of $Cp^*_2Nb(CH_2{=}CHC_6H_5)H$ (5).

Data Collection.

A yellow crystal of $Cp^*_2Nb(CH_2{=}CHC_6H_5)H$ (5), grown from petroleum ether/benzene (1:1), was mounted in a glass capillary under a nitrogen atmosphere. A series of oscillation and Weissenberg photographs established the crystal as orthorhombic. Unit cell parameters were obtained by least squares refinement of fifteen centered reflections ($22° < 2\theta < 33°$): a = 14.626(3), b = 18.134(4), c = 18.147(4); $\alpha,\beta,\gamma = 90°$. The systematic absences led to the unambiguous assignment of the space group P_{bca} (h0l: l = odd, 0kl: k = odd, hk0: h = odd).

A total of 8188 reflections (+h, +k, ±l, $4° < 2\theta < 30°$) was collected on a locally modified Syntex $P2_1$ diffractometer with graphite monochromator and Mo radiation (λ = 0.7107 Å). Three check reflections were remeasured after every 197 reflections, and no decay was indicated. No absorption corrections were applied (μ = 0.49 mm^{-1}, $0.25 < \mu \cdot d < 0.38$). A summary of the data collection information is given in Table V.

Structure Determination and Refinement.

The coordinates of the niobium atom were derived from the Patterson map; subsequent Fourier and difference Fourier maps revealed the remainder of the structure. Several cycles of full-matrix least squares refinement with anisotropic Gaussian amplitudes for all non-hydrogen atoms resulted in $R = \{\Sigma w|Fo|-|Fc/k|w/|Fo|\} = 0.0588$ (3264 reflns with I>0)and $GOF = \{\Sigma w(Fo_2 - Fc_2/k))_2/n_o - n_p)\}^{1/2} = 1.51$, where n_o is the number of reflections and n_p is the number of parameters (4124 reflections). The parameters for the Cp^* hydrogens H111-H253 and the phenyl ring H4-H8 were not refined. There was no residual electron density greater than 0.4 $e^-/Å^3$ remaining in the final difference Fourier map. The final values for the atom coordinates and Gaussian amplitudes are given in Table VI and VII; Table VIII lists the final hydrogen atom coordinates and B's; bond lengths and angles are located in Table IX.

The molecular structure of $Cp^*_2Nb(CH_2=CHC_6H_5)H$ is shown in Figure III; a skeletal view of niobium coordination with notable bond lengths and angles is shown in Figure IV.

REFERENCES

1. (a) Halpern, J.; Okamoto, T.; Zakchariev, A. *J. Mol. Catal.* **1976**, *2*, 65–68. (b) Byrne, J. W.; Blaser, H. U.; Osborn, J. A. *J. Am. Chem. Soc.* **1975**, *97*, 3871–3873. (c) Chaudret, B. N.; Cole–Hamilton, D. J.; Wilkinson, G. *Acta Chem. Scand., Ser. A* **1978**, A32, 763–769. (d) Pardy, R. A.; Taylor, M. J.; Constable, E. C.; Mersh, J. D.; Sanders, J. K. M. *J. Organomet. Chem.* **1982**, *231*, C25–C30. (e) Roe, D. C. XIth International Conference on Organometallic Chemistry, Callaway Gardens, Pine Mountain, Georgia, Oct 10–14, 1983, Abstracts, p 133. (f) Roe, D. C. *J. Am. Chem. Soc.* **1983**, *105*, 7771–7772. (g) Halpern, J.; Okamoto, T. *Inorg. Chim. Acta* **1984**, *89*, L53-L54.

2. (a) McGrady, N. D.; McDade, C.; Bercaw, J. E. In *Organometallic Compounds: Synthesis, Structure, and Theory*; Shapiro, B.L., Ed.; Texas A&M University Press; College Station, TX, 1983; pp 46–85. (b) Doherty, N. M. Ph. D. Thesis, California Institute of Technology, **1984**. (c) Doherty, N. M.; Bercaw, J. E. *J. Am. Chem. Soc.* **1985**, *107*, 2670–2682.

3. Johnson, C. D. *The Hammett Equation*; Cambridge University Press: Cambridge, England, 1973; Chapter 1.

4. Becker, E. D. *High Resolution NMR*; Academic: New York, 1980; p.283.

5. (a) Guggenberger, L. J.; Meakin, P.; Tebbe, F. N. *J. Am. Chem. Soc.* **1974**, *96*, 5420–7. (b) References 2b. (c) Cohen, S. A.; Auburn, P. R.; Bercaw, J. E. *J. Am. Chem. Soc.* **1983**, *105*, 1136-1143.

6. Scheme I is taken from Reference 2b.

7. Reference 4, Chapter 11.

8. Sandstrom, J. *Dynamic NMR Spectroscopy*; Academic Press: London, England, 1982; Chapter 6.

9. An average value for $\Delta S^{\ddagger}$ of -10 e.u. was taken from measured values for the olefin insertion reaction of $Cp^*_2Nb(CH_2{=}CH_2)H$ and $Cp^*_2Nb(CH_2{=}CHC_6H_5)H$; see Reference 2c.

10. Lowry, T. H.; Richardson, K. S. *Mechanism and Theory in Organic Chemistry* 2nd Ed., Harper and Row, Publishers: New York, New York, 1981, 130-145.

11. There is a small electron withdrawing effect by resonance of the CF_3 group as illustrated below (delocalization of the negative charge over all three F's). This effect, though, is much smaller than the inductive effect. The ratio of the resonant effect to the inductive effect for the CF_3 group has been determined to be 0.29. Swain, C. G.; Lupton, Jr., E. C. *J. Am. Chem. Soc.* **1968**, *90*, 4328-4337.

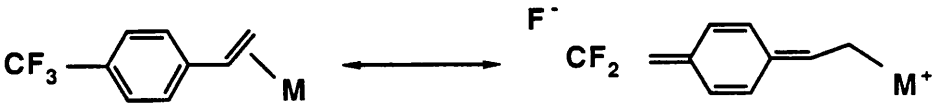

12. There is some transmission of resonance effects from the *meta*-position, with substituents such as OCH_3 and NMe_2. This effect is attributed to inductive transmission to the *meta*-position of the resonance perturbation at the *ortho*- and *para*- positions. Reference 3.

13. (a) Mayer, J. M.; Wolczanski, P. T.; Santarsiero, B. D.; Olson, W. A.; Bercaw, J. E. *Inorg. Chem.* **1983**, *22*, 1149-1155. (b) Messerle, L. W.; Jennische, P.; Schrock, R. R.; Stucky, G. *J. Am. Chem. Soc.* **1980**, *102*, 6744-6752. (c) Schultz, A. S.; Brown, R. K.; Williams, J. M.; Schrock, R. R. *J. Am. Chem. Soc.* **1981**, *103*, 169-176. (d) Gibson, V. C.; McDade, C.; Bercaw, J. E. submitted for publication in *Organometallics.*

14. Bartell, L. S.; Roth, E. A.; Hollowell, C. D.; Kuchitzu, K.; Young, J. E. *J. Chem. Phys.* **1965**, *42*, 2683-2686.

15. Ittel, S. D.; Ibers, J. A. *Adv. Organomet. Chem.* **1976**, *14*, 33-61.

16. For a description of the frontier molecular orbitals of bent metallocene complexes, see: Lauher, J. W.; Hoffmann, R. *J. Am. Chem. Soc.* **1976**, *98*, 1729.

17. Wilson, R. D.; Koetzle, T. F.; Hart, D. W.; Kvick, A.; Tipton, D. L.; Bau, R. *J. Am. Chem. Soc.* **1977**, *99*, 1775–1781.

18. (a) Guggenberger, L. J.; Tebbe, F. N. *J. Am. Chem. Soc.* **1971**, *93*, 5924–5925. (b) Guggenberger, L. J. *Inorg. Chem.* **1973**, *12*, 294–301.

19. Baldwin, J. E.; Kapecki, J. A. *J. Am. Chem. Soc.* **1970**, *92*, 4869-73.

22. Bell, R. A.; Cohen, S. A.; Doherty, N. M.; Threlkel, R. S.; Bercaw, J. E. *Organometallics* **1986**, *5*, 972-5.

21 Reference 8, Chapter 7.

CHAPTER II

Ethylene and Alkyne Insertion Reactions of Permethylscandocene Alkyl Complexes

INTRODUCTION

Olefin insertion into a metal-carbon bond has long been postulated as the mode of propagation in the Ziegler-Natta polymerization of ethylene and other olefins (the Cossee-Arlee mechanism)[1] (equation 1).

$$M\text{-}R + CH_2{=}CHR' \longrightarrow MCH_2CHRR' \qquad (1)$$

Recently, however, there has been a growing interest in demonstrating the validity of this assumption in light of the fact that there is little evidence for well characterized olefin alkyl metal complexes which undergo this insertion reaction.[2] An alternative mechanism for this requisite step in olefin polymerization, which has been postulated by Green and co–workers,[3] involves α-abstraction to form an alkylidene species (see Scheme I).

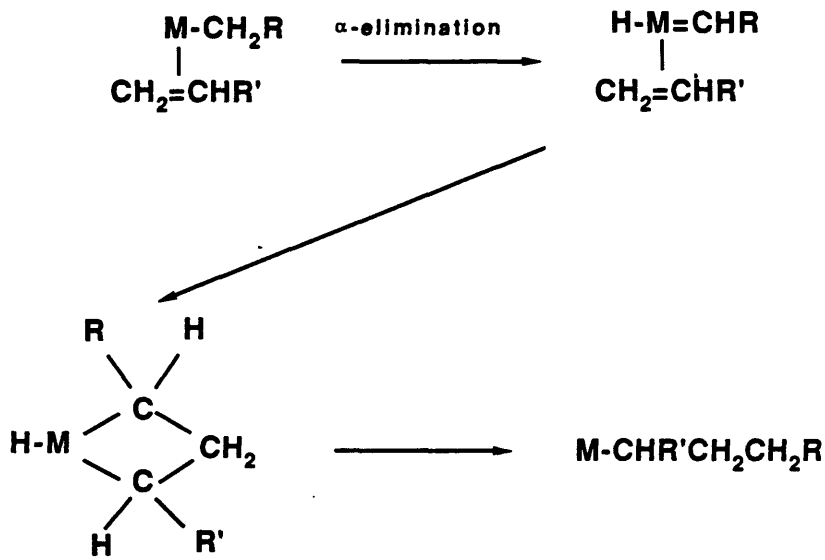

Scheme I. Green–Rooney Mechanism for Olefin Polymerization.

Organometallic chemists working on the subject of metal-catalyzed olefin polymerization have focused on at least two different issues. This first approach has been to provide evidence for the identity of the active species in the Ziegler-Natta (Cp_2TiCl_2-R_nAlCl_{3-n}) system. This has long been postulated as being a cationic Ti(IV) alkyl complex formed by an alkyl transfer reaction between a titanium salt and an aluminum alkyl.[4] The role of the aluminum alkyl cocatalyst has been suggested to be two-fold: alkylation of the titanium and weakening (possibly to the point of cleavage) of the titanium chloride bond (see 1 and 2, below).[5]

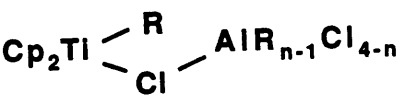

1

2

Recently, Eisch and co–workers reported[6] that treatment of titanocene dichloride and methylaluminum dichloride with a bulky internal alkyne, trimethyl(phenylethynyl) silane, afforded dicyclopentadienyl [E-2-methyl-2-phenyl-1-(trimethysilyl)ethenyl]titanium (IV) tetrachloroaluminate, the identity of which was confirmed by x-ray crystallography (equation 2). This highly substituted alkyne was chosen as a "surrogate" for ethylene to preclude against multiple insertions.

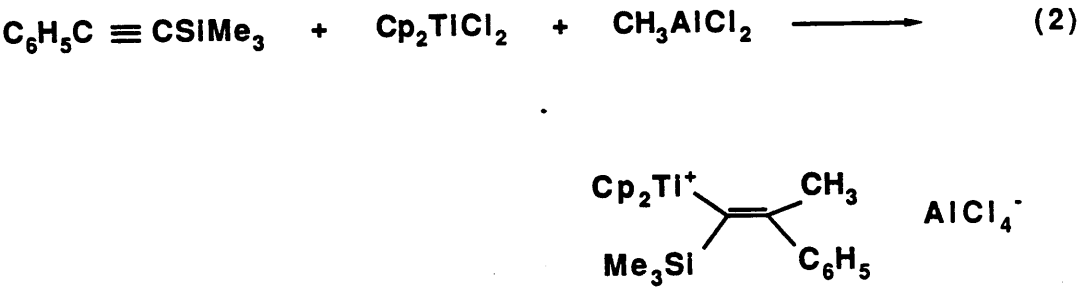

(2)

Product formation was presumed to proceed via regiospecific and *syn*-stereospecific insertion of the highly substituted alkyne into the Ti-C bond of $[Cp_2TiCH_3]^+[AlCl_4]^-$ which is in equilibrium with the aluminum alkyl adduct shown below. This equilibrium between **3** and **4** lies far to the left, preventing detection of **4** by spectroscopic means.

$$\underset{\mathbf{3}}{Cp_2TiCl_2 \bullet Cl_2AlCH_3} \rightleftharpoons \underset{\mathbf{4}}{Cp_2Ti^+\text{-}CH_3\ \ AlCl_4^-}$$

These findings were interpreted as good evidence that a titanium alkyl cation is the active species in the Ziegler- Natta system.

Along the same lines, Jordan and co–workers have reported[7] their efforts toward the preparation, characterization and delineation of reactivity patterns of cationic $[Cp_2M(IV)R]^+$ complexes. Cationic complexes have been prepared which are stabilized by the presence of coordinated Lewis bases. Specifically, $[Cp_2ZrCH_3(L)]^+[X]^-$ (L=THF, CH_3CN; X=BPh_4, PF_6) have been prepared as shown below (equations 3-5).

$$Cp_2Zr(CH_3)X + M[PF_6] \xrightarrow{CH_3CN} [Cp_2Zr(CH_3)(CH_3CN)][PF_6] + MX \qquad (3)$$

X=Cl, M=Ag; X=I, M=Tl

$$Cp_2Zr(CH_3)_2 + Ag[BPh_4] \longrightarrow [Cp_2Zr(CH_3)(CH_3CN)][BPh_4] + Ag^0 + 1/2\ C_2H_6 \qquad (4)$$

$$[Cp_2Zr(CH_3)(CH_3CN)][BPh_4] \xrightarrow{THF} [Cp_2Zr(CH_3)(THF)][BF_4] \qquad (5)$$

These complexes have been found to be active toward ethylene polymerization. The polymerization is inhibited by the presence of L (the complexes are unreactive toward ethylene in

THF solution), suggesting that the 14e$^-$ solvent free complex is the true polymerization catalyst. In accord, the cationic complexes show much higher activity when they are generated in the absence of donor ligands; their stability is, however, markedly decreased.

An alternate approach that has been taken in studying metal catalyzed olefin polymerizations is to address the issue of propagation. Well defined model systems and their reactivity toward olefins have been investigated in an attempt to discern between the Cossee-Arlman and Green-Rooney mechanisms for polymer propagation. About five years ago, Watson reported[8] that $Cp^*_2LuCH_3 \cdot OEt_2$ was an active ethylene polymerization and propylene oligomerization catalyst. No olefin adduct was observed prior to insertion (as expected for a d^0 metal center). In addition, the α-abstraction mechanism (Green-Rooney) can be ruled out in this oxidatively inert system. Similarly, Marks *et al.*[9] have prepared a series of lanthanide hydride dimers, $[Cp^*_2MH]_2$ (M = La, Nd, Lu) and have shown that these complexes are highly active toward the polymerization of ethylene.

Grubbs and co–workers[10] have investigated the kinetic isotope effect of ethylene polymerization in the Ziegler system in an attempt to differentiate between the two proposed modes of propagation. Since no kinetic isotope effect was observed ($k_H/k_D = 1$), the Green–Rooney mechanism was disfavored in that it involves α-hydrogen activation (and thus a primary kinetic isotope effect should be observed). In addition, the absence of a kinetic isotope effect on the stereochemistry of the Lewis acid catalyzed cyclization reaction of a series of complexes, $Cp_2Ti[CHD(CH_2)_nCH{=}CH_2]Cl$,[11] was taken as good evidence that α-hydrogens are not involved, again consistent with rate determining olefin insertion.

Recent efforts in our research group have focused on the synthesis and reactivity of permethylscandocene alkyl complexes, Cp^*_2ScR.[12] These complexes have been shown to react with olefins by two distinct routes (see Scheme II). Insertion of the olefin into the Sc–C bond (path a) occurs for all scandium alkyl and aryl complexes when the olefin is ethylene, and

for the scandium methyl complex when the olefin is propene (multiple insertions of ethylene are observed; a single insertion is observed with propene). For all other olefins, path b is preferred, in which "σ bond metathesis" to produce a scandium alkenyl complex and free alkane occurs.

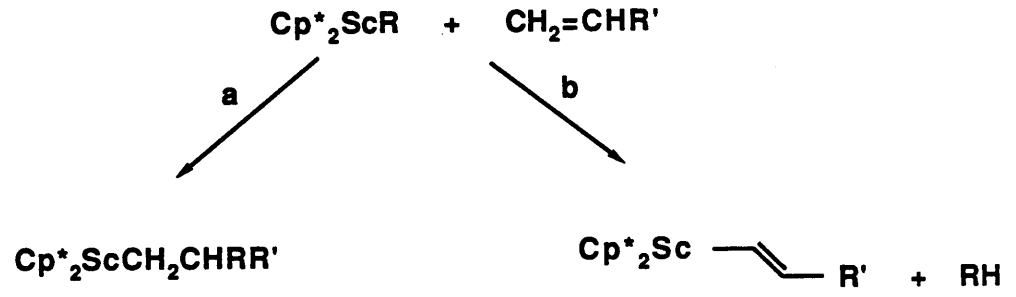

Scheme II. Reaction of Permethylscandocene Alkyl Complexes with Olefins (a: insertion; b: sigma bond metathesis).

From the examples listed above, it appears that the Cossee-Arlman mechanism is operative, at least for the electron deficient early transition metal, lanthanide and actinide systems.[13]

Efforts to gain insight into the mechanism of the actual olefin insertion step have in the past been met with limited success. This is in large part due to the fact that olefin insertion is quite fast (diffusion controlled, in most cases[14]), and unlike CO, which only undergoes a single insertion, most olefins undergo multiple insertions to form oligomers and polymers. It is known from previous studies that the rate of olefin insertion varies markedly with the nature of the olefin; that is, the more highly substituted the olefin, the less reactive (ethylene >> propene > 1-butene > 2-butene).[15] Little is known about the effect that the identity of the alkyl group (the migrating group) has on the rate of olefin insertion. A study aimed at elucidating the effect of the alkyl

group on olefin insertion rate would be of interest in contributing to an understanding of the mechanism of olefin insertion. Additionally it would have important implications in the molecular weight distributions of the polymers generated using different metal alkyl complexes as catalysts.

The permethylscandocene alkyl complexes previously reported can be prepared as monomers, free of any coordinating solvent. Additionally, they react with olefins in the absence of any Lewis acid cocatalysts. Consequently, these complexes are quite amenable to mechanistic studies and would serve as an ideal system with which to explore the mechanism of olefin insertion.

Selectively labeled (^{13}C) permethylscandocene alkyl complexes have been prepared and their rate of ethylene insertion measured by ^{13}C NMR. Kinetic measurements of the stoichiometric reaction of scandium alkyl complexes with internal alkynes were performed in an attempt to model a single insertion in the ethylene polymerization reaction. Herein we present the results of ethylene and alkyne insertion reactions of permethylscandocene alkyl complexes.

RESULTS AND DISCUSSION

Ethylene Insertion Reactions with Permethylscandocene Alkyl Complexes–Results.

The second order rate constants for ethylene insertion into the Sc-C bond of Cp^*_2ScR (R = CH_3, CH_2CH_3, $CH_2CH_2CH_3$) have been measured by ^{13}C NMR. ^{13}C NMR has been used extensively in the characterization of polyolefins due to its sensitivity to the position of a carbon atom in a hydrocarbon chain.[16] Although ^{13}C spectra of polymers and organometallic complexes are routinely obtained using the natural abundance of ^{13}C (1.1 %), acquisition times on the order of an hour (depending on sample concentration, number of equivalent nuclei, etc.) are usually required for high resolution spectra. In standard acquisitions, short pulse delays are utilized to achieve maximum signal to noise; all quantitative information (signal intensity as a measure of concentration) is lost, however. In order for quantitative information to be obtained from the spectra, the long carbon translational relaxation times (T_1) require that long pulse delays be employed to ensure adequate relaxation between pulses. Techniques which allow quantitative information to be obtained from ^{13}C NMR spectra have been developed.[17] These include the use of long pulse delays (PD > $5T_1$) or addition of paramagnetic relaxation agents (*e.g.* $Cr(acac)_3$) to ensure complete relaxation of the carbon nuclei and gated pulse sequences to eliminate NOE effects. Consequently, spectra obtained using these parameters, while containing valuable quantitative information, require very long acquisition times (usually on the order of a day) to obtain the same resolution obtained above with the short pulse delays. Therefore the use of quantitative ^{13}C NMR for kinetic measurements would be limited to reactions with very long half lives if samples with natural abundance ^{13}C are used. The use of ^{13}C–enriched samples was deemed necessary in this system so that spectra with adequate signal to noise could be obtained with a minimum number of acquisitions (and hence, kinetic measurements could be made on systems with much shorter reaction times).

The initial polymerization experiments were conducted using ^{13}C labeled ethylene and natural abundance (^{13}C) permethylscandocene alkyl complexes. In view of the complexity associated with the spectra obtained in this manner (see Figure I), an alternative approach was taken. The use of selectively labeled (^{13}C) scandium alkyl complexes and natural abundance ethylene (1.1 % ^{13}C) greatly simplified the spectra recorded. Under the experimental conditions employed, only one signal (or two in the case of the scandium ethyl complex, see below) for the alkyl ligand of each scandium complex in solution was observed. In both cases (Figures I and II), the resonances in the spectra were assigned by comparison with spectra recorded for each isolated scandium alkyl complex (see Table I). The selectively labeled (^{13}C) scandium alkyl complexes were prepared as shown below (equations 6-8); the syntheses of $Cp^*_2Sc^{13}CH_3$ and $Cp^*_2Sc^{13}CH_2{}^{13}CH_3$ have been previously reported.[12c]

$$Cp^*_2ScCl + {}^{13}CH_3Li \longrightarrow Cp^*_2Sc^{13}CH_3 \qquad (6)$$

$$Cp^*_2ScCH_3 \xrightarrow[-CH_4]{H_2} [Cp^*_2ScH] \xrightarrow{{}^{13}CH_2{}^{13}CH_2} Cp^*_2Sc^{13}CH_2{}^{13}CH_3 \qquad (7)$$

$$Cp^*_2ScCH_3 \xrightarrow[-CH_4]{H_2} [Cp^*_2ScH] \xrightarrow{CH_2CH^{13}CH_3} Cp^*_2ScCH_2CH_2{}^{13}CH_3 \qquad (8)$$

Kinetic measurements were carried out at –80(±1) °C under conditions of *ca.* 0.1 M scandium complex and 1-1.5 M ethylene in toluene-d_8 (see Experimental Section for details of sample preparation and spectra acquisition). Figure II shows a partial spectrum acquired during a kinetics run of $Cp^*_2Sc^{13}CH_3$ and C_2H_4. The resonance for the methyl ligand (δ 25.4) is considerably broadened (fwhh = 29 Hz, –80 °C) due to its proximity to the quadrupolar scandium nucleus (I = 7/2, 100% abundance, –0.22 barns[18]). The sharp singlets at δ 22.8 and δ 14.7 are assigned to the terminal carbons of the propyl and pentyl complexes, respectively (the signal for

the terminal carbon of longer chain alkyl complexes cannot be resolved from that of the pentyl complex, see Table I). The methyl groups on the Cp^* rings for the scandium alkyl complexes in solution are not resolved but rather appear as a single resonance at δ 11.5. The septet at δ 20.4 is due to the solvent ($C_6D_5CD_3$). Resonances due to unreacted ethylene, ferrocene (added as an internal standard) and the other solvent signals are not shown in this partial spectrum.

From each spectrum, the relative integrations of the two starting materials, $Cp^*_2Sc^{13}CH_3$ and C_2H_4, were determined. Since the ethylene reaction is not stoichiometric, standard techniques for obtaining second order rate constants do not apply.[19] Rather, data were plotted as for pseudo first order kinetics with a correction made at each data point to compensate for the decreasing concentration of ethylene in solution.[20] A representative kinetics plot ($\ln\{[ScR][C_2H_4]_t/[C_2H_4]_0\}$ vs. time) for the reaction of $Cp^*_2Sc^{13}CH_3$ and ethylene is shown in Figure III. From the slope an observed rate constant, k_{obs}, was obtained. The second order rate constant, k_2, could then be calculated: $k_2 = k_{obs}/[C_2H_4]_0$ where $[C_2H_4]_0$ represents the initial ethylene concentration.

Rate constants were obtained analogously for $Cp^*_2Sc^{13}CH_2{}^{13}CH_3$ and $Cp^*_2ScCH_2CH_2{}^{13}CH_3$; these data are contained in Table II. Attempts to obtain rate constants at different temperatures were unsuccessful; lower temperatures resulted in viscosity and solubility problems and reaction rates too fast for NMR measurement were observed at higher temperatures.

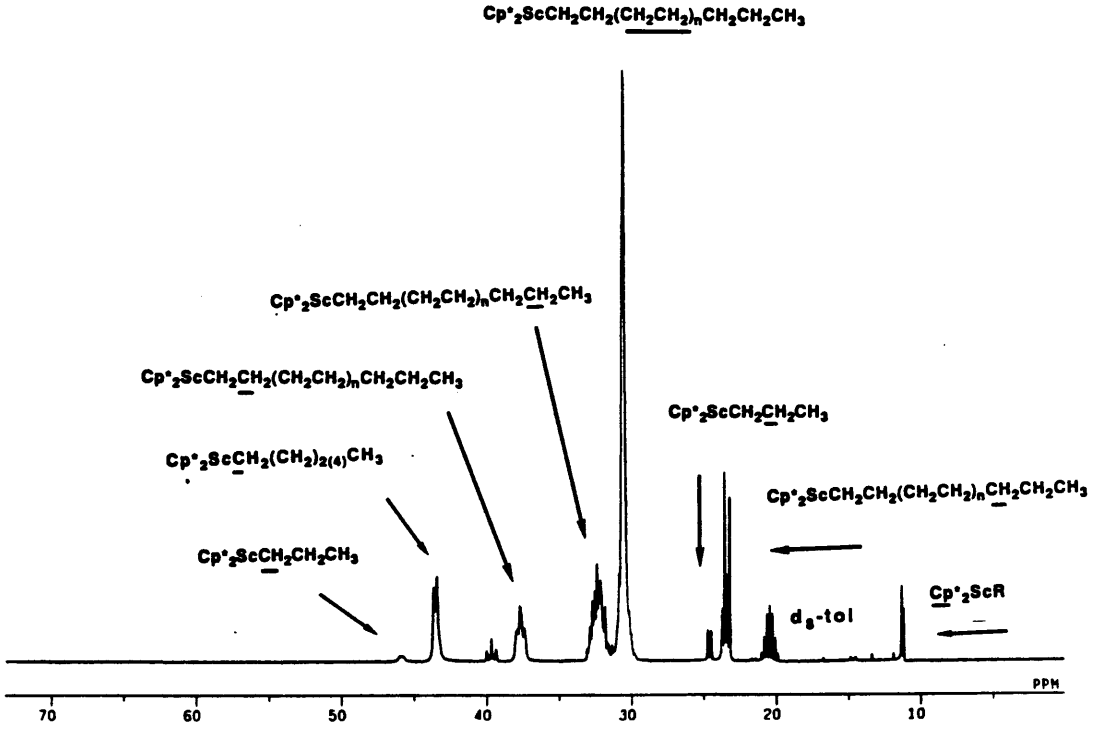

Figure I. Partial ^{13}C NMR Spectrum of the Reaction of $Cp^*_2ScCH_3$ with $^{13}CH_2=^{13}CH_2$ (d_8-tol, -50°C).

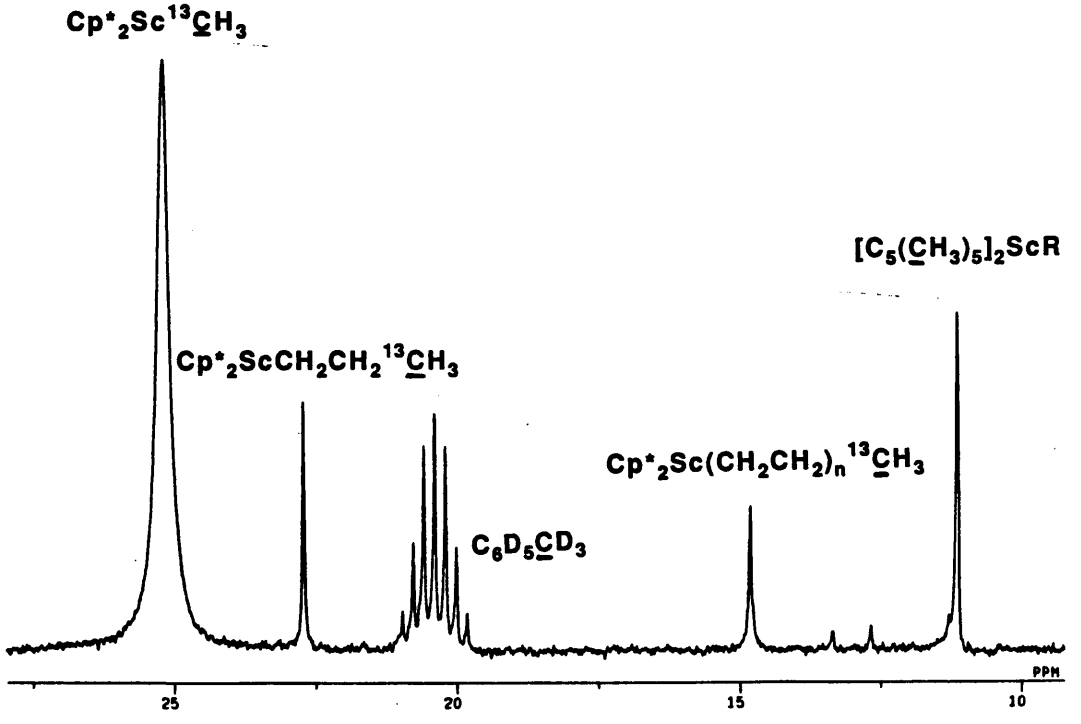

Figure II. Partial ^{13}C NMR Spectrum of a Polymerization Run of $Cp^*_2Sc^{13}CH_3$ and $CH_2=CH_2$ (d_8-tol, –80°C).

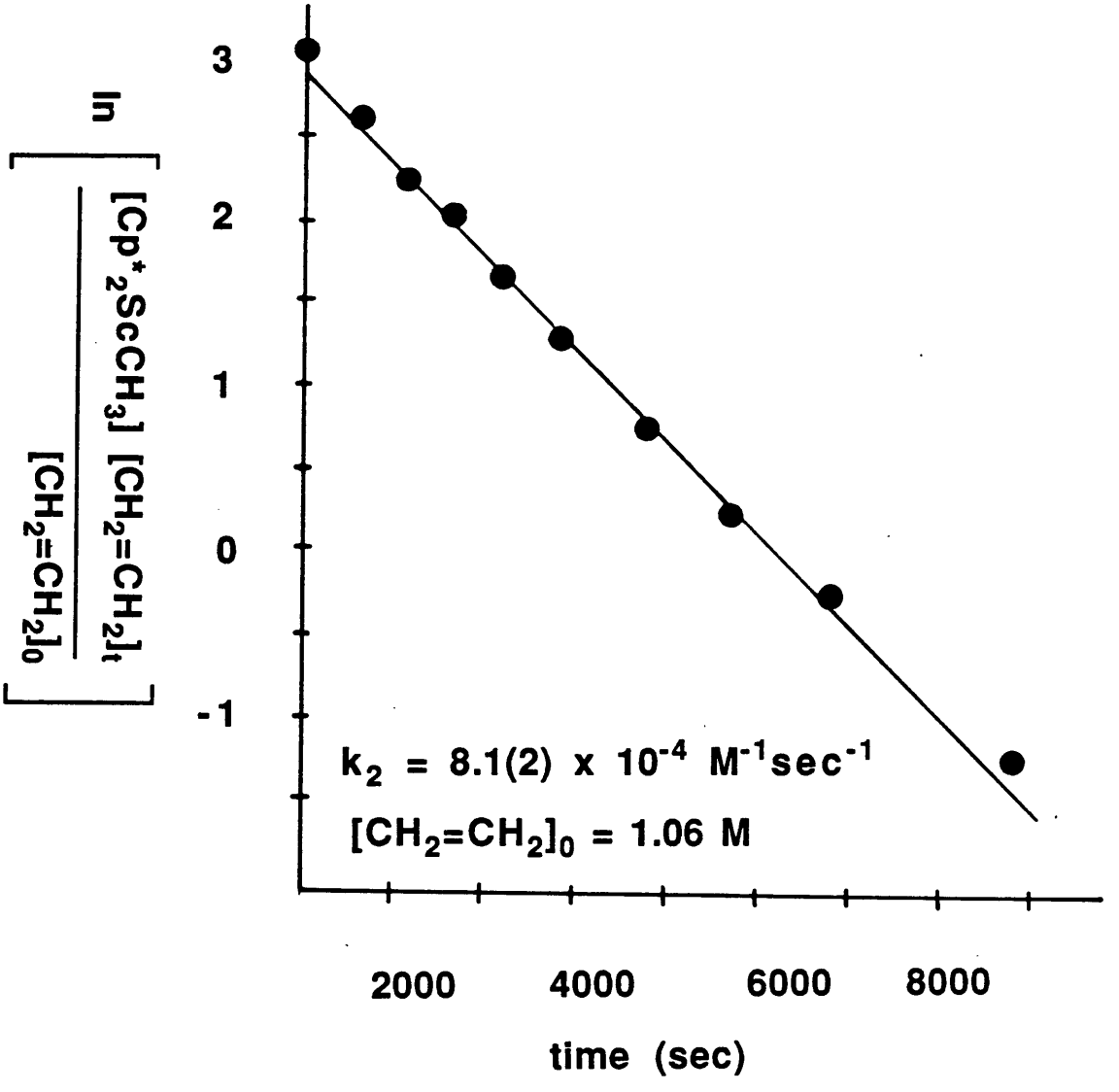

Figure III. Representative Kinetics Plot for the Reaction of $Cp^*_2Sc^{13}CH_3$ and $CH_2=CH_2$ (d_8-tol, −80°C).

Ethylene Insertion Reactions–Discussion.

The second order rate constants for ethylene insertion for Cp^*_2ScR (R = CH_3, CH_2CH_3, $CH_2CH_2CH_3$) have been measured and are listed in Table II. It is clear that the rate of ethylene insertion is dependent on the nature of the alkyl group bound to scandium. A relative ordering of the reaction rate of scandium alkyl complexes with ethylene is shown below.

(Sc-H >>) $Sc\text{-}CH_2CH_2CH_3 \approx Sc\text{-}CH_2CH_2CH_2CH_3 > Sc\text{-}CH_3 > ScCH_2CH_3$ (> ScC_6H_5)

The scandium hydride complex is the fastest to insert ethylene, too fast to measure by conventional NMR techniques. An NMR tube containing the scandium hydride complex and ethylene was prepared as described in the Experimental Section. The frozen tube was loaded into the precooled NMR probe at –80°C; all of the scandium hydride complex was however reacted by the time one spectrum (^1H NMR) was recorded. From this crude experiment, a lower limit of *ca.* 10^{-2} $M^{-1}sec^{-1}$ can be estimated for the reaction of the scandium hydride with ethylene.

The greater insertion rate for the scandium propyl complex over the scandium methyl can be understood in terms of thermodynamic considerations. A transition state wherein scandium–carbon bond breaking and making occur concertedly has been proposed for the insertion reactions (*vide infra*). Accordingly, the strength of the metal–carbon bond has a direct effect on the magnitude of the activation barrier; a stronger metal–carbon bond will result in a higher activation barrier (slower insertion rate). Although thermochemical measurements have not been obtained for the scandium alkyl bond strengths, data have been obtained for a related actinide system. Marks and co–workers have measured the metal-carbon bond strengths for a series of hydride, alkyl and aryl derivatives of permethylthorocene, $Cp^*_2ThR_2$.[21] Their results indicate that the Th-C bond strength in the methyl complex is stronger than in the longer chain alkyls $ThCH_2CH_3$ and $ThCH_2CH_2CH_2CH_3$. The difference in bond strengths is attributed to steric effects. This finding is in agreement with that reported for an iridium system,

$Ir[P(CH_3)_3]_2(CO)(I)R$.[22] Our experimental results substantiate initial observations which suggested that the scandium methyl complex inserts the first equivalent of ethylene slower than subsequent insertions.[23] Bond strength considerations undoubtedly are also behind the relative inactivity of the scandium phenyl complex toward ethylene.[24]

The observation that the scandium ethyl complex is the slowest to insert ethylene cannot be rationalized by metal-carbon bond strength considerations. An examination of its structure provides insight into the decreased reactivity toward ethylene (relative to the other alkyl complexes studied). Evidence has been accumulated which points to a β-agostic interaction in the ground state as shown below.

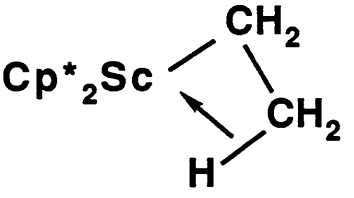

Although the ^{13}C and ^{1}H NMR were not diagnostic of a static agostic interaction,[25] the IR spectrum of **3** exhibits low energy C-H bands attributable to the agostic interaction. The crystal structure of **3** was attempted; severe disorder in the Cp^* rings precluded accurate resolution of the ethyl ligand. The best that can be said is that the location of the two carbons of the ethyl ligand (virtually equidistant from the scandium center) is not inconsistent with an agostic interaction.

A similar β-agostic interaction in the scandium propyl complex, although favorable electronically, would be discouraged sterically. Donation of electron density from one of the β-C-H bonds into an empty orbital on scandium requires that the bond be held in the equatorial plane. As such, the methyl group on the β-carbon would be directed toward one of the Cp^* rings (as

shown in A below). These unfavorable steric interactions for the propyl complex destabilize an agostic interaction and accordingly, the IR spectrum of the scandium propyl complex shows no low energy C-H bands indicative of structure A below.

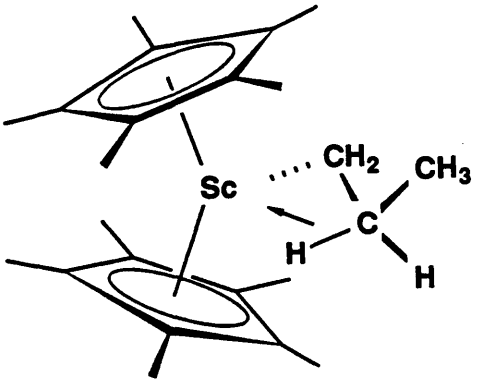

A

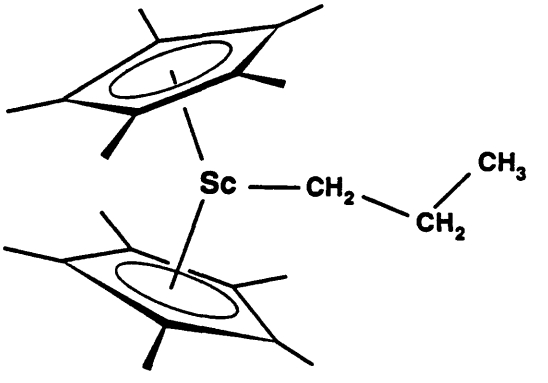

B

The investigation of complexes with agostic ground state structures has been focused primarily on the development of the methods of detection and towards a better understanding of when such an interaction will occur.[26] Little attention has been directed toward the effect that an agostic interaction has on the reactivity of the metal complex. Schmidt and Brookhart[2e] have proposed a correlation between an agostic β-hydrogen interaction in an olefin hydride complex and the propensity toward which the corresponding metal alkyl complex will undergo olefin alkyl migration. A series of complexes, $CpCo(L)(CH_2CH_2)H$, where L is a phosphine or phosphite ligand were shown to adopt agostic structures and to be active polymerization catalysts. The polymerization experiments were monitored by ^1H NMR and, notably, the products of ethylene insertion also contain bridging structures. Although rate constants were not obtained, it appears that the first insertion of ethylene is slower than subsequent insertions. These workers suggest that the same factors that favor a bridging over terminal hydride structure will facilitate alkyl migration (Figure IV).

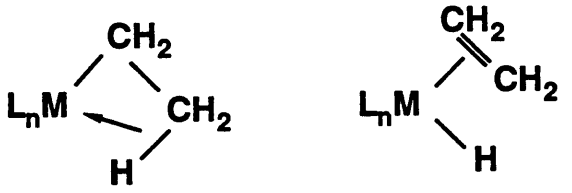

Figure IV.

The agostic interaction of the scandium ethyl complex results in a ground state stabilization relative to that of a 14e⁻ alkyl complex (*i.e.* $Cp^*_2ScCH_2CH_2CH_3$). In order for the complex to insert ethylene, this interaction must be broken.

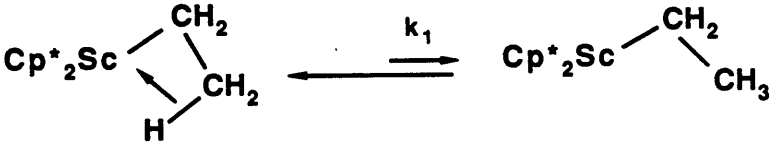

We propose that this dissociation energy (associated with k_1) results in an increased barrier toward ethylene insertion relative to the other alkyl complexes. Our results are not contradictory with Brookhart's but rather provide a further understanding of the factors that affect the rate at which a metal alkyl complex undergoes ethylene insertion. Our findings indicate that an alkyl complex which is coordinatively unsaturated will be even more reactive toward alkyl migration than one in which there is an agostic interaction (which Brookhart et al. have shown to be more reactive than a traditional olefin hydride) (Figure V).

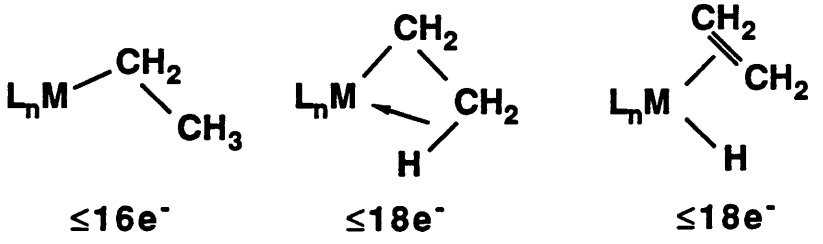

Figure V. **increasing olefin insertion**

Reaction of $Cp^*_2ScCH_3$ With Internal Alkynes–Results.

Previous studies[12b] have shown that $Cp^*_2ScCH_3$ reacts with 2-butyne to form the product of a single insertion, $Cp^*_2ScC(CH_3)=C(CH_3)_2$, **2** (equation 9).

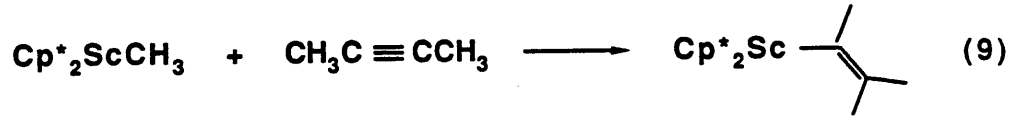

(9)

No further reaction is observed, even under excess butyne, high temperature and long reaction times (>35 equivalents, one day at 80° C). The kinetics for the formation of **2** can be followed conveniently by ^1H NMR (toluene-d_8) and serve as a model for a single insertion step in the polymerization of ethylene discussed previously. Pseudo first order kinetics were obtained which were linear over at least 2 half lives. Second order rate constants were obtained over the temperature range 245-265 K and are included in Table III. Activation parameters, derived from the Arrhenius plot shown in Figure VI, are listed below:

$$\Delta G^{\ddagger}(265\ K) = 18.95(1)\ kcal/mol$$

$$\Delta S^{\ddagger} = -36(2)\ eu$$

$$\Delta H^{\ddagger} = 9.7(3)\ kcal/mol$$

The insertion reaction described in equation 9 occurs for a variety of different internal alkynes. With unsymmetrical alkynes two products can arise, depending on the orientation of the alkyne (equation 10). Isomeric assignment of **A** and **B** were made by comparison with authentic samples (see Experimental Section).

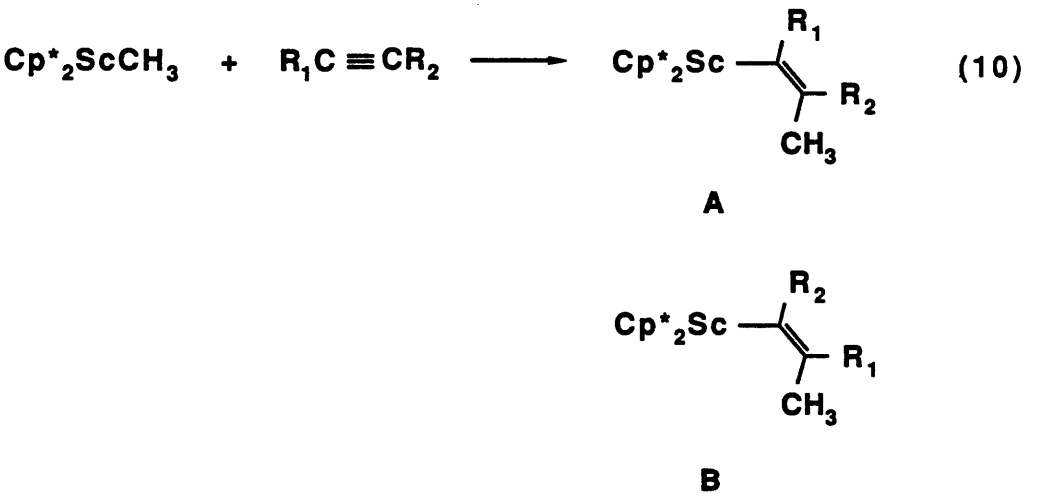

(10)

The kinetics for the formation of **A** and **B** were monitored as described above for the reaction of $Cp^*_2ScCH_3$ with 2-butyne; the rate constant obtained from the pseudo first order plots, k_{obs}, in these experiments is a sum of the rate constants for the formation of **A** and **B**: $k_{obs} = k_A + k_B$; the ratio of products obtained yields k_A/k_B.[27] Kinetic data obtained for the reactions shown in equation 10 are compiled in Table IV.

Alkyne Insertion Reactions–Discussion.

The stoichiometric reaction of $Cp^*_2ScCH_3$ with 2-butyne serves as a useful model for a single insertion step in the polymerization of ethylene. Second order rate constants have been measured for this reaction over a range of temperatures allowing the determination of activation parameters. This reaction is characterized by a modest enthalpy of activation ($\Delta H^{\ddagger}$ = 9.7(3) kcal/mol) and a very large negative entropy of activation ($\Delta S^{\ddagger}$ = -36(2) eu). These findings are consistent with a highly ordered four-centered transition state, illustrated below (Figure VI). In this transition state, scandium–carbon bond breaking and forming occur in concert. Although electronic effects have not been addressed in the insertion reactions, it is clear from this model that a stronger scandium–carbon bond would result in a decreased rate of insertion (*vide supra*).

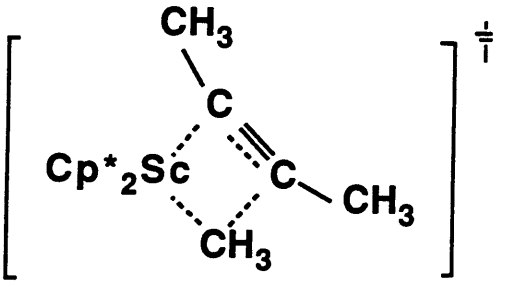

Figure IV. Proposed Transition State for Insertion of 2-Butyne with $Cp^*_2ScCH_3$.

The importance of steric effects in these insertion reactions is illustrated by the reactions of $Cp^*_2ScCH_3$ with unsymmetrical alkynes. From the isomeric mixures obtained with these reactions (see Table V), it is apparent that increasing the bulk on one end of the alkyne (relative to the other) serves to disfavor formation of the isomer in which the bulky substituent is geminal to the scandium center. Indeed, when the alkyne is 4-methyl-2-pentyne [$(CH_3)_2CHC{\equiv}CCH_3$], only

isomer, that with the isopropyl group directed away from the scandium is formed. Although electronic effects may play some role in determining product distribution,[28] these are presumably much smaller than the steric effects.

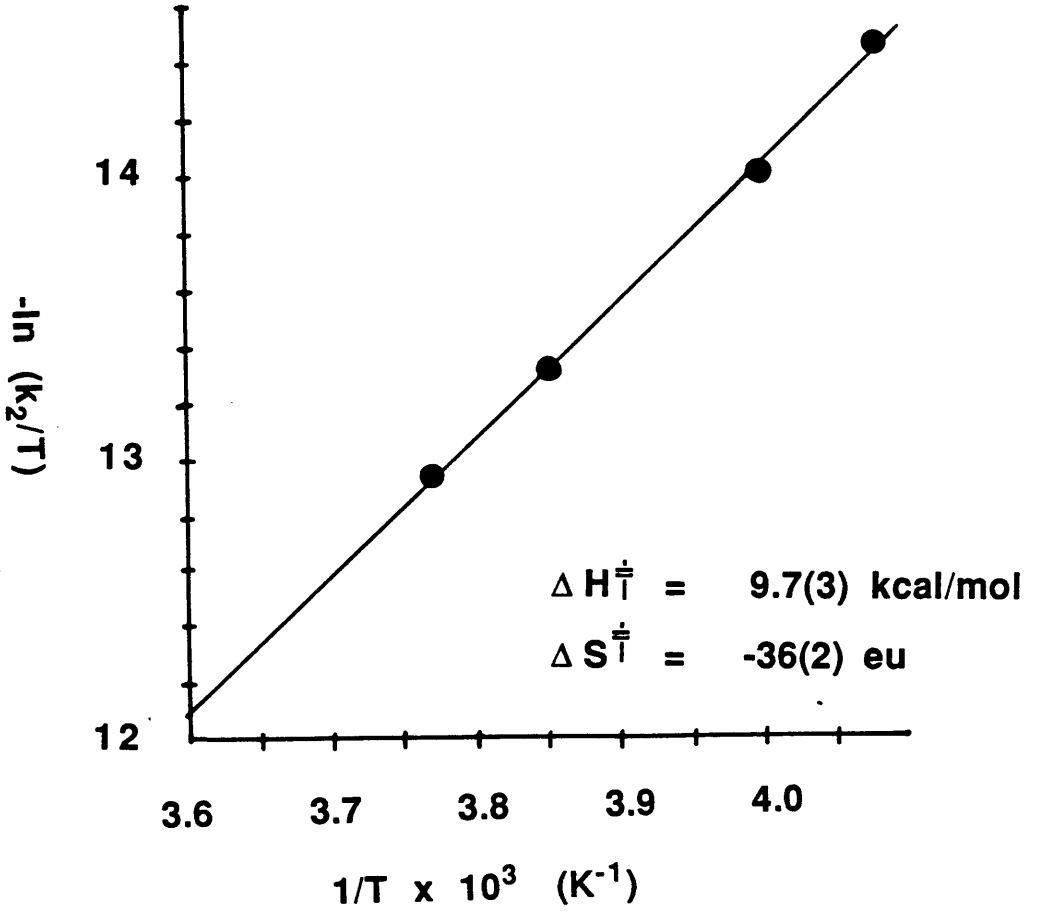

Figure VI. Eyring Plot for the Reaction of $Cp^*_2ScCH_3$ and 2-Butyne.

CONCLUSIONS

The rate of ethylene insertion into a series of permethylscandocene alkyl complexes has been measured by ^{13}C NMR. From this studies some knowledge of the influence of the migrating alkyl group on the rate of olefin insertion has been gained. A ground state stabilizing β-agostic interaction serves to retard the ethylene insertion rate over a coordinatively unsaturated alkyl complex. The metal-carbon strength affects the insertion rate; a stronger bond results in a slower rate of insertion. The results obtained for a single insertion of ethylene have implications in the area of catalyst design. One criterion for narrow molecular weight distribution in polymer synthesis is that chain initiation must be rapid (or at least as fast) compared to chain propagation. From these findings one would conclude that beginning the ethylene polymerization with a scandium alkyl complex where initial chain length has at least three carbons (propyl or longer) should lead to polyethylene with a narrow molecular weight distribution.

The stoichiometric reaction of $Cp^*_2ScCH_3$ with internal alkynes has been examined as a possible model for a single insertion in the ethylene polymerization reaction. A highly ordered four centered transition state has been proposed. Due to the highly congested coordination sphere of the scandium center, steric effects play a dominant role in the transition state of the insertion reaction.

Table I. ^{13}C NMR data for Cp^*_2ScR Complexes.[a]

R	Cp^*	α	β	γ	δ	ϵ	ζ
CH_3	118.92[c] 11.14[d]	25.36 br s J_{CH} = 111					
CH_2CH_3	116.78[c] 11.89[d]	36.86 t J_{CH} = 119	20.46 J_{CH} = 120				
$(CH_2)_2CH_3$	118.60[c] 11.19[d]	45.8 J_{CH} = 117	24.58	22.76			
$(CH_2)_3CH_3$[b]	119.29[c] 11.42[d]	43.43	30.70	34.74	14.49		
$(CH_2)_4CH_3$[b,e]	119.24[c] 11.43[d]	43.80	31.73	40.25	23.61	14.69	
$(CH_2)_5CH_3$[b,e]	119.27[c] 11.45[d]	43.96	32.99	32.08	37.70	23.71	14.68

[a] ^{13}C (100.25 MHz) NMR spectra were taken in d_8-toluene at −50 °C unless otherwise noted. Chemical shifts are reported in parts per million (δ) from tetramethylsilane referenced from solvent signal. Coupling constants ($J_{13C\text{-}1H}$) were obtained from a gated (^1H NOE enhanced) spectrum and are reported in hertz. Coupling constants for the α carbons were obtained from a sample in which the α carbon was isotopically enriched.
[b] Spectrum recorded in d_{12}-cyclohexane, ambient temperature.
[c] Resonance assigned to the $\underline{C}_5(CH_3)_5$ carbons.
[d] Resonance assigned to the $C_5(\underline{C}H_3)_5$ carbons.
[e] Assignment of the internal carbons (β,γ,δ) was made by comparison with published ^{13}C NMR data for alkanes.[29]

Table II. Second Order Rate Constants (k_2) for the Reaction of Ethylene with Cp^*_2Sc-R Complexes.[a]

R	k_2 (-80 °C) ($M^{-1}sec^{-1}$)
$^{13}CH_3$	$8.1(2) \times 10^{-4}$
$^{13}CH_2{}^{13}CH_3$	$4.4(2) \times 10^{-4}$
$CH_2CH_2{}^{13}CH_3$	$6.1(2) \times 10^{-3}$

[a]Rate constants were measured using a continuous accumulation stacking routine with sufficient duration allowed between pulses to enable quantitative information to be derived from relative integration of resonances of interest.

Table III. Second Order Rate Constants (k_2) for the Reaction of $Cp^*_2ScCH_3$ and 2-Butyne.[a]

T(K)	$k_2 \times 10^4$ ($M^{-1}sec^{-1}$)
245	1.28(3)
250	2.34(4)
260	4.31(8)
265	6.38(14)

[a]Butyne concentrations were measured using an internal standard (Cp_2Fe) of known concentration.

Table IV. Second Order Rate Constants (k_2) for the Reaction of $Cp^*_2ScCH_3$ and Unsymmetrical Alkynes (RC≡CR').[a]

R	R'	k_A(255 K) x 10^5 ($M^{-1}sec^{-1}$)	k_B(255 K) x 10^5 ($M^{-1}sec^{-1}$)	A:B
CH_3	CH_3	15(1)	15(1)	50:50
CH_3	CH_2CH_3	21(1)	10(1)	68:32
CH_3	C_6H_5	1.4(1)	0.91(1)	61:39
CH_3	$CH(CH_3)_2$	0.16(1)	—	100:0

[a]Products A and B are as shown in equation 10 (see text). The rate constants, k_A and k_B, are for the formation of A and B, respectively.

EXPERIMENTAL SECTION

General Considerations.

All air sensitive manipulations were carried out using glove box or high vacuum line techniques. Solvents were dried over $LiAlH_4$ or sodium benzophenone ketyl and stored over titanocene. Toluene-d_8 was dried over activated 4Å molecular sieves and stored over titanocene.

Argon, nitrogen and hydrogen were purified over MnO on vermiculite and activated molecular sieves. Ethylene (Matheson), propylene (Matheson), ^{13}C-C_2H_4 (99% isotopic purity, MSD Isotopes), ^{13}C-C_3-propylene (99% isotopic purity, MSD Isotopes) were purified by three cycles of freeze-pump-thaw at −196°C and then vacuum transferred at 25°C. ^{13}C-C_1-propylene was prepared by addition of acetaldehyde to ^{13}C-C_1-methylenetriphenylphosphorphorane.

All of the alkynes used in this study were purchased and dried over activated molecular sieves prior to use: 2-butyne (Aldrich), phenylpropyne (Aldrich), 2-pentyne (Wiley) and 4-methyl-2-pentyne (Wiley). Cp_2Fe, used as an internal standard for NMR tube kinetic experiments, was sublimed before use.

NMR spectra were recorded on Varian EM-390 (^1H, 90 MHz), JEOL FX90Q (^1H, 89.56 MHz; ^{13}C, 22.50 MHz) and JEOL GX400Q (^1H, 399.78 MHz; ^{13}C, 100.38 MHz) spectrometers. Infrared spectra were recorded on a Beckman 4240 spectrometer and reported in cm^{-1}. All elemental analyses were conducted by L. Henling of the Caltech Analytical Laboratory.

The synthesis of $Cp^*_2ScCH_3$, $Cp^*_2Sc^{13}CH_3$, and $Cp^*_2Sc^{13}CH_2{}^{13}CH_3$ have been reported previously.[12b,12c]

Ethylene Insertion Reactions: Sample Preparation.

A typical sample was prepared in a glove box by loading the Cp^*_2ScR complex (*ca.* 25 mg, 0.05 mmol) and 0.5 ml toluene-d_8 (containing a known amount of Cp_2Fe as an internal standard) into a sealable NMR tube which was then attached to a calibrated gas volume. The toluene solution was degassed at −78°C. Ethylene (*ca.* 0.5 mmol), was admitted to the gas volume and condensed into the NMR tube at −196°C. While keeping the tube at −196°C and open to the manifold, nitrogen (300 torr) was admitted to the system. The tube was then sealed at −196°C. Fully immersed in a dry ice/ diethyl ether bath (−100°C), the tube was sloshed to effect dissolution of the ethylene into the toluene solution. The solution was then refrozen at −196°C while the top half of the NMR tube was heated to thermally decompose any residual scandium complex on the walls of the tube.[30] Warming in the dry ice/ diethyl ether bath was required to affix the NMR tube spinner onto the tube; the tube was then returned to the −196°C dewar. The sample was loaded, frozen, into the precooled NMR probe.

Ethylene Insertion Reactions: Measurement of Rate Constants Using ^{13}C NMR.

The insertion rates of ethylene into the Sc-C bond of **2-4** were measured using ^{13}C NMR (100.13 MHz) on a JEOL GX400Q spectrometer. One pulse FT spectra were recorded automatically at preset time intervals by using a stack routine (with INIWT as the variable parameter). A listing of the parameters for this stack routine (AUTO01) is included in Appendix 1. A heteronuclear decoupled pulse (SGBCM) was employed with a delay between pulses (92 sec) of sufficient duration[31] to enable quantitative information to be derived from relative integration of resonances of interest.[32]

The free induction decays, measured as described above, were added together using an automated sequence employing the ADDBL command.[33] Listings of the programs used for this procedure (SUM.GLG and SUM.LNK) are also contained in Appendix 1. A series of fifteen

FID's were added together to produce a single spectrum; the average time for the spectrum was taken as that of the start of the accumulation of the eighth FID. By this process, approximately 35 data points could be collected from a two hour acquisition time.

The labeled resonance was integrated (relative to Cp_2Fe as an internal standard) along with the ethylene in solution. The observed rate constant was obtained from the slope of the plot of $\ln\{(Cp^*_2ScR/Cp_2Fe)[(C_2H_4)_t/(C_2H_4)_0]\}$ vs. time.

The temperature of the probe was measured after each kinetic run with a standard CH_3OH reference tube.

Kinetics of the Reaction of $Cp^*_2ScCH_3$ with 2-Butyne.

Sealed NMR tube samples were prepared by dissolving $Cp^*_2ScCH_3$ (*ca.* 25mg) in 0.5 ml d_8-tol stock solution (with a known concentration of Cp_2Fe) in a sealable NMR tube. The NMR tube was then attached to a calibrated gas volume. On the vacuum line, the tube was evacuated (at −78°C). 2-butyne (*ca.* 10-15 equivalents) was admitted to the gas bulb and condensed into the NMR tube at −196°C. The tube was sealed and stored at −196°C. The NMR probe was cooled to the desired temperature and the sample was placed in a dry ice/acetone (−78°C) slush to thaw the solution. Just prior to loading into the precooled probe, the tube was shaken several times to effect dissolution of the butyne. Approximately 20 spectra were recorded at regular intervals over the duration of 2-3 half lives. The temperature of the probe was measured after the experiment was over with a CH_3OH sample. Peak intensities of the Cp_2Fe, $Cp^*_2ScCH_3$ and 2-butyne were measured for each spectra. The observed rate constants (k_{obs}) were obtained from the slope of the plots of $\ln([Cp^*_2ScCH_3]/[Cp_2Fe])$ vs. time. Second order rate constants, k_2, were obtained by dividing the observed rate constants by the average concentration of butyne ($k_2 = k_{obs}/[\text{2-butyne}]_{ave}$). Activation parameters were obtained by measuring k_2 at four different temperatures. A plot of $\ln(k_2/T)$ vs. $1/T$ (T = temperature in degrees Kelvin) results in a slope of

$-\Delta H^{\ddagger}/R$ and an intercept of $[(\Delta S^{\ddagger}/R) + 23.76]$. Reported errors in the rate constants represent one standard deviation from the least squares fit of the experimental data. These errors were used in determining the uncertainty in the activation parameters.

Kinetics of $Cp^*_2ScCH_3$ with Unsymmetrial Alkynes.

Samples were prepared as above except that the sealable NMR tube was fitted with a rubber septum rather than a gas volume before removing from the glove box. The tube was cooled to −196°C and the alkyne added via syringe. The tube was then sealed and the NMR experiment was carried out as before for 2-butyne. With unsymmetrical alkynes, two isomeric products (A,B) are formed (see equation 10 for assignment of isomers); the Cp* peak intensities of the alkenyl complexes along with $Cp^*_2ScCH_3$ and Cp_2Fe were measured for each spectrum. A plot of $\ln([Cp^*_2ScCH_3]/[Cp_2Fe])$ vs. time again resulted in a k_{obs} which, when divided by the average concentration of alkyne, $[alkyne]_{ave}$, yielded k_2. The second order rate constant is a sum of two rate constants for the formation of the two isomeric products, $k_2 = k_a + k_b$; the ratio of products obtained yields k_a/k_b.

The isomeric products **A** and **B** were assigned by comparison with authentic samples. For example, in the reaction of $Cp^*_2ScCH_3$ and phenylpropyne, the two products formed are $Cp^*_2ScC(CH_3)=C(CH_3)(Ph)$, **A**, and $Cp^*_2ScC(Ph)=C(CH_3)_2$, **B**. Compound **B** was prepared independently in an NMR tube by the σ bond metathesis reaction of $Cp^*_2ScCH_3$ and $Ph(H)C=C(CH_3)_2$ (equation 11).

REFERENCES

1. (a) Cossee, P. *J. Catal.* **1964**, *3*, 80; (b) Arlman, E. J.; Cossee, P. *J. Catal.* **1964**, *3*, 99.

2. Evidence for olefin alkyl complexes that undergo this olefin insertion reaction has been put forth by: (a) Evitt, E. R.; Bergman, R. G. *J. Am. Chem. Soc.* **1980**, *102*, 7003-7011. (b) Evitt, E. R.; Bergman, R. G. *J. Am. Chem. Soc.* **1979**, *101*, 3973-3974. (c) Pardy, R. B. A. *J. Organomet. Chem.* **1981**, *216*, C29-C34. (d) Flood, T. C.; Bitler, S. P. *J. Am. Chem. Soc.* **1984**, *106*, 6076-6077. (e) Schmidt, G. F.; Brookhart, M. *J. Am. Chem. Soc.* 1985, *107*, 1443.

3. Ivin, K. J.; Rooney, J. J.; Stewart, C. D.; Green, M. L. H.; Mahtab, R. *J. Chem. Soc., Chem. Commun.* **1978**, 604-606.

4. (a) Long, W. P.; Breslow, D. S. *J. Am. Chem. Soc.* **1959**, *81*, 81. (b) Breslow, D. S.; Newburg, N. R. *J. Am. Chem. Soc.* **1960**, *82*, 1953.

5. Boor, J., Jr. *Ziegler-Natta Catalysts and Polymerization*; Academic Press: New York, New York, 1979, p. 670.

6. Eisch, J. J.; Piotrowski, A. M.; Brownstein, S. K.; Gabe, E. J.; Lee, F. L. *J. Am. Chem. Soc.* **1985**, *107*, 7219-7221.

7. (a) Jordan, R. F.; Dasher, W. E.; Echols, S. F. *J. Am. Chem. Soc.* **1986**, *108*, 1718-1719. (b) Jordan, R. F.; Bajgur, C. S.; Willett, R.; Scott, B. *J. Am. Chem. Soc.* **1986**, *108*, 7410-7411.

8. (a) Watson, P. L. *J. Am. Chem. Soc.* **1982**, *104*, 337-339. (b) Watson, P. L.; Roe, D. C. *J. Am. Chem. Soc.* **1982**, *104*, 6471-6473.

9. Jeske, G.; Lauke, H.; Mauermann, H.; Swepston, P. N.; Schumann, H.; Marks, T. J. *J. Am. Chem. Soc.* **1985**, *107*, 8091.

10. Soto, J.; Steigerwald, M. L.; Grubbs, R. H. *J. Am. Chem. Soc.* **1982**, *104*, 4479.

11. Clawson, L.; Soto, J.; Buchwald, S. L.; Steigerwald M. L.; Grubbs, R. H. *J. Am. Chem. Soc.* **1985**, *107*, 3377-3378.

12. (a) Thompson, M. E.; Bercaw, J. E. *Pure Appl. Chem.* **1984**, *56*, 1. (b) Thompson, M. E., Ph. D. Thesis, California Institute of Technology, **1985**. (c) Thompson, M. E.; Baxter, S. M.; Bulls, A. R.; Burger, B. J.; Nolan, M. C.; Santarsiero, B. D.; Schaefer, W. P.; Bercaw, J. E. *J. Am. Chem. Soc.* **1987**, *109*, 203-219.

13. For a system which appears to support the Green-Rooney mechanism for chain propagation, see: Turner, H. W.; Schrock, R. R. *J. Am. Chem. Soc.* **1982**, *104*, 2331-2333.

14. Gates, B. C.; Katzer, J. R.; Schuit, G. C. A. *Chemistry of Catalytic Processes*; McGraw-Hill: New York, 1979, p.150.

15. Collman, J. P.; Hegedus, L. S.; Norton, J. R.; Finke, R. G. *Principles and Applications of Organometallic Chemistry*; University Science Books: Mill Valley, California, 1987, p. 578.

16. For a good review on the use of ^{13}C NMR in polymer characterization, see: Randall, J. C. in *Polymer Characterization by NMR and ESR*; Woodward, A. E.; Bovey, F. A., Ed.; ACS Symposium Series 142; American Chemical Society: Washington, D. C., 1980; Chapter 6.

17. Shoolery, J. N. *Progr. NMR Spect.* **1977**, *11*, 79-93.

18. Becker, E. D. *High Resolution NMR*; Academic: New York, 1980; p. 282.

19. Moore, J.W.; Pearson, R.G. *Kinetics and Mechanism*; Wiley-Interscience: New York, N.Y., 1981, Chapter 8.

20. The correction factor applied to each data point is $[C_2H_4]_t/[C_2H_4]_0$, which accounts for the continuous disappearance of ethylene. For example, when the ethylene supply is 75% depleted, the rate of disappearance of Cp^*_2ScR is one quarter of the initial rate or the rate if the ethylene concentration could be held constant. Therefore the correction factor of 1/4 is included to yield an apparent pseudo first order reaction.

21. Bruno, J. W.; Marks, T. J.; Morss, L. R. *J. Am. Chem. Soc.* **1983**, *105*, 6824-6832.

22. Yoneda, G.; Blake, D. M. *Inorg. Chem.* **1981**, *20*, 67-71.

23. When $Cp^*_2ScCH_3$ was treated with three equivalents of ethylene at −78 °C and then slowly warmed to room temperature, the ethylene was consumed by less than half of the starting scandium complex, suggesting that the initial insertion was slower than subsequent insertions, see Reference 12b.

24. There was a slow reaction between Cp^*_2ScPh and C_2H_4 at room temperature, however the rate of this reaction was not quantified.

25. Coupling constants ($J_{C\alpha-H}$) for $Cp^*_2ScCH_2CH_3$ and $Cp^*_2ScCH_2CH_2CH_3$ were measured from the ^{13}C NMR spectra of isotopically enriched samples. Values of 122 and 117 Hz were obtained for the ethyl and propyl complexes, respectively. While the difference is small, the larger C_α coupling constant may reflect a smaller Sc-C_α-C_β angle relative to that found in the propyl complex.

26. (a) Brookhart, M.; Green, M. L. H. *J. Organomet. Chem.* **1983**, *250*, 395. (b) Lammanna, W.; Brookhart, M. *J. Am. Chem. Soc.* **1981**, *103*, 989. (c) Brookhart, M.; Lamanna, W.; Humphrey, M. B. *J. Am. Chem. Soc.* **1982**, *104*, 2117. (c) Brookhart, M.; Lamanna, W.; Pinhas, A. R. *Organometallics* **1983**, *2*, 638. (d) Dawoodi, Z.; Green, M. L. H.; Mtetwa, V. S. B.; Prout, K. *J. Chem. Soc., Chem. Commun.* **1982**, 802. (e) Dawoodi, Z.; Green, M. L. H.; Mtetwa, V. S. B.; Prout, K.; Schultz, A. J.; Williams, J. M.; Koetzle, T. F. *J. Chem. Soc., Dalton Trans.*, in press. (f) Berry, A.; Dawoodi, Z.; Derome, A. E.; Dickinson, J. M.; Downs, A. J.; Green, J. C.; Green, M. L. H.; Hare, P. M.; Payne, M. P.; Rankin, D. W. H.; Robertson, H. E. *J. Chem. Soc., Chem. Commun.*, in press.

27. Reference 19, p.22-25.

28. In Chapter III of this thesis, a transition state wherein there is development of positive charge on the β-carbon is proposed for the β-hydrogen elimination reaction. If similar electronic effects are operative in the insertion reaction, orienting the alkyne such that the more electron releasing substituent is *trans* to the scandium will be favored. Electronic effects on the insertion reaction were not, however, addressed in this study.

29. Grant, D. M.; Paul, E. G. *J. Am. Chem. Soc.* **1964**, *86*, 2984-2990.

30. Only the lower portion (*ca.* 25%) of the NMR tube is cooled with the variable temperature apparatus in the NMR tube. Thus, any residual scandium compound on the sides of the NMR tube is not cooled and draws the ethylene out of solution by rapidly polymerizing it. Heating the upper portion of the tube with a heat gun prior to the NMR experiment effects decomposition of any residual complex on the walls and alleviates this problem.

31. A pulse delay of greater than $10T_1$ was employed to ensure complete relaxation of all ^{13}C nuclei. Values for T_1 were measured using the inversion-recovery method and analyzed using the non-linear least squares method contained in the GXJEOL400 software.

32. The NOE enhancement is expected to be equivalent for all terminal methyl groups of permethylscandocene alkyl complexes. Therefore, a decoupled pulse was chosen to optimize S/N.

33. GXJEOL 400 Manual, Version GX-OPR2-3.

CHAPTER III

β-Elimination Reactions of Permethylscandocene Alkyl Complexes

INTRODUCTION

The decomposition of metal alkyl complexes containing β-hydrogens occurs primarily by β-hydrogen elimination to form a metal hydride and olefin (free or coordinated) (equation 1).[1]

$$MCH_2CH_2R \longrightarrow M\text{-}H + CH_2{=}CHR \qquad (1)$$

The facility of the above reaction is manifested by the fact that metal complexes with ligands containing β-hydrogens, in many instances, cannot be prepared or are of limited stability. There has been, however, considerable interest in studying the process of β-hydrogen elimination, from both a theoretical and an experimental approach.[2] This process is a requisite step in both olefin hydrogenation and hydroformylation and is a chain termination step in olefin polymerization. From the experimental studies to date, it has been learned that β-hydrogen elimination occurs on a single metal center. Both a vacant coordination site and a small M-C-C-H dihedral angle are required to permit transfer of the hydrogen from the alkyl group to the metal center. As a result, coordinatively saturated metal alkyl complexes containing β-hydrogens and complexes with unsuitable M-C-C-H dihedral angles (*e.g.* as in a metallocycle) in general are more resistant to β-hydrogen elimination.

As with the olefin insertion reactions described previously, the β-hydrogen elimination reaction often is not rate limiting. For example, with coordinatively saturated complexes, thermal extrusion of a ligand (to generate an open coordination site) generally requires higher temperatures than β-hydrogen transfer. Whitesides has reported[3] that there is no kinetic isotope effect ($k_H/k_D = 0.97$) on the decomposition of $(PPh_3)_2Pt(CH_2CH_2CH_2CH_3)_2$. This supports a rate determining phosphine dissociation step to form a three-coordinate complex, $(PPh_3)Pt(CH_2CH_2CH_2CH_3)_2$ which rapidly decomposes via β-hydrogen elimination and reductive elimination to form a mixture of 1-butene and butane (see Scheme I).

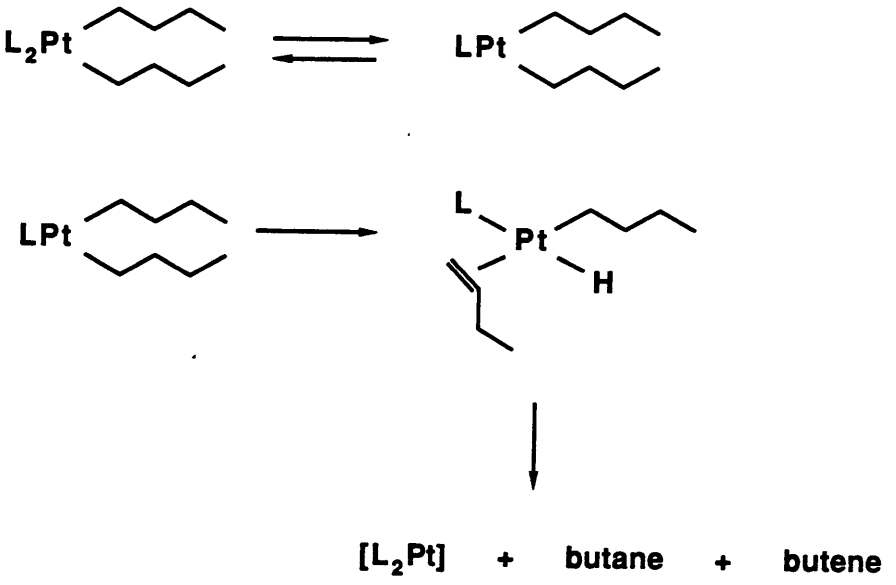

Scheme I. Decomposition of $(PPh_3)_2Pt(CH_2CH_2CH_2CH_3)_2$ (L=PPh_3).

One approach that has been taken to circumvent rate limiting formation of the coordinatively unsaturated species (thereby observing β-elimination directly) is to enact ligand extrusion by photochemical means. Wrighton[4] has studied the low temperature decomposition of $CpW(CO)_2CH_2CH_3$ generated by CO loss from $CpW(CO)_3CH_2CH_3$. Warming of the solution resulted in β-hydrogen elimination and isomerization to form *trans*-$CpW(CO)_2(CH_2{=}CH_2)H$. An upper limit of 10 kcal/mol was placed on the β-hydrogen elimination step. Rate determining isomerization, however, precluded the extraction of any further information regarding the elimination reaction. Due to the difficulties described with isolating the β-elimination reaction, there has been no systematic study done to date which has addressed the steric and electronic effects of this common metal alkyl decomposition route.

Previous efforts in our research group have been directed toward the synthesis and reactivity of permethylscandocene alkyl complexes.[5] Complexes with β-hydrogens have been prepared and appear to be moderately stable in solution. They are, however, coordinatively unsaturated, and as such, could decompose by formation of a scandium hydride complex and

liberation of an olefin (an olefin adduct of a d^0 metal center would not be expected to be stable). Although β-hydrogen elimination has been predicted to be thermodynamically unfavorable in d^0 and d^0f^n systems[6] (equation 2), it could be kinetically significant.

$$Cp^*_2ScCH_2CH_2R \rightleftharpoons Cp^*_2ScH + CH_2=CHR \qquad (2)$$

Indeed, evidence from our ethylene polymerization studies (Chapter 2) suggests that β-elimination is a major termination pathway for this reaction.[7]

A general route has been developed for the synthesis of scandium alkyl complexes which have β-hydrogens. By this method, a series of alkyl complexes of permethylscandocene, including a series of *para*–substituted phenethyl complexes, have been prepared in order to probe the steric and electronic factors of the β-hydrogen elimination reaction.

In contrast to the common occurrence of the β-hydrogen elimination reaction, there have only been a few examples reported in the literature of the decomposition of metal alkyl complexes by β-alkyl elimination (equation 3), the microscopic reverse of olefin insertion into a metal-carbon bond.

$$MCH_2CHRR' \longrightarrow M\text{-}R' + CH_2=CHR \qquad (3)$$

The paucity of examples of this reaction is undoubtedly due to the fact that metal alkyl complexes with β-hydrogens decompose primarily by β-hydrogen elimination. Metal alkyl complexes without β-hydrogens are often stable or decompose by other pathways including homolytic M-C bond cleavage and α or γ eliminations.[8] Thus, for β-alkyl elimination to occur for a complex which also contains β-hydrogens, the more favorable β-hydrogen must be reversible and/or

and/or discouraged. In addition, there should be a driving force for alkyl elimination such as release of strain energy associated with the alkyl ligand or removal of steric congestion around the metal center.

Watson has reported[9] that $Cp^*_2LuCH_2CH(CH_3)_2$ decomposes by competitive β-hydrogen and β-alkyl elimination (equation 4).

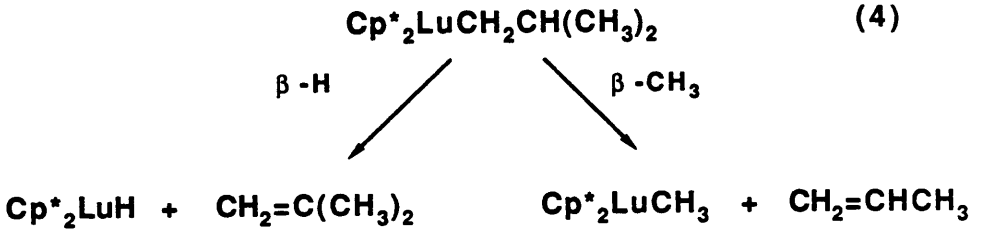

(4)

The kinetic scheme is not straightforward since the liberated propene and isobutene undergo insertion reactions with the lutetium alkyl and hydride complexes in solution. Nevertheless, a ratio of *ca.* 1:3 was obtained for the hydrogen and methyl elimination reactions, respectively. That β-alkyl elimination is more favorable is presumably due to steric congestion encountered in the transition state of β-hydrogen elimination (*vide infra*).

Flood has shown that β-alkyl elimination is the exclusive decomposition route for *trans*-$(PMe_3)_2PtCl(CH_2\overline{CCH_3CH_2CH_2CH_2})$ (equation 5).[10] Abstraction of the chloride ligand with $AgBF_4$ results in ring opening *via* β-alkyl elimination; rearrangement leads to a mixture of substituted allyl complexes.

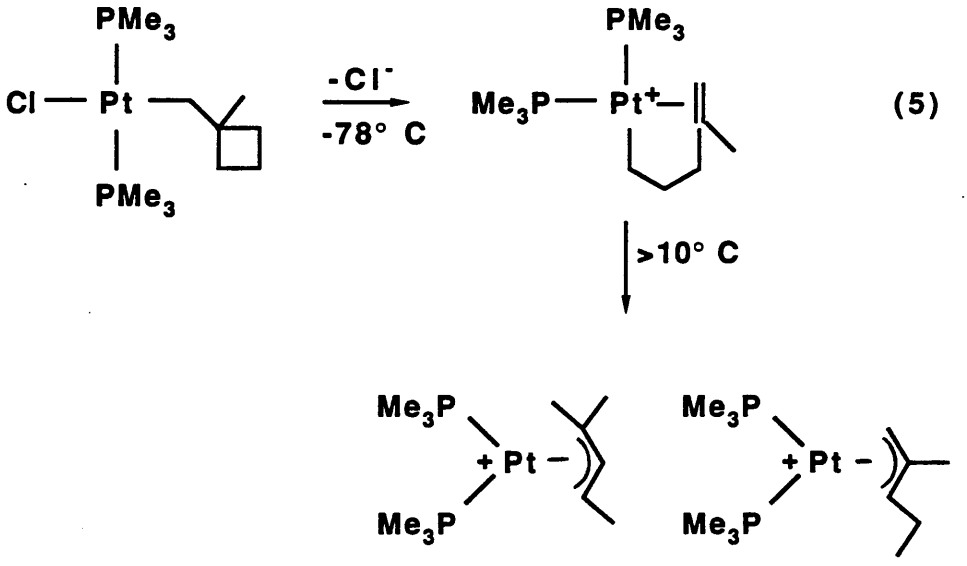

(5)

The alkyl ligand above was chosen for two particular reasons. First of all, all β-hydrogens were removed to prevent decomposition of the metal complex by the more favorable β-hydrogen elimination. Secondly, the alkyl group contains a four membered ring, the strain energy of which is removed upon β-alkyl elimination.

The cycloalkylmethyl complexes of permethylscandocene, $Cp^*_2ScCH_2CH(CH_2)_nCH_2$, provide an opportunity to investigate the β-alkyl elimination reaction. Specifically, the preference for β-alkyl over β-hydrogen elimination (equation 6) and the equilibrium between ring opening and cyclization (alkyl elimination *vs.* olefin insertion) (equation 7) was studied as a function of n (ring size). Expulsion of the olefin in the β-hydrogen and β-alkyl elimination has been shown, in the cases of $Cp^*_2LuCH_2CH(CH_3)_2$[9] and $Cp^*_2ScCH_2CH_3$,[11] to lead to competitive side reactions. In the proposed complexes, β-alkyl elimination results in the formation of a new alkyl complex with a pendent olefin. Tethering the olefin in this way simplifies reactivity patterns.

$$M\text{-}H + CH_2{=}CRR' \underset{}{\overset{k_1}{\longleftarrow}} MCH_2CHRR' \xrightarrow{k_2} M\text{-}R' + CH_2{=}CHR \qquad (6)$$

$$k_1/k_2 = ?$$

$$M\text{-}CH_2\overbrace{CH(CH_2)_nCH_2} \overset{K}{\rightleftharpoons} M\text{-}CH_2(CH_2)_nCH{=}CH_2 \qquad (7)$$

$$K = ?$$

Finally, we have begun to investigate the synthesis and decomposition routes of permethylscandocene alkyl complexes wherein the alkyl group contains a heteroatom (X) bonded to the β-carbon, $Cp^*_2ScCH_2CH_2X$ (X = halide, OR, PR_2, SiR_3). In general, there are few examples in the literature of metal alkyl complexes of this type due to rapid decomposition via expulsion of ethylene and formation of an M-X bond (equation 8).[12]

$$M\text{-}CH_2CH_2X \longrightarrow M\text{-}X + CH_2{=}CH_2 \qquad (8)$$

Herein, we present our results on the β-hydrogen, alkyl and X elimination of permethylscandocene alkyl complexes.

RESULTS AND DISCUSSION

β-Hydrogen Elimination of Permethylscandocene Alkyl Complexes.

While investigating the stoichiometric reactions of permethylscandocene alkyl complexes with internal alkynes,[5d] it was observed that no insertion took place for scandium alkyl complexes containing β-hydrogens (equation 9).

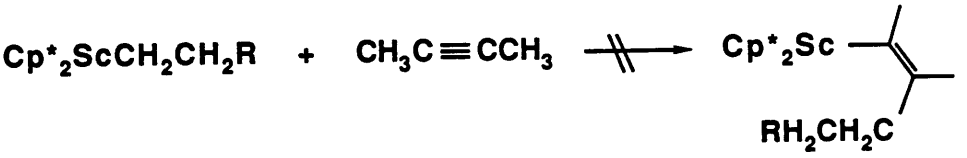

(9)

Rather, the products of this reaction were *cis*-$Cp^*_2Sc(CH_3)C{=}CH(CH_3)$, **1**, and free olefin, $CH_2{=}CHR$. These products are consistent with β-hydrogen elimination to form free olefin and Cp^*_2ScH, the latter of which is readily trapped by the alkyne in solution (equations 10 and 11).

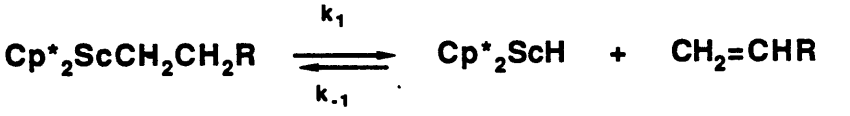

(10)

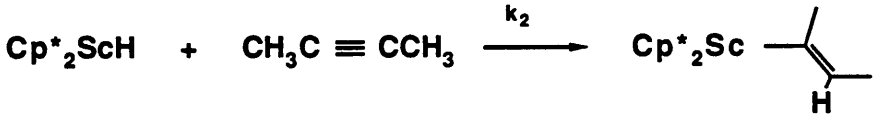

(11)

The synthesis of **1** from the reaction of $[Cp^*_2ScH]$ with 2-butyne has been reported.[5b] Further evidence that reversible β-hydrogen elimination occurs in solution is garnered from the observation of deuterium incorporation in the β-position when the scandium alkyl complex is dissolved in C_6D_6 (equation 12).[13] Deuterium incorporation likely proceeds via the reversible reaction of Cp^*_2ScH with C_6D_6. The reactions of Cp^*_2ScR with C_6D_6 have been previously investigated in our research group.[5c]

$$Cp^*_2ScCH_2CH_2R \xrightarrow[C_6D_6]{} Cp^*_2ScCH_2CHDR \qquad (12)$$

A series of permethylscandocene alkyl complexes have been prepared in order to probe the steric and electronic effects of the β-hydrogen elimination reaction. The complexes used in this study include the following: Cp^*_2ScR where R = CH_2CH_3 (2), $CH_2CH_2CH_3$ (3), $CH_2CH_2CH_2CH_3$ (4), $CH_2CH_2SiMe_3$ (5), $CH_2CH_2C_6H_5$ (6), $CH_2CH_2C_6H_4$-*p*-NMe_2 (7), $CH_2CH_2C_6H_4$-*p*-CF_3 (8), and $CH_2CH_2C_6H_4$-*p*-Me (9). The syntheses of the ethyl and propyl complexes have been previously reported;[5c] the syntheses of all the other complexes are described in the following section.

Synthesis and Characterization of Permethylscandocene Alkyl Complexes.

Treatment of a petroleum ether solution of $[Cp^*_2ScH]$[14] with one equivalent of the appropriate *para*–substituted styrene results in the formation of the phenethyl complexes, 6-9.

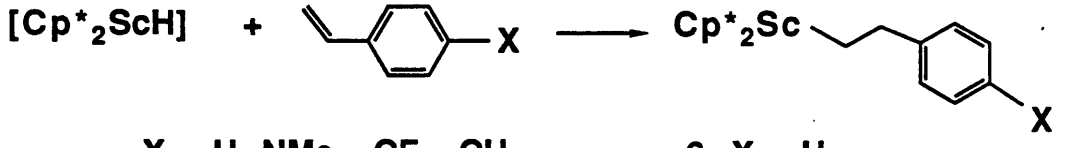

X = H, NMe_2, CF_3, CH_3

6 X = H

7 X = NMe_2

8 X = CF_3

9 X = CH_3

Concentration of the solution and cooling to –78 °C effected crystallization of the light yellow complexes. Owing to their high solubility, isolated yields ranged from 40-65%.

Attempts to prepare the *para*-methoxy derivative, $Cp^*_2ScCH_2CH_2C_6H_4$-*p*-OCH_3 were unsuccessful. Preparative reactions resulted in a dark orange oil from which no solid could be extracted; a ^1H NMR spectrum of an NMR tube reaction of equimolar amounts of Cp^*_2ScH and 4-vinylanisole (CH_2=CHC_6H_4-*p*-OCH_3) showed a multitude of Cp^*–containing products suggesting involvement of the methoxy group in this reaction.

Complexes **6-9** were characterized by ^1H and ^{13}C NMR and elemental analysis. The ^1H NMR spectra of **6-9** are all similar and each spectrum is characterized by a single Cp^* resonance, resonances attributable to the phenyl ring (and its *para*–substituent) and a pair of AA'BB' multiplets for the $ScCH_2CH_2R$ protons. Resonances for the hydrogens on the carbon bound to scandium (α) are characteristically shifted upfield (approximately δ 0.2 ppm) relative to aliphatic hydrogens, whereas the hydrogens on the β–carbon give rise to a multiplet at *ca.* δ 2.4.

$^{13}C\{^1H\}$ NMR spectra were obtained for complexes **6-9** using ^1H NOE enhancement techniques (see Table II). The spectra are not exceptional except that as a result of the quadrupolar nature of the scandium nucleus (I=7/2, 100% natural abundance) resonances for carbons bound to scandium are often difficult to observe either at room temperature or without isotopic enrichment. The resonance for the α carbon of complex **9**, however, was observed as a broad triplet (J_{CH} = 116.3 Hz) at δ 42.7. This chemical shift is similar to that observed for α carbons of other scandium alkyl complexes.[15] Signals for the β carbons were observed in all cases as triplets at *ca.* δ 36 ppm. The coupling constants, J_{CH}, were typically 118-122 Hz.

$Cp^*_2ScCH_2CH_2SiMe_3$ (**3**) and $Cp_2ScCH_2CH_2CH_2CH_3$ (**4**) were synthesized by an analogous method to that described above. A petroleum ether solution of $[Cp^*_2ScH]$ was treated with a stoichiometric amount of the appropriate olefin (equations 13 and 14). Owing to their high solubility, complexes **3** and **4** could not be isolated by cold filtration but rather were obtained as powders after removal of all volatiles from the reaction mixture. Characterization of these complexes was accomplished by ^1H and ^{13}C NMR (see Tables I and II).

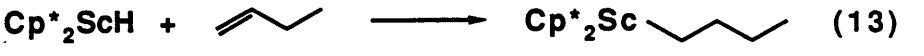

(13)

$$Cp^*_2ScH + CH_2{=}CHSiMe_3 \longrightarrow Cp^*_2ScCH_2CH_2SiMe_3 \quad (14)$$

β-Hydrogen Elimination Rate–Kinetic Measurements.

The observed rate constants for the reaction of $Cp^*_2ScCH_2CH_2Ph$ with 2-butyne (toluene-d_8, ^1H NMR, 280 K) were found to be independent of butyne concentration (over the range 0.46-3.0 M). The observed rate constants along with the measured butyne concentration are given in Table III.

From equations 10 and 11, the rate expression shown below can be written for the reaction of $Cp^*_2ScCH_2CH_2R$ with 2-butyne.

$$\frac{d[Cp^*_2ScCH_2CH_2R]}{dt} = k_{obs}[Cp^*_2ScCH_2CH_2R]$$

$$\text{where} \quad k_{obs} = k_1\left[1 - \frac{k_{-1}[CH_2{=}CHR]}{k_{-1}[CH_2{=}CHR] + k_2[CH_3C{\equiv}CCH_3]}\right]$$

The insensitivity of the observed rate constant to butyne concentration (in the range specified above) indicates that the second term in the above expression can be neglected; that is, $k_{obs} \approx k_1$. From this result, it is clear that the β-hydrogen elimination rate of a scandium alkyl complex can be measured by observing the rate of its reaction with 2-butyne.

Rate constants for the β-hydrogen elimination rate of complexes **2-9** were measured as described above. A representative kinetics plot for the reaction of $Cp^*_2ScCH_2CH_2CH_2CH_3$ with 2-butyne is shown in Figure I. The first order rate constants (k_1) and free energies of activation ($\Delta G^{\ddagger}$) at 290 K are listed for each complex in Table IV. A complete listing of all rate constants measured is given in Table V. Activation parameters for the decomposition of $Cp^*_2ScCH_2CH_2C_6H_5$ and $Cp^*_2ScCH_2CH_2C_6H_4$-*p*-CH_3, derived from Eyring plots are listed below.

Complex	$Cp^*_2ScCH_2CH_2Ph$	$Cp^*_2ScCH_2CH_2Ph$-*p*-CH_3
$\Delta G^{\ddagger}$(280 K)	21.19(8) kcal/mol	20.82(8) kcal/mol
$\Delta S^{\ddagger}$	−11(2) eu	−10(1) eu
$\Delta H^{\ddagger}$	17.98(44) kcal/mol	18.04(28) kcal/mol

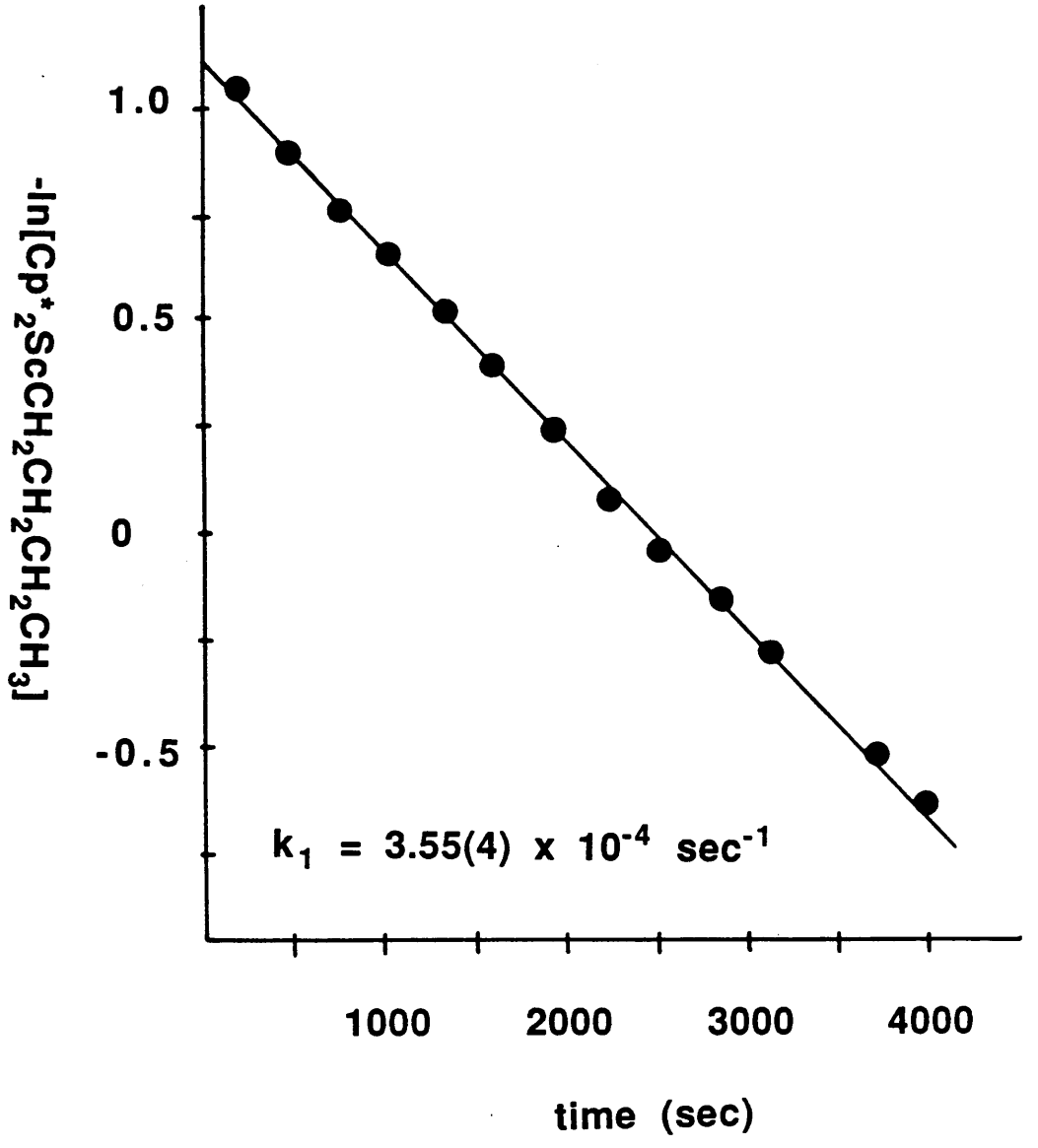

Figure I. Kinetics Plot of the Reaction of $Cp^*_2ScCH_2CH_2CH_2CH_3$ with 2-butyne (d_8-tol, 2 °C, 1.11 M 2-butyne).

Deuterium Kinetic Isotope Effect on the β-Hydrogen Elimination.

The deuterium kinetic isotope effect on the β-hydrogen elimination rate was measured for $Cp^*_2ScCH_2CHDC_6H_5$, **6-β-d_1**. Complex **6-β-d_1** was prepared by adding one equivalent of styrene to a petroleum ether solution of $[Cp^*_2ScD]$ (equation 15).

$$Cp^*_2ScCH_3 \xrightarrow{D_2} [Cp^*_2ScD] \xrightarrow{CH_2CHPh} \underset{\textbf{6-}\beta\textbf{-}d_1}{Cp^*_2ScCH_2CHDPh} \quad (15)$$

High field NMR (^2H, ^1H) showed conclusively that the deuterium was located solely in the β position and that incorporation was greater than 95%.

Treatment of **6-β-d_1** with excess 2-butyne in C_6D_6 at room temperature afforded a mixture of products (equation 16).

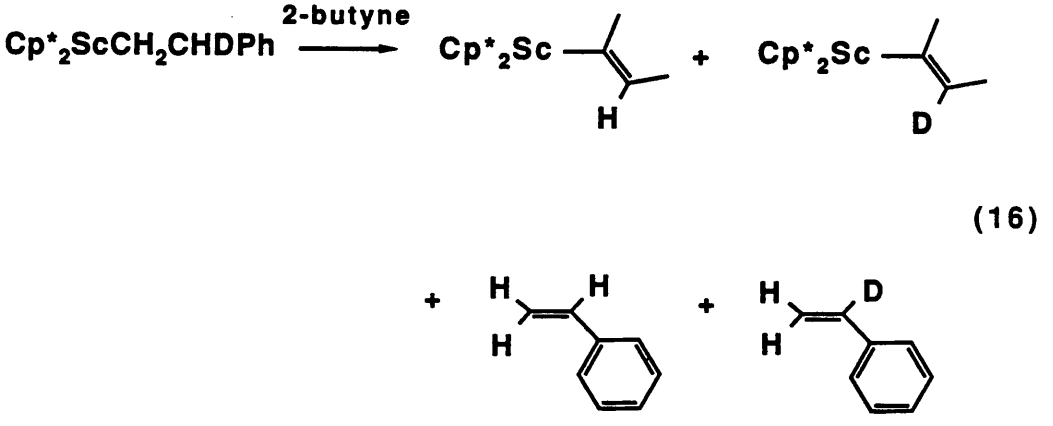

(16)

The ratio of $CH_2{=}CHC_6H_5$ to $CH_2{=}CDC_6H_5$ was determined by cutting and weighing the peaks corresponding to the hydrogen *cis* to the phenyl group from the ^1H NMR spectrum (400 MHz). A deuterium kinetic isotope effect (k_H/k_D) of 2.0(3) was obtained from the ratio of d_1- to d_0-styrene.

β-Hydrogen Elimination–Discussion.

The β-hydrogen elimination rate for a series of permethylscandocene alkyl complexes has been measured by trapping kinetics. From the data given in Table IV, it is clear that the β-hydrogen elimination rate is sensitive to the nature of the substituent(s) on the β carbon. Substitution of a hydrogen at the β-carbon by an alkyl group (CH_3 or CH_2CH_3), or a phenyl group caused a modest increase in the β-hydrogen elimination rate. Thes relative order R = H > Ph > CH_2CH_3 > CH_3 for $Cp^*_2ScCH_2CH_2R$ can be rationalized by a transition state wherein there is a partial positive charge on the β-carbon. The alkyl groups are inductively electron releasing relative to hydrogen[16] and thus stabilize the proposed transition state. A phenyl group, while electron releasing by resonance, is inductively electron withdrawing. That the phenethyl complex is slightly more resistant to the β-hydrogen elimination than the ethyl complex might suggest that the electronic effect of the phenyl group is largely inductive in nature (*vide infra*). Substitution of a hydrogen at the β-carbon by a trimethylsilyl group resulted in a dramatic decrease in the rate of β-hydrogen elimination. Again, consistent with the model proposed above, due to its electropositivity silicon destabilizes positive charge on the adjacent carbon. Undoubtedly, sterics also contribute to this large activation for β-hydrogen elimination of $Cp^*_2ScCH_2CH_2SiMe_3$ (*vide infra*).

In an attempt to focus on electronic effects, the β-hydrogen elimination rates for a series of *para*-substituted permethylscandocene phenethyl complexes were measured. Electronic effects can be transmitted from the substituent to the β carbon through the polarizable arene π cloud. The data shown in Table IV for these complexes can be understood in terms of the model described above. That is, an electron withdrawing substituent (CF_3) in the *para* position serves to retard the β-hydrogen elimination rate (relative to H). In contrast, an electron donating substituent (CH_3 or NMe_2) facilitates this decomposition reaction. These data can be used to construct a Hammett Plot (log k vs. σ_p)[16,17] which is shown in Figure II. The data give a good

linear correlation with σ_p (R = 0.9967) with a slope (ρ) of −1.87(11). These data correlate better with σ_p than σ_+ (R = 0.9653 for log k_1 vs σ_+), indicating that direct resonance between the phenyl ring and the β-carbon in the transition state is not maximized. A possible explanation for this result is that as the hydrogen is transferred from the β-carbon to the scandium center, the phenyl group is twisted out of resonance with the β carbon to avoid steric interactions with the Cp^* rings. Similar arguments have been used to explain the correlation of the olefin insertion rate with σ_p for a series of *para*-substituted styrene hydride complexes of permethylniobocene previously studied in our research group.[18]

The slightly faster decomposition rate of the propyl complex over that of the butyl complex further suggests that steric factors are operative in the transition state. As the hydrogen is transferred to the metal, the α- and β-carbons rehybridize from sp^3 to sp^2, causing the substituents on the β-carbon to be directed toward the Cp^* rings. As such, the steric bulk of the substituent on the β-carbon will have a direct effect on the magnitude of the activation barrier for hydrogen transfer. Consequently, the butyl complex with a larger ethyl group on the β–carbon has a greater activation barrier and slower β-hydrogen elimination rate than the propyl complex. In accord, the analogous scandium β-trimethylsilylethyl complex undergoes very slow β-hydrogen elimination and the scandium cyclopentylmethyl complex does not decompose *via* β-hydrogen elimination (*vide infra*). This reasoning implies that hydrogen transfer precedes Sc-C_α bond breaking. The results from this study are in contrast with those seen for pseudo-octahedral cobalt complexes [Co(acac)R_2L_2] (L = PR_3),[19] and alkylcobalamins[20] and the organocopper(I) compounds, L_nCuR (L = PPh_3).[21] For these complexes, steric bulk in the alkyl group appears to accelerate the β-hydrogen elimination rate. In addition, the β-elimination reactions for these complexes exhibit similar activation parameters to other processes involving homolytic metal carbon bond scission. These observations have been taken as good evidence that metal-carbon bond rupture occurs concurrently with hydrogen transfer.

The β-hydrogen elimination rates for $Cp^*_2ScCH_2CH_2Ph$ and $Cp^*_2ScCH_2CH_2Ph$-*p*-CH_3 were measured over a range of temperatures, allowing activation parameters to be determined. These reactions are characterized by small, negative entropies of activation (–11(2) and –10(1) eu, respectively) consistent with the four centered transition state proposed above. A similar value has been obtained for the gas phase β-hydrogen elimination of $[(CH_3)_2CHCH_2]_3Al$.[22] Egger interpreted the gas phase results in terms of a reasonably tight four centered transition state with restricted rotation around the Al-C, C-C and C-H bond.

A kinetic isotope effect of 2.0(3) was measured for the β-hydrogen elimination of $Cp^*_2ScCH_2CHYC_6H_5$ (Y = H,D). This value is in accord with that observed in other systems wherein hydrogen transfer is rate determining.[23]

From the results described above, a detailed understanding of the transition state for β-hydrogen elimination of permethylscandocene alkyl complexes has been achieved. The proposed transition state is four centered with a partial positive charge on the β-carbon. The hydrogen is transferred in the transition state from the β-carbon to the electrophilic scandium center as H^-.

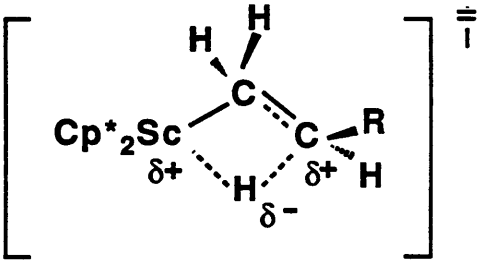

The electronic effects observed in the *para*-substituted phenethyl complexes are primarily inductive in nature, suggesting that the phenyl group is not in resonance with the β-carbon during

the hydrogen transfer step. In addition, steric considerations suggests that Sc-C_α bond rupture follows hydrogen transfer.

A curious result from this study is the relative ordering of the scandium ethyl and propyl complexes. As described previously (Chapter II), evidence points to the existence of a β-agostic interaction in the ground state structure of the ethyl complex (*and* no such interaction in the propyl complex). Since agostic interactions have been viewed as "arrested transition states" for hydride olefin insertion (and by microscopic reversibility, β-hydrogen elimination),[26e] it was somewhat surprising that the ethyl complex is more resistant to β-hydrogen elimination than the propyl complex. The larger relative activation barrier for the ethyl complex undoubtedly arises from a ground state stabilization attributed to the agostic interaction and a transition state destabilization due to the inability to delocalize the positive charge away from the β-carbon. This reasoning can be used to construct *qualitative* partial free energy surfaces for the β-hydrogen elimination of $Cp^*_2ScCH_2CH_3$ and $Cp^*_2ScCH_2CH_2CH_3$, which are shown in Figure III.

Although the activation barriers can be determined for the β-hydrogen elimination, the alkyl complexes cannot be placed on the same energy surface. Attempts to obtain ground state energies by equilibration methods[24] were not successful; competing σ bond metathesis reactions such as that shown below (equation 17) interfered with the measurement of equilibrium constants.

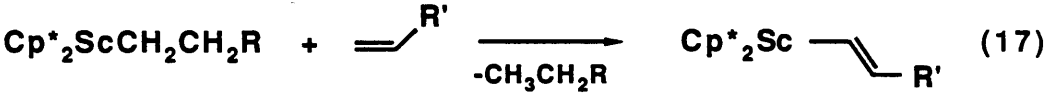

(17)

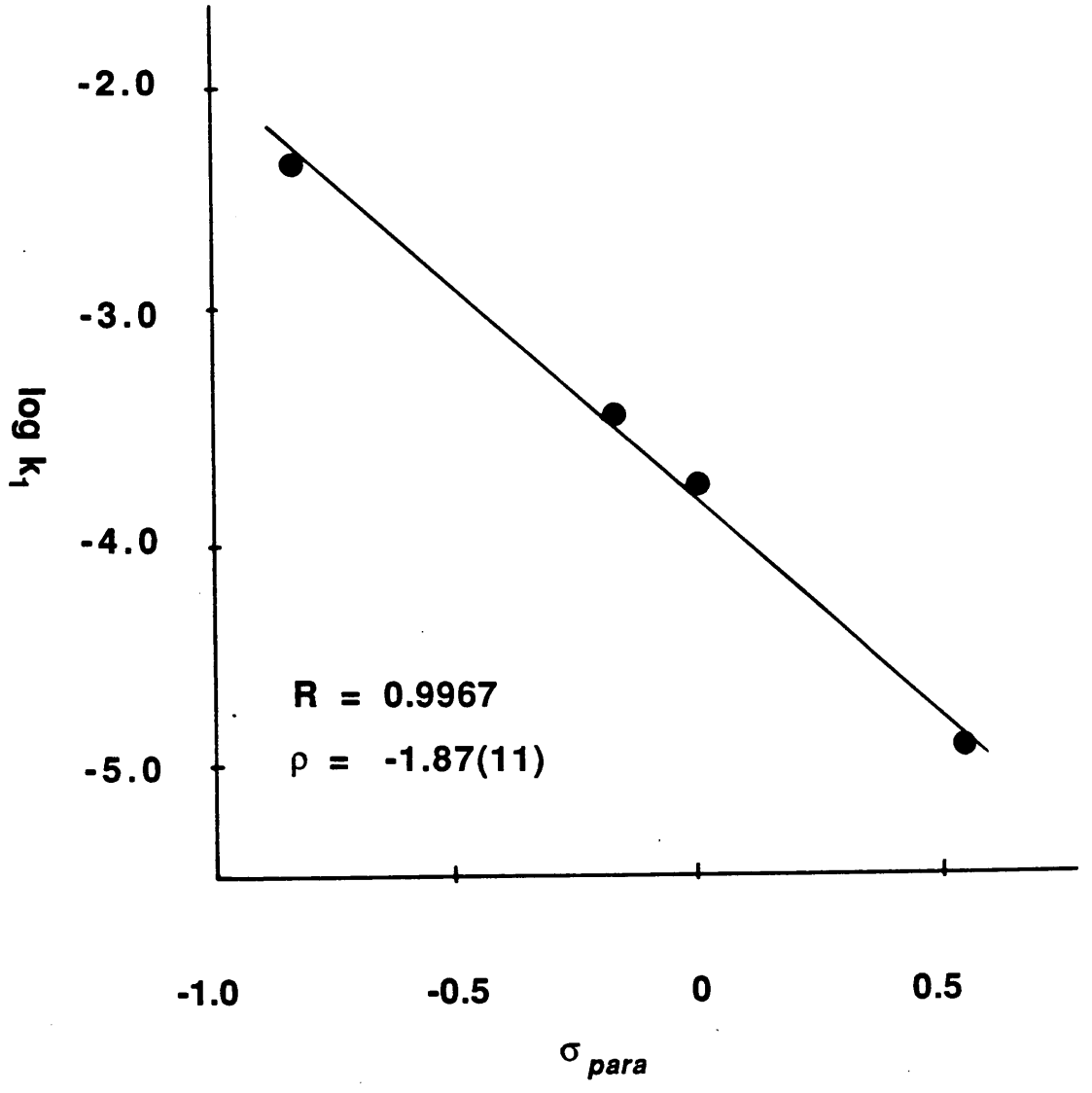

Figure II. Hammett Plot for the β-Hydrogen Elimination of Permethylscandocene Alkyl Complexes.

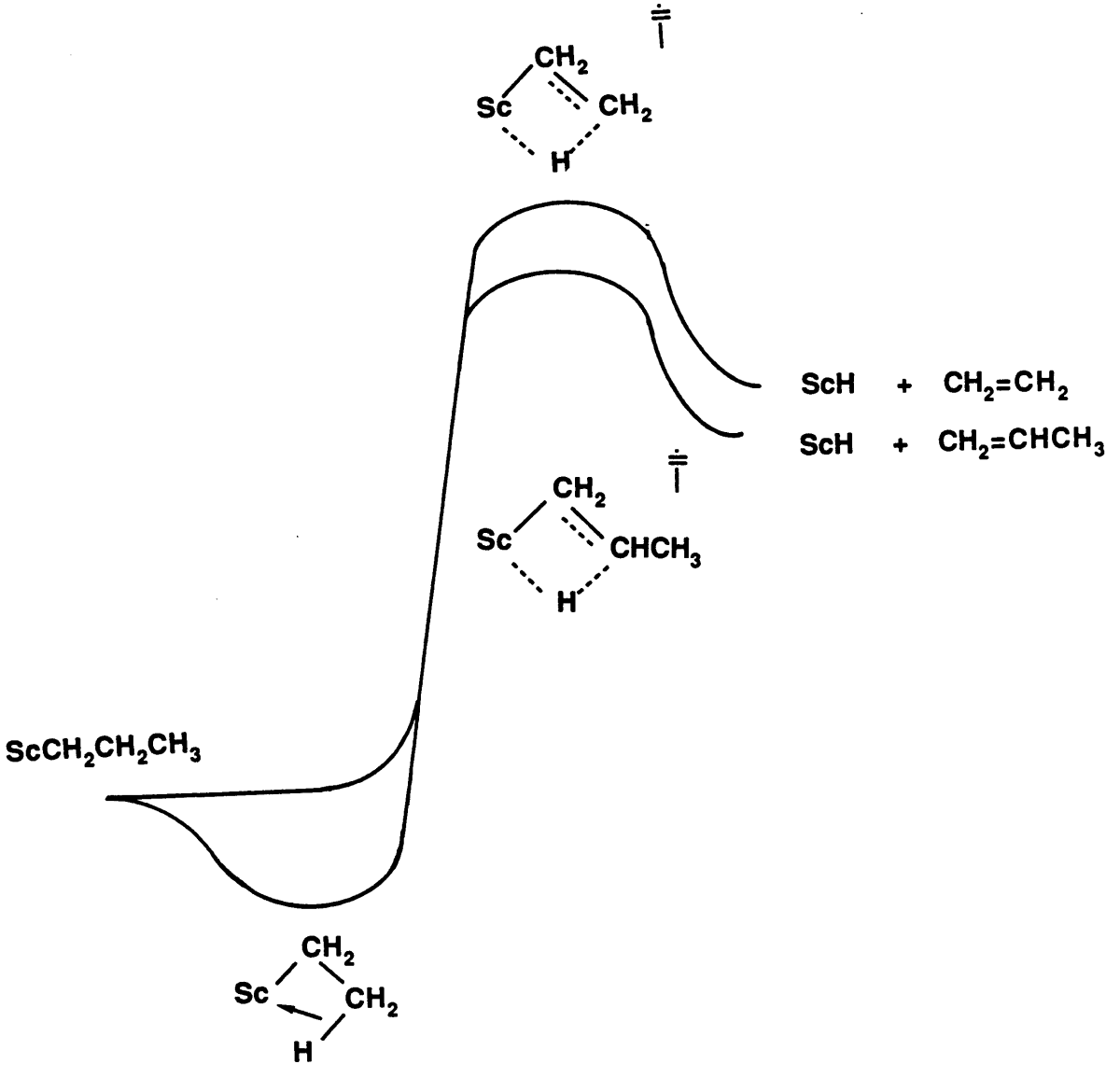

Figure III. Partial Free Energy Surfaces for β-Hydrogen Elimination of $Cp^*_2ScCH_2CH_3$ and $Cp^*_2ScCH_2CH_2CH_3$.

β-Alkyl Elimination of Permethylscandocene Alkyl Complexes: Reactions of Cp^*_2ScH With Dienes and Exo-cyclic Olefins.

In order to prepare complexes of the general types, $Cp^*_2ScCH_2\overline{CH(CH_2)_nCH_2}$ and $Cp^*_2ScCH_2(CH_2)_nCH{=}CH_2$ with which to study β-alkyl elimination, the reactions of $[Cp^*_2ScH]$ with exocyclic olefins and dienes were investigated.

The smallest exocyclic olefin, methylenecyclopropane, reacts with Cp^*_2ScH to form the η^3-crotyl complex, $Cp^*_2Sc(\eta^3\text{-}CH_2CHCHCH_3)$, **12** (equation 18).

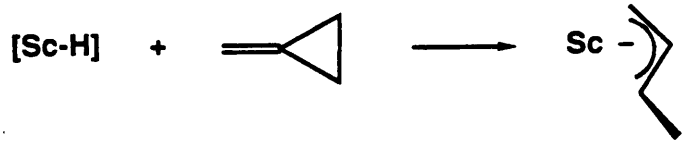

(18)

Although no intermediates are observed, a likely mechanism involves initial insertion to form a cyclopropylmethyl complex (**10**) which undergoes rapid β-alkyl elimination and subsequent rearrangement to the crotyl complex (**12**) (Scheme II). Excess methylenecyclopropane is converted to butadiene by β-hydrogen elimination of **11**.

Compound **12** can also be prepared by treatment of $Cp^*_2Sc(THF)H$ with butadiene and is isolated as a light orange solid in *ca.* 60% yield from cold petroleum ether (equation 19).

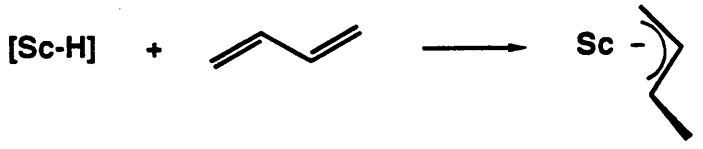

(19)

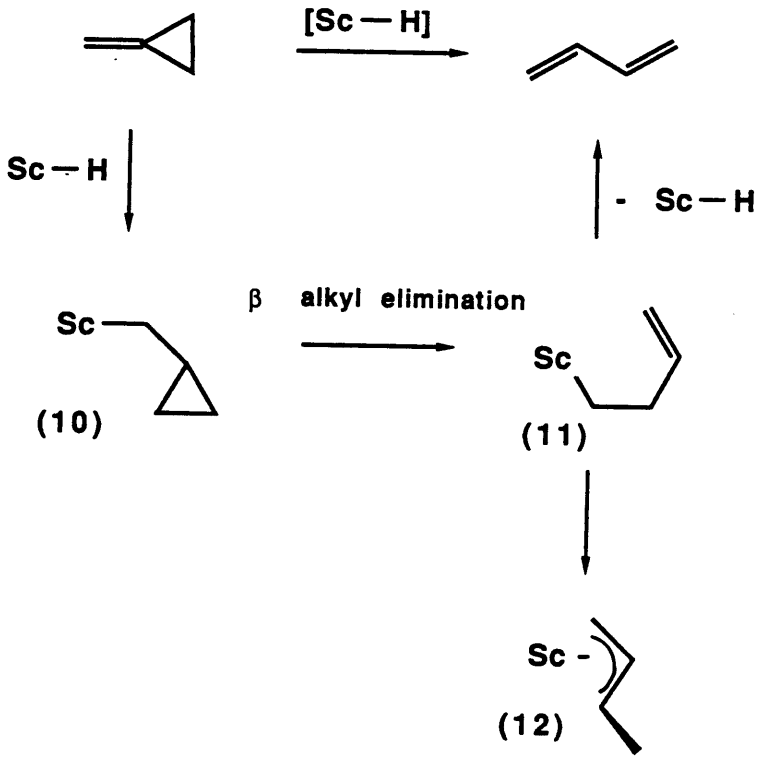

Scheme II. Formation of $Cp^*_2Sc(\eta^3\text{-}CH_2CHCHCH_3)$.

At room temperature, the ^1H NMR spectrum (400 MHz, C_6D_6, see Table I) of **12** shows a single resonance for both Cp^* rings and a single resonance for the *syn* and *anti* protons of the allyl ligand, indicating that η^3-η^1 conversion is rapid on the NMR time scale.[25] A static structure is observed (inequivalent Cp^* rings and distinct resonances for the *syn* and *anti* protons) when the sample is cooled to –80 °C. This variable temperature NMR behavior is similar to that observed for the parent allyl complex, $Cp^*_2Sc(\eta^3\text{-}CH_2CHCH_2)$, reported previously.[5c]

Formation of a metal crotyl complex from the reaction of a metal hydride and methylenecyclopropane occurs for a variety of transition metals.[26] The driving force for β-alkyl elimination is undoubtedly release of the strain energy associated with the three membered ring.

Treatment of [Cp^*_2Sc-H] with methylenecyclobutane results in the formation of the pentyl-bridged dimer shown below (equation 20).

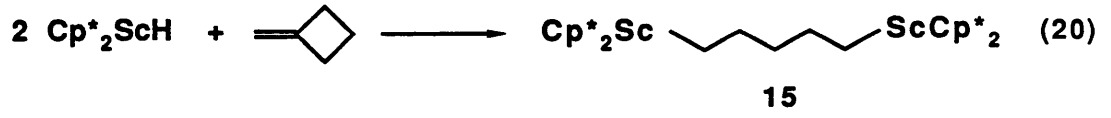

(20)

Compound **15** was isolated as a bright yellow solid in 72% yield from a cold concentrated solution of petroleum ether. It has been characterized by ^1H and ^{13}C NMR (see Tables I and II) and elemental analysis. Compound **15** has also been prepared by treatment of Cp^*_2Sc-H with 0.5 equivalent of 1,4-pentadiene.[27]

A likely mechanism for the formation of **15** is shown in Scheme III. The scandium cyclobutylmethyl complex (**13**), formed from initial insertion of methylenecyclobutane into the Sc-H bond, is not observed, even at low temperature. The ^1H NMR spectrum of Cp^*_2Sc-H and one equivalent CH_2=$CCH_2CH_2CH_2$ at –80 °C (without prior warming) shows only compound **15**. Unreacted methylenecyclobutane, but not 1,4-pentadiene, is observed at this temperature.

When Cp^*_2Sc-H is treated with one equivalent of methylenecyclobutane at –20 °C, a mixture of **14** and **15** is formed in a ratio of 1:6.2. Free methylenecyclobutane is also observed at this temperature. Observation of **15** as the major scandium species in solution suggests that β-alkyl elimination and reaction of **14** with another molecule of Cp^*_2Sc-H are faster than initial insertion of CH_2=$CCH_2CH_2CH_2$ into the Sc-H bond.

As the sample is warmed to room temperature, 1,4-pentadiene begins to form (at the expense of the methylenecyclobutane). This observation can be understood by β-hydrogen elimination from **14** or two consecutive eliminations from **15**. First order rate constants for the β-

hydrogen elimination of 15 have been measured by the method described previously (reaction with 2-butyne) and are listed below.[27]

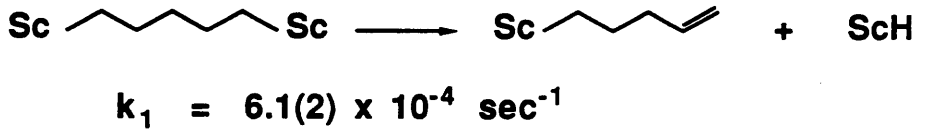

$k_1 = 6.1(2) \times 10^{-4}\ sec^{-1}$

$k_1 = 0.8(1) \times 10^{-4}\ sec^{-1}$

The reversibility of the β-alkyl elimination step (alkyl elimination $\rightleftharpoons$ olefin insertion) is demonstrated by a labeling experiment with $Cp^*_2Sc\text{-}H$ and $^{13}CH_2{=}\overline{C}CH_2CH_2\overline{CH_2}$. The dimeric product 15 that results from this reaction shows that the label appears in both the α and γ positions (equation 21). With excess $^{13}CH_2{=}\overline{C}CH_2CH_2\overline{CH_2}$, free 1,4 pentadiene is observed with the ^{13}C label incorporated in the 1 and 3 positions. Incorporation of the label in the γ position of the pentyl bridged dimer and in the 3 position of the free 1,4 pentadiene likely proceeds by the mechanism shown in Scheme IV.

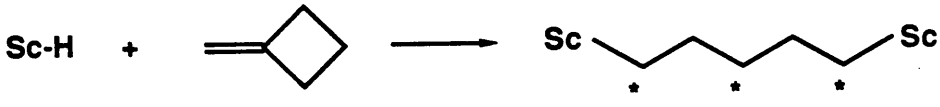

(21)

Sc-H = $(C_5Me_5)_2$Sc-H, * = ^{13}C label

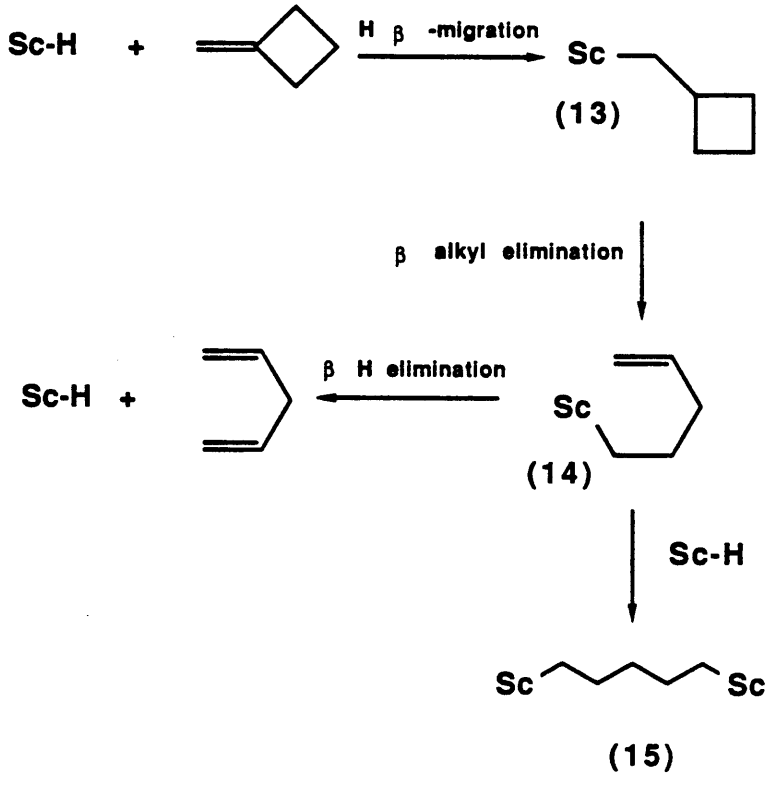

Scheme III. Formation of $Cp^*_2ScCH_2CH_2CH_2CH_2CH_2ScCp^*_2$.

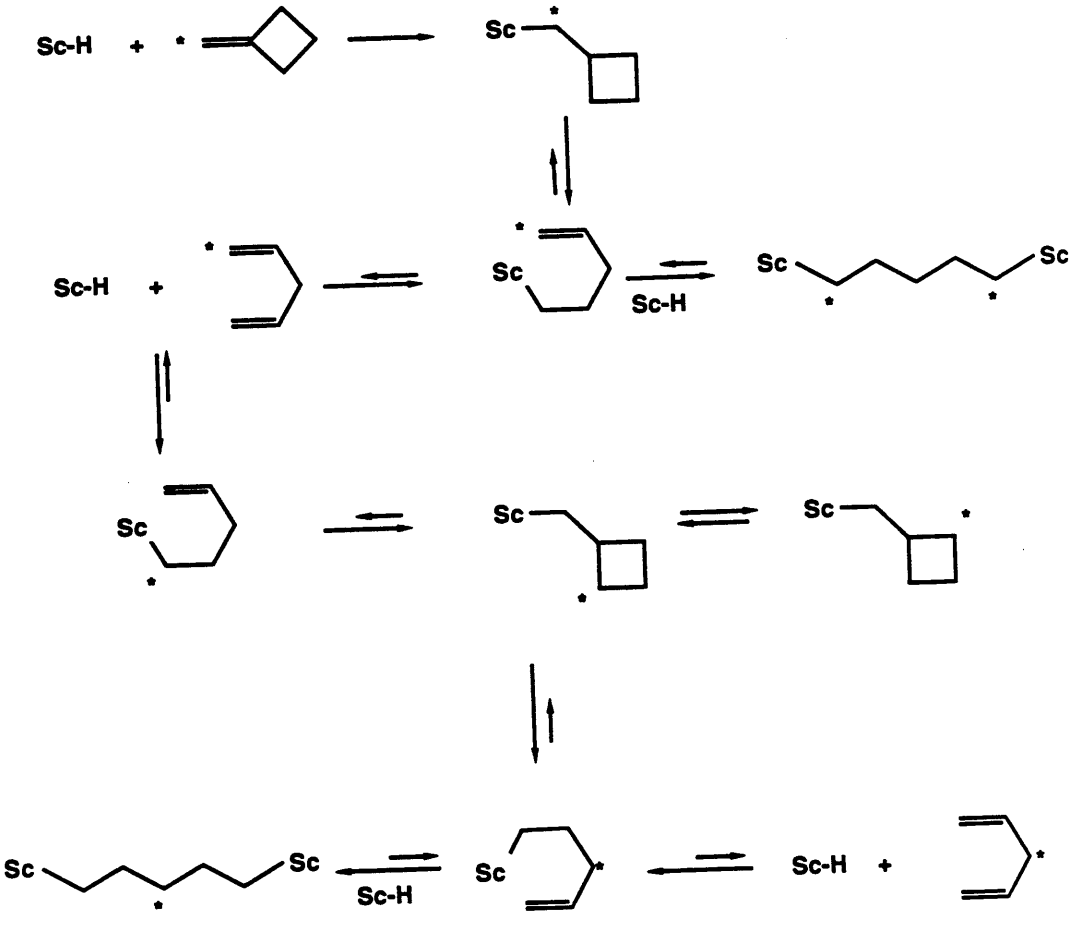

Scheme IV. Reversible Olefin Insertion/ Alkyl Elimination ($Cp^*_2ScH + {}^{13}CH_2{=}\overline{CCH_2CH_2CH_2}$).

Reaction of Cp^*_2Sc-H with 1,4-pentadiene results in the formation of **15** as described above. With one equivalent of pentadiene, a mixture of **14** and **15** is formed (in the ratio of *ca.* 1:2). Formation of **15** as the major product under these conditions suggests that the reaction of **14** with another molecule of Cp^*_2Sc-H is faster than the initial reaction of Cp^*_2Sc-H with pentadiene ($k_2 > k_1$).

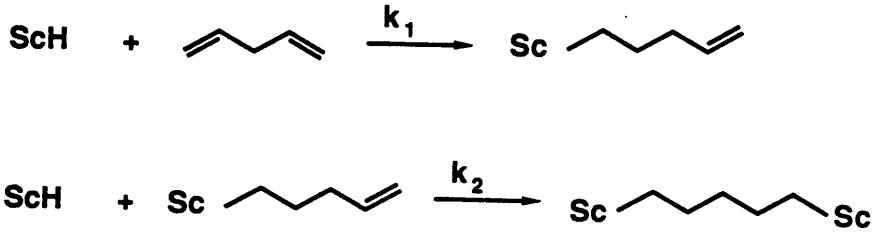

Although compound **14** cannot be isolated free from **15**, it can be characterized in solution by its ^1H NMR spectrum (toluene-d_8). Multiplets at δ 5.7 and 4.9 are assigned to the three protons of the pendent olefin. Resonances at δ 0.6, 0.8, 1.1 (all multiplets) correspond to the aliphatic hydrogens on the α, β and γ carbons, shifted characteristically upfield by the electropositive scandium. The two Cp^* rings give rise to a singlet at δ 1.94.

Treatment of Cp^*_2Sc-H with one equivalent of methylenecyclopentane results in quantitative formation of the expected insertion product, $Cp^*_2ScCH_2\overline{CHCH_2CH_2CH_2CH_2}$, **16**, which can be isolated as light yellow crystals in 40 % yield from petroleum ether (equation 22).

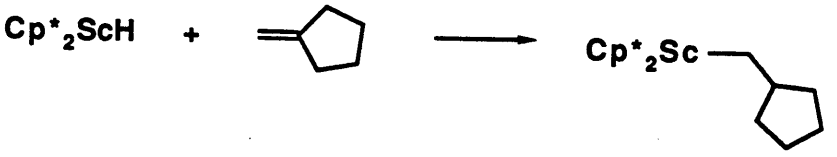

(22)

Compound **16** has been characterized by ^1H NMR, ^{13}C NMR (see Tables I and II) and elemental analysis. Characteristic of alkyl complexes of permethylscandocene, the ^1H NMR spectrum contains an upfield signal (δ 0.71 d J_{HH} = 7.3 Hz, C_6D_6) attributed to the hydrogens on the carbon

bound to scandium. The resonance for the carbon bound to scandium was observed in the ^{13}C NMR by preparing the isotopically enriched compound. The signal is a broad (fwhh = 66 Hz) triplet (J_{HH} = 110) at δ 50.8, quite characteristic of other sp^3 carbons bound to scandium.

Compound **16** undergoes σ bond metathesis reactions, not unlike other scandium alkyl complexes. Indeed, if the reaction in equation 22 is carried out with an excess of methylenecyclopentane, another product is readily formed, which has been identified as $Cp^*_2ScCH=CCH_2CH_2CH_2CH_2$ (**17**) by ^1H and ^{13}C NMR (equation 23).

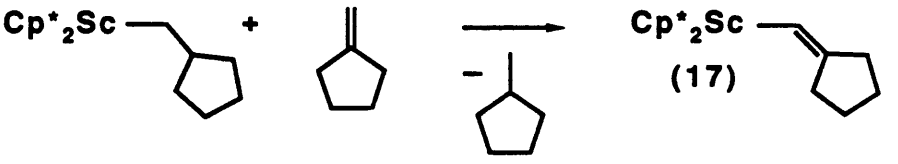

(23)

In addition, compound **16** reacts with styrene and allene to give the expected products of sigma bond metathesis (equations 24 and 25). Compound **18** (the scandium allenyl) has been independently prepared by the reaction of $Cp^*_2ScCH_3$ with allene (see Experimental Section); compound **19** (the scandium styrenyl) was identified by comparison of its ^1H NMR spectrum to that of $Cp^*_2ScCH=CHC_6H_4$-X (X=CH_3, OCH_3, CF_3) previously reported.[5b,c] In all three of the reactions, methylcyclopentane was identified in the ^1H NMR by comparison with a spectrum of an authentic sample.

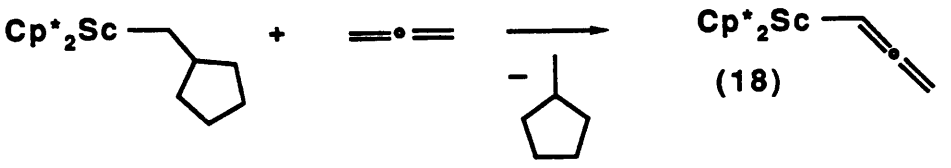

(24)

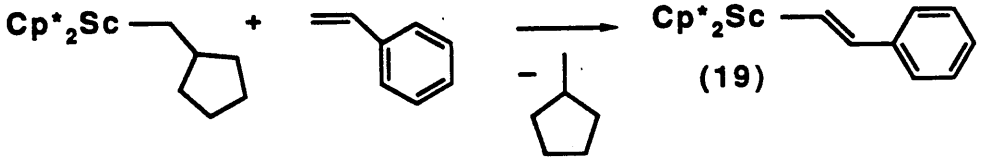

(25)

Unlike all of the compounds with β hydrogens discussed previously, $Cp^*_2ScCH_2CHCH_2CH_2CH_2CH_2$ does not react with 2-butyne to give *cis*-$Cp^*_2Sc(CH_3)C{=}CHCH_3$ and free olefin (methylenecyclopentane) (equation 26).

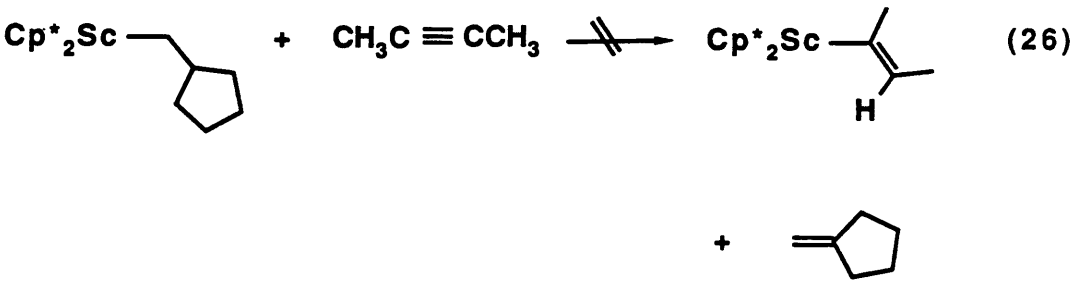

(26)

Rather, treatment of **16** with butyne results in the slow formation of *cis*-$Cp^*_2Sc(CH_3)C{=}CHCH_3$ and 1,5-hexadiene (equation 27). This reaction is not clean; observation of free methylcyclopentane indicates that involvement of the Cp^* rings by intramolecular σ bond metathesis occurs concurrently.

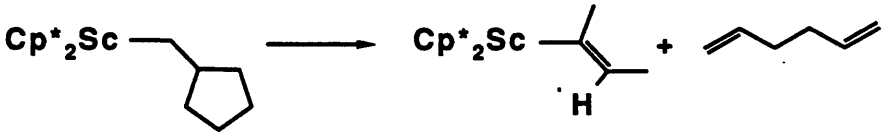

(27)

Treatment of Sc-H with one equivalent of ^{13}C-C_1-methylenecyclopentane results in the formation of the cyclopentylmethyl complex in which the ^{13}C label appears not only in the α position but also in the two equivalent γ positions (equation 28). Reversible β-alkyl elimination is invoked to rationalize incorporation of the label into the γ positions as shown in Scheme V.

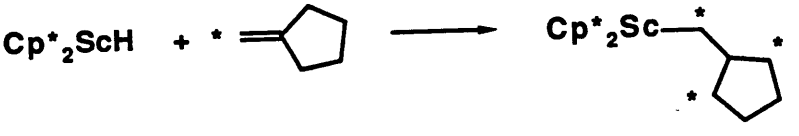

(28)

Reaction of Cp^*_2ScH with 1,5-hexadiene gives a product which by ^1H NMR was consistent with a hexyl bridged dimer, $Cp^*_2ScCH_2CH_2CH_2CH_2CH_2CH_2ScCp^*_2$. In the presence of excess diene, alkenyl products are formed suggesting that σ bond metathesis was taking place. This reaction was not pursued.

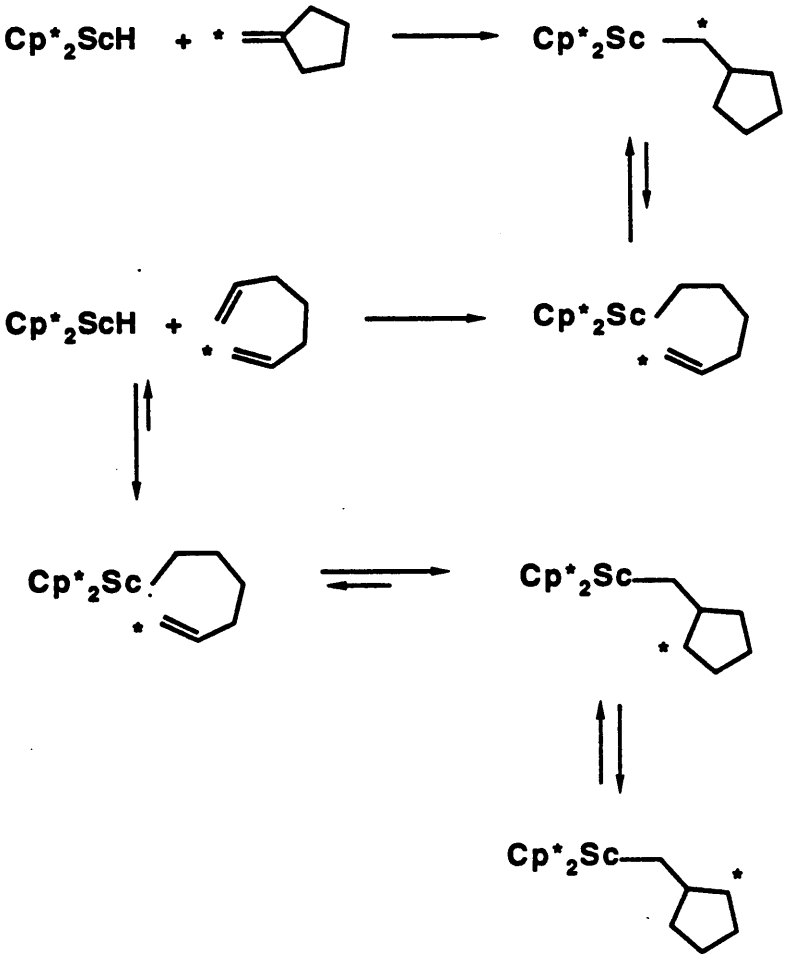

Scheme IV. Reversible Olefin Insertion/ Alkyl Elimination (Cp^*_2ScH + $^{13}CH_2$=$CCH_2CH_2CH_2CH_2$).

β-Alkyl Elimination-Discussion.

The reactions of Cp^*_2ScH with a series of exo-cyclic olefins and dienes have been investigated. β-Alkyl elimination has been shown to occur irreversibly in the reaction with methylenecyclopropane and reversibly with methylenebutane and methylenepentane. β-Alkyl elimination has been shown to be more favorable than β-hydrogen elimination for the scandium cyclopentylmethyl complex.

The equilibrium between alkyl elimination/olefin insertion can be understood by comparing the heats of formation for the exocyclic olefins and the corresponding dienes.

Compound	ΔH_f (kcal/mole)	$\Delta(\Delta H_f)$ (kcal/mole)
methylenecyclopropane[28]	47.9	21.9
butadiene[29]	26.0	
methylenecyclobutane[29]	29.1	3.8
1,4-pentadiene[30]	25.3	
methylenecyclopentane[31]	3.5	-17.3
1,5-hexadiene[30]	20.2	

Thus, the observations that the scandium hydride complex catalyses the ring opening of methylenecyclopropane and methylenecyclobutane and the final scandium complexes obtained in these reactions are derived from the products of ring opening are in accord with the thermodynamic data listed above. Also consistent with the data above, methylenecyclopentane is not ring opened catalytically by the scandium hydride complex but rather reacts stoichiometrically to produce the stable cyclopentylmethyl complex.

Although it would be thermodynamically favorable, there is no evidence for catalytic ring closure of 1,5-hexadiene (to methylenecyclopentane) by the scandium hydride complex. From the labeling experiment with ^{13}C-C_1-methylenecyclopentane, it is known that the scandium hexenyl complex does undergo intramolecular olefin insertion. In the presence of free Sc-H, however, dimer formation appears to be more favorable (equation 29).

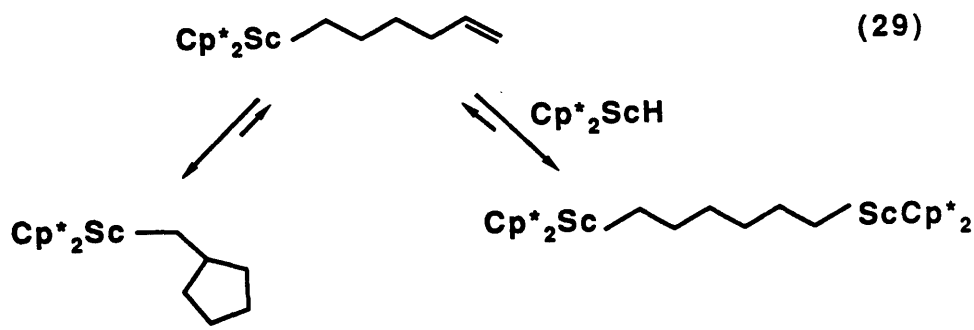

(29)

The subtle effects which dictate why the [Cp^*_2ScH] complex reacts with 1,4-pentadiene and 1,5-hexadiene to preferentially form polymethylene bridged dimers while the less sterically encumbered scandium hydride, [$(C_5Me_4)_2SiMe_2$]ScH, described below catalyzes the cyclization of 1,5-hexadiene and 1,6-heptadiene, are not well understood.[32]

Unfavorable steric interactions in the transition state are undoubtedly responsible for the observation that β-alkyl elimination is more favorable than β-hydrogen elimination for the scandium cyclopentylmethyl complex. In order to transfer the hydrogen from the β-carbon to the scandium, the cyclopentyl group must be oriented toward the bulky Cp^* rings. In contrast, the transition state for β-alkyl elimination is much less sterically congested with the cyclopentyl ring located in the equatorial wedge between the two Cp^* rings. These two transition states are illustrated in Figure III. Thus, although the cyclopentyl group would stabilize the transition state proposed for β-hydrogen elimination on electronic grounds (the electron releasing cycloalkyl group would stabilize positive charge development at the β carbon), unfavorable steric interactions prevent decomposition by this route. Consequently, β-alkyl elimination occurs. The

ring opening is thermodynamically unfavorable and reversible. In the presence of a Cp^*_2ScH trap (2-butyne), hexadiene is slowly formed and the scandium hexenyl complex ($Cp^*_2ScCH_2CHCH_2CH_2CH{=}CH_2$) is not observed, suggesting that the ring cyclization occurs at a much higher rate than either β-hydrogen elimination of the scandium hexenyl complex or β-alkyl elimination of the starting cyclopentylmethyl complex.

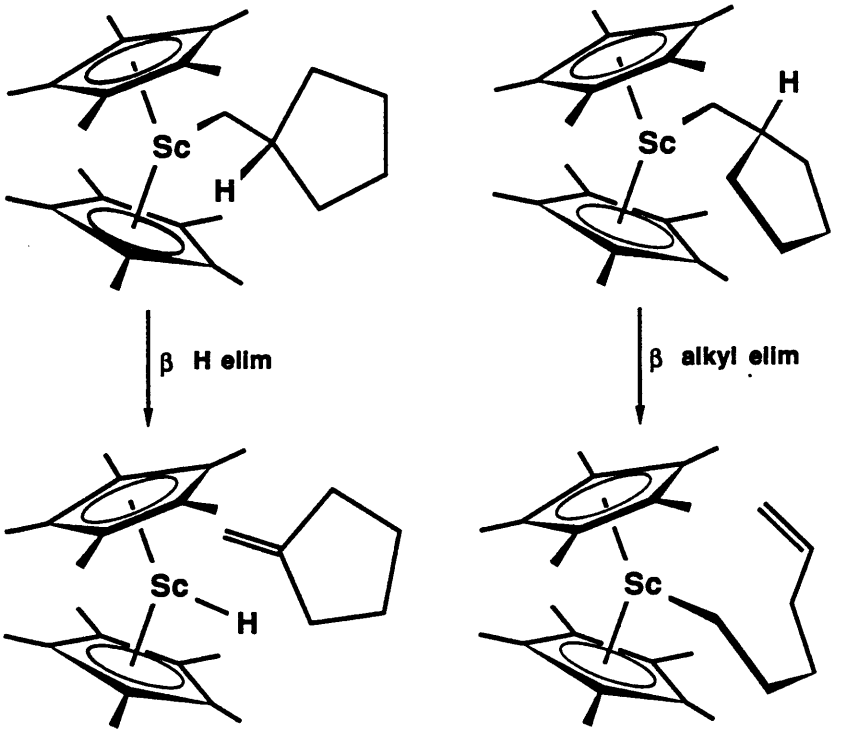

Figure III. Transition States for β-Hydrogen and β-Alkyl Elimination of $Cp^*_2ScCH_2CHCH_2CH_2CH_2CH_2$.

The reactivity of $Cp^*_2ScCH_2CHCH_2CH_2CH_2CH_2$ contrasts with the results obtained with analogous $[(C_5Me_4)_2SiMe_2]Sc$ complexes. By tethering the two rings with the $SiMe_2$ bridge, the R1-Sc-R2 (R1 and R2 are the ring centroids) angle increases significantly (A value of 144.6(10) was found for $Cp^*_2ScCH_3$;[5c] an angle of 117.0(2) was measured in the crystal structure of $[(C_5Me_4)_2SiMe_2]ScCH(SiMe_3)_2$). Thus, steric effects are likely to be greatly reduced in reactions with these tethered complexes. In accord, the isobutyl complex, $[(C_5Me_4)_2SiMe_2]ScCH_2CH(CH_3)_2$, decomposes by both β-hydrogen and β-methyl elimination, with the β-hydrogen elimination being much more favorable. Additionally, the corresponding cyclopentylmethyl complex has been prepared and undergoes a straightforward reaction with 2-butyne to afford the butenyl complex and free methylenecyclopentane. It does not, however, show any evidence for ring opening by β-alkyl elimination.[33]

β-X-Elimination: Reactions of Cp^*_2ScR with Polar Monomers (CH_2=CHX).

In order to study the decomposition of scandium alkyl complexes of the general type $Cp^*_2ScCH_2CRHX$ (R = H, CH_3; X = halogen, OR, PR_2, $SiMe_3$) by β-X elimination, the reactions of Cp^*_2ScR with polar monomers (CH_2=CHX) were investigated.

Treatment of Cp^*_2ScH with one equivalent of ethyl vinyl ether at low temperature (–80 °C) results in the formation of a roughly equal mixture of $Cp^*_2ScOCH_2CH_3$ **(20)** and $Cp^*_2ScCH_2CH_3$ **(2)** (equation 30).

$$2\ Cp^*_2ScH + CH_2{=}CHOEt \xrightarrow{-80^\circ C} Cp^*_2ScOEt + Cp^*_2ScCH_2CH_3 \qquad (30)$$

Cp^*_2ScH has reacted completely at this temperature by the time a spectrum can be run and no intermediates are seen in this reaction. As the sample is warmed to room temperature, the concentrations of ethyl vinyl ether and $Cp^*_2ScCH_2CH_3$ decrease while the concentration of $Cp^*_2ScOCH_2CH_3$ increases.

$Cp^*_2ScCH_3$ reacts with ethyl vinyl ether to form $Cp^*_2ScOCH_2CH_3$ and propene (equation 31).

$$Cp^*_2ScCH_3 + CH_2{=}CHOEt \xrightarrow{25^\circ C} Cp^*_2ScOEt + CH_2{=}CHCH_3 \qquad (31)$$

As above, no intermediates are seen in this reaction. However, the $Cp^*_2ScCH_3$ reacts much slower than the hydride complex; the rate is first order in $[Cp^*_2ScCH_3]$ and has a half life of *ca.* 1 hour at room temperature ($[CH_2$=CHOEt$] \approx 1.0$ M, $[Cp^*_2ScCH_3]_0 \approx .1$ M). This reaction rate is comparable to that seen for the insertion of propene into the Sc-CH_3 bond.

Even at 80°C, there is no reaction observed between $Cp^*_2ScC_6H_4$-*p*-CH_3 and ethyl vinyl ether.

Vinyl fluoride reacts with permethylscandocene hydride and alkyl complexes in much the same way as ethyl vinyl ether. That is, treatment of Cp^*_2ScH with one equivalent of vinyl fluoride at low temperature (–80°C) results in the formation of a roughly equimolar mixture of Cp^*_2ScF (21) and $Cp^*_2ScCH_2CH_3$ (equation 32). As above, the reaction is complete by the time a spectrum is recorded and when the sample is warmed to room temperature, the concentrations of the scandium ethyl complex and vinyl fluoride decrease while the concentration of Cp^*_2ScF increases.

$$2\ Cp^*_2ScH + CH_2{=}CHF \xrightarrow{-80^0C} Cp^*_2ScF + Cp^*_2ScCH_2CH_3 \quad (32)$$

$Cp^*_2ScCH_3$ reacts with vinyl fluoride to form Cp^*_2ScF and propene at a rate similar to that observed above with ethyl vinyl ether (equation 33).

$$Cp^*_2ScCH_3 + CH_2{=}CHF \xrightarrow{25^0C} Cp^*_2ScF + CH_2{=}CHCH_3 \quad (33)$$

Cp^*_2ScH reacts at low temperature (–80° to –20°C) with vinyldiphenylphosphine to produce the β-diphenylphosphinoethyl compound, $Cp^*_2ScCH_2CH_2PPh_2$ (22), shown below (equation 34).

$$Cp^*_2ScH + CH_2{=}CHPPh_2 \longrightarrow Cp^*_2ScCH_2CH_2PPh_2 \quad (34)$$

Compound **22** can be obtained at low temperature as a yellow crystalline solid but decomposes upon warming (*vide infra*). All characterization and reactivity studies have therefore been done with samples which have been prepared *in situ* in an NMR tube (not isolated).

The ^{1}H NMR spectrum of **22** (–20 °C, toluene-d_8, 400 MHz) contains multiplets assigned to the α and β protons at δ 0.74 and 0.94, respectively. The ^{13}C NMR spectrum (^{1}H NOE enhanced) shows a triplet at δ 33.6 (J_{CH} = 117 Hz) for the α carbon and a triplet of doublets at 27.2 (J_{CH} = 125.1, J_{CP} = 27.1 Hz) assigned to the β carbon. Compound **22** decomposes upon warming to room temperature to form **23** and ethylene (equation 35).

$$Cp^*_2ScCH_2CH_2PPh_2 \longrightarrow Cp^*_2ScPPh_2 + CH_2{=}CH_2 \quad (35)$$

Free ethylene is not, however, observed (^{1}H NMR); presumably it is polymerized by starting material. Compound **23** has been independently prepared by stirring a petroleum ether solution of Cp^*_2ScH with vinyldiphenylphosphine at room temperature and by treating Cp^*_2ScCl with $LiPPh_2$ in petroleum ether. In both cases, a dark blue oil is obtained; attempts to obtain a solid material were not successful.

The reaction shown in equation 34 can be followed conveniently by ^{1}H NMR. The reaction is first order in [$Cp^*_2ScCH_2CH_2PPh_2$] and the first order rate constant at 280 K is 1.90(7) x 10^{-4} sec^{-1}. The presence of excess 2-butyne does not affect the rate of this decomposition and *cis*-$Cp^*_2Sc(CH_3)C{=}C(CH_3)H$ is not observed, implying that β-phosphine elimination occurs exclusively (over β-hydrogen elimination).

The synthesis of $Cp^*_2ScCH_2CH_2SiMe_3$ has been previously described. Despite the slow rate of β-hydrogen elimination for this complex, there is no evidence for β-$SiMe_3$ elimination.

β-X Elimination–Discussion.

The reactions of Cp^*_2ScR (R = H, CH_3) with a variety of polar monomers have been investigated. The reactions involving Cp^*_2ScH and CH_2=CHX (X = OEt, F) can be accounted for by either of two mechanisms which are described below. The first of these, which involves a β-ethoxyethyl intermediate, is shown in equations 36 and 37.

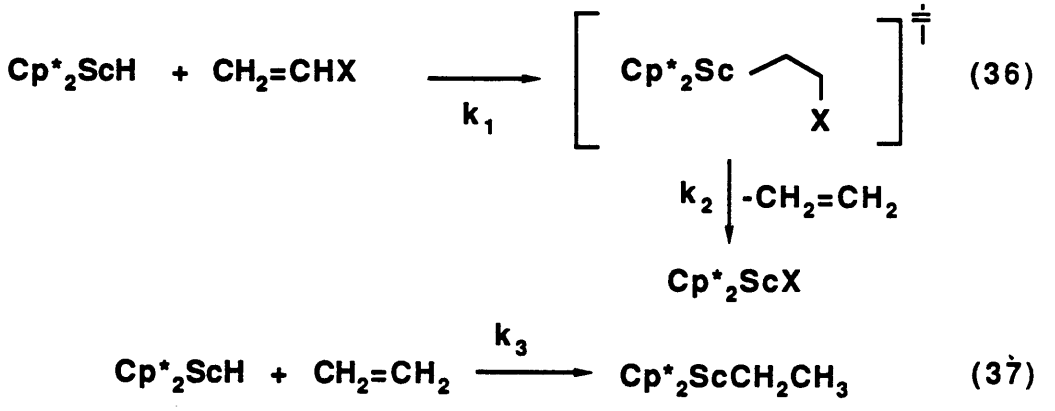

In this mechanism, the presence of $Cp^*_2ScCH_2CH_3$ at low temperatures suggests that β-X elimination (k_2) and reaction of ethylene with Cp^*_2ScH (k_3) are faster than initial insertion of CH_2=CHX in the Sc-H bond (k_1). As the temperature is increased from –80°C, the $Cp^*_2ScCH_2CH_3$ undergoes β-hydrogen elimination to form Cp^*_2ScH and free ethylene, the former of which is trapped by CH_2=CHX. This mechanism (rate determining initial olefin insertion followed by rapid β-X elimination) can also be used to explain the reactions of vinyl fluoride and ethyl vinyl ether with $Cp^*_2ScCH_3$.

An alternative mechanism for these reactions involves a direct σ-bond metathesis as shown below (equation 38). Activation of C-X bonds has been previously observed in the reaction of permethylscandocene alkyl complexes with alkyl halides.[5c] As above, the liberated ethylene reacts with Cp^*_2ScH in solution to form the observed $Cp^*_2ScCH_2CH_3$.

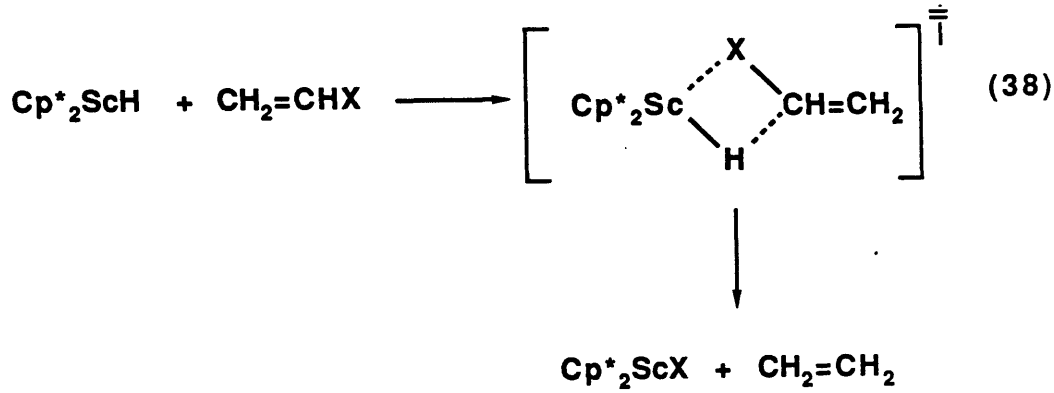

(38)

Since no intermediates are seen in the reactions shown in equations 30 and 32, it is not possible to discount either of the above two mechanisms. If the first mechanism is operative, the β-X elimination is not observed, since it occurs at a much faster rate than the rate determining insertion of the olefin into the Sc-H bond. Discouraging the elimination reaction by the use of sterically demanding vinyl ethers such as CH_2=CHOR (R = Ph, *t*-Bu) might allow for detection of a β-alkoxyethyl intermediate (and thus discount the second mechanism). These experiments must, however, await further study.

The β-X ethyl (X = PPh_2, $SiMe_3$) complexes were prepared by reaction of [Cp^*_2ScH] with vinyldiphenylphosphine and vinyltrimethylsilane. In the case of the former, the compound is only stable at low temperature, decomposing via β-PPh_2 elimination upon warming. The stability of this complex over a β-ethoxyethyl or β-fluoroethyl presumably arises from a decreased driving force for decomposition by β-X elimination and unfavorable steric interactions between the bulky diphenylphosphide group and the Cp^* rings. Preferential β-PPh_2 elimination is understood on both electronic and steric grounds: formation of the strong Sc-P bond is favored over the Sc-H bond and transfer of a hydrogen from the β-carbon necessitates directing the diphenylphosphide group toward one of the Cp^* rings. The β-trimethylsilylethyl complex undergoes very slow β-hydrogen elimination and shows no tendency to decompose via β-$SiMe_3$. Presumably the electropositive nature of the silyl group and the steric congestion around the scandium center

discourages formation of the Sc-Si bond. It would be of interest to explore the reactivity of similar complexes of this type where the steric congestion around the scandium center is decreased.

CONCLUSIONS

Permethylscandocene alkyl complexes have been prepared and used to study the processes of β-hydrogen, β-alkyl and β-X elimination. A model for the transition state for β-hydrogen elimination has been developed. In accord with that proposed by others, the transition state is four centered, and has a partial positive charge on the β carbon. The hydrogen is transferred to the scandium as H^-. The importance of steric effects in the transition state are underscored by the decreased rates of β-hydrogen elimination for the scandium cyclopentylmethyl and scandium β-trimethylsilylethy complexes and suggest that hydrogen transfer precedes Sc-C_α bond cleavage.

β-Alkyl elimination occurs for the scandium cycloalkylmethyl complexes (alkyl = propyl, butyl, pentyl). The ring opening has been shown by labeling experiments to be reversible in the last two cases. The scandium cycloalkylmethyl complex preferentially undergoes β-alkyl over β-hydrogen elimination.

The reaction of Cp^*_2ScH with CH_2=CHX (X = F, OEt) results in the formation of an equimolar mixture of Cp^*_2ScX and $Cp^*_2ScCH_2CH_3$. Two mechanisms are proposed to account for the products formed: a stepwise mechanism involving rate determining olefin insertion to produce a β-X ethyl intermediate followed by rapid β-X elimination and alternatively, a concerted σ bond metathesis mechanism. From the experiments performed, it is not possible to discount either mechanism. β-X-Ethyl complexes have been prepared for X = PPh_2 and $SiMe_3$; β-X occurs below room temperature for $Cp^*_2ScCH_2CH_2PPh_2$ and is not observed for $Cp^*_2ScCH_2CH_2SiMe_3$.

Table I. ^{1}H NMR Data.[a]

Compound	Assignment	δ (ppm)	Coupling (Hz)
$Cp^*_2ScCH_2CH_2CH_2CH_3$ (4)[c]	$[C_5(CH_3)_5]$	1.88 s	
	α-CH_2	0.90 t	J_{HH}=7.4
	β,γ,δ-CH_2(3)	0.56-0.61 m	
$Cp^*_2ScCH_2CH_2SiMe_3$ (5)[c]	$[C_5(CH_3)_5]$	1.86 s	
	$CH_2CH_2SiMe_3$	0.52 m	
	$CH_2CH_2SiMe_3$	-0.90 m	
	$Si(CH_3)_3$	0.08 s	
$Cp^*_2ScCH_2CH_2C_6H_5$ (6)[b]	$[C_5(CH_3)_5]$	1.84 s	
	$CH_2CH_2C_6H_5$	1.01 m	AA'BB'
	$CH_2CH_2C_6H_5$	2.38 m	AA'BB'
	$CH_2CH_2C_6H_5$	7.48 d	$^3J_{HH}$ = 7.0
	$CH_2CH_2C_6H_5$	7.30 d	$^3J_{HH}$ = 8.0
	$CH_2CH_2C_6H_5$	7.124 t	$^3J_{HH}$ = 7.5
$Cp^*_2ScCH_2CH_2C_6H_4$-p-NMe_2 (7)[c]	$[C_5(CH_3)_5]$	1.89 s	
	$CH_2CH_2C_6H_4$	1.11 m	AA'BB'
	$CH_2CH_2C_6H_4$	2.27 m	AA'BB'
	$CH_2CH_2C_6H_4$	7.04 d	$^3J_{HH}$ = 8.5
	$CH_2CH_2C_6H_4$	6.57 d	$^3J_{HH}$ = 8.5
	$N(CH_3)_2$	2.82 s	
$Cp^*_2ScCH_2CH_2C_6H_4$-p-CF_3 (8)[b]	$[C_5(CH_3)_5]$	1.82 s	
	$CH_2CH_2C_6H_4$	0.84 m	AA'BB'
	$CH_2CH_2C_6H_4$	2.38 m	AA'BB'
	$CH_2CH_2C_6H_4$	7.48 d	$^3J_{HH}$ = 8.0
	$CH_2CH_2C_6H_4$	7.35 d	$^3J_{HH}$ = 8.0
$Cp^*_2ScCH_2CH_2C_6H_4$-p-CH_3 (9)	$[C_5(CH_3)_5]$	1.85 s	
	$CH_2CH_2C_6H_4$	1.15 m	AA'BB'
	$CH_2CH_2C_6H_4$	2.42 m	AA'BB'
	$CH_2CH_2C_6H_4$	7.19 d	$^3J_{HH}$ = 7.8
	$CH_2CH_2C_6H_4$	7.51 d	$^3J_{HH}$ = 7.8
	CH_3	2.25 s	

$Cp^*_2Sc(\eta^3\text{-}CH_2CHCHCH_3)$ **(12)**	$[C_5(CH_3)_5]$	1.89 s	
	$CH_2CHCHCH_3$	2.22 d	J_{HH} = 10
	$CH_2CHCHCH_3$	6.65 m	J_{HH} = 10,13
	$CH_2CHCHCH_3$	4.60 m	J_{HH} = 6,13
	$CH_2CHCHCH_3$	1.30 m	J_{HH} = 6
$Cp^*_2Sc(\eta^3\text{-}CH_2CHCHCH_3)$ **(12)**[d]	$[C_5(CH_3)_5]$	1.83 s	
	$[C_5(CH_3)_5]$	1.92 s	
	$CHHCHCHCH_3$	1.62 d	J_{HH} = 10.5
	$CHHCHCHCH_3$	3.13 d	J_{HH} = 10.5
	$CH_2CHCHCH_3$	6.65 m	J_{HH} = 10,13
	$CH_2CHCHCH_3$	4.60 m	J_{HH} = 6,13
	$CH_2CHCHCH_3$	1.30 m	J_{HH} = 6
$Cp^*_2ScCH_2CH_2CH_2CH_2CH_2ScCp^*_2$ **(15)**[c]	$[C_5(CH_3)_5]$	1.89 s	
	α-CH_2	0.68 m	
	β-CH_2	0.39 m	
	γ-CH_2	1.62 m	

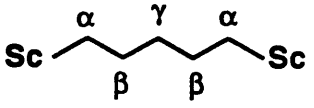

$Cp^*_2ScCH_2CHCH_2CH_2CH_2CH_2$ **(16)**	$[C_5(CH_3)_5]$	1.87 s	
	α-CH_2	0.71 d	J_{CH}=7.3
	β-CH	2.65 m	
	γ-CH_2	1.25 m	
	δ-CH_2	1.70 m	

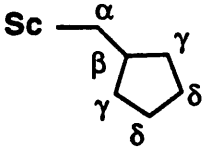

$Cp^*_2ScCH{=}CCH_2CH_2CH_2CH_2$ **(17)**	$[C_5(CH_3)_5]$	1.87 s	
	α-CH	6.31 br s	
	γ-CH_2	2.60 m	
	δ-CH_2	(not found)	

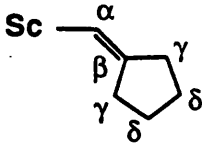

$Cp^*_2ScCH{=}C{=}CH_2$ **(18)**	$[C_5(CH_3)_5]$	1.84 s	
	$CH{=}C{=}CH_2$	3.46 t	J_{HH}=2.9
	$CH{=}C{=}CH_2$	2.64 d	J_{HH}=2.9
$Cp^*_2ScCH{=}CHC_6H_5$ **(19)**	$[C_5(CH_3)_5]$	1.84 s	
	$CH{=}CHC_6H_5$	6.15 d	J_{HH}=20

	$CH{=}CHC_6H_5$	7.82 d	J_{HH}=20
	$CH{=}CHC_6H_5$[e]		
$Cp^*_2ScOCH_2CH_3$ **(20)**[b]	$[C_5(CH_3)_5]$	1.95 s	
	OCH_2CH_3	3.18 q	$^3J_{HH}$ = 7
	OCH_2CH_3	1.41 t	$^3J_{HH}$ = 7
Cp^*_2ScF **(21)**	$[C_5(CH_3)_5]$	1.88 s	
$Cp^*_2ScCH_2CH_2P(C_6H_5)_2$ **(22)**[f]	$[C_5(CH_3)_5]$	1.81 s	
	CH_2CH_2P	0.74 m	
	CH_2CH_2P	0.94 m	
	$P(C_6H_5)_2$	7.39 td	J_{HH}=7,2
		7.66 t	J_{HH}=7
		7.16 t	J_{HH}=7
		7.07 d	J_{HH}=7
		7.05 d	J_{HH}=7
$Cp^*_2ScP(C_6H_5)_2$ **(23)**[c]	$[C_5(CH_3)_5]$	1.87 s	
	$P(C_6H_5)_2$	7.32 d	J_{HH} = 7.0
		7.16 d	J_{HH} = 7.0
		7.07 d	J_{HH} = 7.1
		6.98 d	J_{HH} = 7.4
		6.85 d	J_{HH} = 7.0

[a]^{1}H (90 and 400 MHz) NMR spectra were taken in benzene-d_6 at ambient temperature, unless otherwise stated. Chemical shifts are reported in parts per million (δ) from tetramethylsilane added as an internal reference or to residual protons in the solvent. Coupling constants are reported in hertz.

[b]Toluene-d_8 at room temperature, 400 MHz

[c]Cyclohexane-d_{12} at room temperature, 400 MHz

[d]Toluene-d_8 at -95°C, 400 MHz

[e]Overlap with free styrene resonances precluded accurate assignment of these signals.

[f]Toluene-d_8 at -20°C, 400 MHz.

Table II. ^{13}C NMR Data.[a]

Compound	Assignment	δ (ppm)	Coupling (Hz)
$Cp^*_2ScCH_2CH_2CH_2CH_3$ (4)[b]	$[C_5(CH_3)_5]$	11.42	
	$[C_5(CH_3)_5]$	119.29	
	α-CH_2	43.43	
	β-CH_2	30.70	
	γ-CH_2	34.47	
	δ-CH_3	14.49	
$Cp^*_2ScCH_2CH_2SiMe_3$ (5)[b]	$[C_5(CH_3)_5]$	11.70 q	J_{CH}= 125
	$[C_5(CH_3)_5]$	118.0 s	
	$CH_2CH_2SiMe_3$	39.16 t	J_{CH}= 124
	$CH_2CH_2SiMe_3$	13.88 t	J_{CH}=118
	$CH_2CH_2Si(CH_3)_3$	-0.48 q	J_{CH}=118
$Cp^*_2ScCH_2CH_2C_6H_5$ (6)[b]	$[C_5(CH_3)_5]$	11.47 q	J_{CH}= 125
	$[C_5(CH_3)_5]$	119.9 s	
	$CH_2CH_2C_6H_5$	(not found)	
	$CH_2CH_2C_6H_5$	36.92 t	J_{CH}=118.8
	$CH_2CH_2C_6H_5$	C_1 149.0 s	
	$CH_2CH_2C_6H_5$	$C_{2,6}$ 127.76 d	J_{CH}=165
	$CH_2CH_2C_6H_5$	$C_{3,5}$ 128.23 d	J_{CH}=161
	$CH_2CH_2C_6H_5$	C_4 124.46 d	J_{CH}=158
$Cp^*_2ScCH_2CH_2C_6H_4$-p-NMe_2 (7)[b]	$[C_5(CH_3)_5]$	11.50 q	J_{CH}= 124.7
	$[C_5(CH_3)_5]$	119.59 s	
	$CH_2CH_2C_6H_4$	(not found)	
	$CH_2CH_2C_6H_4$	36.37 t	J_{CH}=122.5
	$CH_2CH_2C_6H_4$	C_1 148.62 s	
	$CH_2CH_2C_6H_4$	$C_{2,6}$ 128.14 d	J_{CH}=151.9
	$CH_2CH_2C_6H_4$	$C_{3,5}$ 113.44 d	J_{CH}=154.1
	$CH_2CH_2C_6H_4$	C_4 137.35 s	
	$N(CH_3)_2$	41.36 q	J_{CH}=125.2
$Cp^*_2ScCH_2CH_2C_6H_4$-p-CF_3 (8)[b]	$[C_5(CH_3)_5]$	11.42 q	
	$[C_5(CH_3)_5]$	120.30 s	
	$CH_2CH_2C_6H_4$	(not found)	
	$CH_2CH_2C_6H_4$	36.50 t	
	$CH_2CH_2C_6H_4$	C_1 (not found)	
	$CH_2CH_2C_6H_4$	$C_{2,6}$ 127.69	
	$CH_2CH_2C_6H_4$	$C_{3,5}$ 124.91	
	$CH_2CH_2C_6H_4$	C_4 124.87	
	CF_3	(not found)	

$Cp^*_2ScCH_2CH_2C_6H_4$-*p*-CH_3 (9)[b]	$[C_5(CH_3)_5]$	11.49 q	J_{CH}= 124.9
	$[C_5(CH_3)_5]$	119.84 s	
	$CH_2CH_2C_6H_4$	42.67 t	J_{CH}=116.3
	$CH_2CH_2C_6H_4$	36.57 t	J_{CH}=118.1
	$CH_2CH_2C_6H_4$	C_1 145.92 s	
	$CH_2CH_2C_6H_4$	$C_{2,6}$ 127.59 d	J_{CH}=152.6
	$CH_2CH_2C_6H_4$	$C_{3,5}$ 128.51 d	J_{CH}=159.9
	$CH_2CH_2C_6H_4$	C_4 133.21 s	
	CH_3	21.29 q	J_{CH}=124.9
$Cp^*_2Sc(\eta^3$-$CH_2CHCHCH_3)$ (12)	$[C_5(CH_3)_5]$	12.50 q	J_{CH}=124.7
	$[C_5(CH_3)_5]$	118.08 s	
	$CH_2CHCHCH_3$	89.90 d	J_{CH}=137.9
	$CH_2CHCHCH_3$	151.4 d	J_{CH}=139.4
	$CH_2CHCHCH_3$	60.25 t	J_{CH}=135.7
	$CH_2CHCHCH_3$	18.05 q	J_{CH}=125.4
$Cp^*_2ScCH_2CH_2CH_2CH_2CH_2ScCp^*_2$ (15)[c]	$[C_5(CH_3)_5]$	11.57 q	J_{CH}=124.7
	$[C_5(CH_3)_5]$	118.87 s	
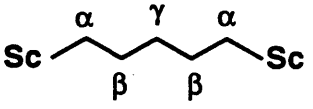	α-CH_2	45.07 t	J_{CH}=115.9
	β-CH_2	33.24 t	J_{CH}=114.4
	γ-CH_2	43.83 t	J_{CH}=127.7
$Cp^*_2ScCH_2CHCH_2CH_2CH_2CH_2$ (16)[c]	$[C_5(CH_3)_5]$	11.55 q	J_{CH}=124.9
	$[C_5(CH_3)_5]$	120.24 s	
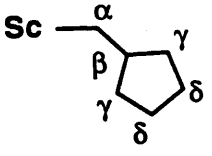	α-CH_2	50.75[e] t	J_{CH}=111.5
	β-CH	44.11 d	J_{CH}=125.4
	γ-CH_2	38.88 t	J_{CH}=125.8
	δ-CH_2	26.0[d]	
$Cp^*_2ScCH{=}CCH_2CH_2CH_2CH_2$ (17)	$[C_5(CH_3)_5]$	11.89 q	J_{CH}=125.2
	$[C_5(CH_3)_5]$	120.45 s	
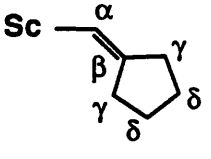	α-CH	176.9[e] d	J_{CH}=102.5[f]
	β-C	147.84 s	
	γ-CH_2	37.95 t	J_{CH}=127
	γ-CH_2	36.57 t	J_{CH}=126
	δ-CH_2	28.63 t	J_{CH}=125
	δ-CH_2	27.45 t	J_{CH}=125

$Cp^*_2ScCH=C=CH_2$ (**18**)[c]	$[C_5(CH_3)_5]$	10.31 q	J_{CH}=126
	$[C_5(CH_3)_5]$	118.42 s	
	$CH=C=CH_2$	94.17 br s	
	$CH=C=CH_2$	151.1 d	J_{CH}=17.5
	$CH=C=CH_2$	50.5 t	J_{CH}=164
$Cp^*_2ScCH_2CH_2P(C_6H_5)_2$ (**22**)[g]	$[C_5(CH_3)_5]$	11.35 q	J_{CH}=124.7
	$[C_5(CH_3)_5]$	118.94 s	
	CH_2CH_2P	33.57 t	J_{CH}=117
	CH_2CH_2P	27.18 td	J_{CH}=125.1
			J_{CP}=27.1
	$P(C_6H_5)_2$[h]	133.63 d	J_{CH}=158.5
		141.02 br s	
		129.2	
		123.5	
$Cp^*_2ScP(C_6H_5)_2$ (**23**)[b]	$[C_5(CH_3)_5]$	12.78 qd	J_{CH}=125.5
	$[C_5(CH_3)_5]$	123.96 s	
			J_{CP}=4.4
	$P(C_6H_5)_2$	148.25 d	J_{CP}=25.7
		127.56 dd	J_{CH}=156.3
			J_{CP}=7
		128.12 d	J_{CH}=158.5
		132.89 d	J_{CH}=157.7
		131.85 d	J_{CH}=155.5

[a] ^{13}C (100.25 MHz) NMR spectra were taken in benzene-d_6 at ambient temperature, unless otherwise stated. Chemical shifts are reported in parts per million (δ) from tetramethylsilane referenced from solvent signal. Coupling constants ($J_{13C\text{-}1H}$) were obtained from a gated (^1H NOE enhanced) spectrum and are reported in hertz.

[b] Cyclohexane-d_{12} at room temperature, 100.25 MHz.

[c] Toluene-d_8 at room temperature, 100.25 MHz.

[d] Chemical shift obtained in C_6D_6; the coupling constant was not obtained due to the limited stability of **16** in C_6D_6.

[e] Chemical shift obtained from ^{13}C NMR spectrum of ^{13}C–enriched sample.

[f]Coupling constant obtained from ^{1}H NMR spectrum of ^{13}C–enriched sample.

[g]Toluene-d_8 at –20 °C, 100.25 MHz.

[h]Overlap with toluene signals precluded observation of all carbon phenyl resonances.

Table III. Observed Rate Constants (k_{obs}) for β-Hydrogen Elimination of $Cp^*_2ScCH_2CH_2Ph$ as a Function of 2-Butyne Concentration.[a]

[2-butyne] (M)	$k_{obs} \times 10^4$ (sec^{-1})
0.98	3.16(6)
1.17	2.97(11)
2.87	3.30(5)
3.35	2.98(2)

[a]Rate constants were measured at 285 K. Butyne concentrations were measured using an internal standard (Cp_2Fe) of known concentration.

Table IV. Kinetic Data for β-Hydrogen Elimination of Cp^*_2ScR Complexes.[a]

R	$k_1 \times 10^4$ (sec^{-1})	$\Delta G^{\ddagger}$ (kcal/mol)
CH_2CH_3	0.94(3)	21.51(8)
$CH_2CH_2CH_3$	6.3(1)	20.45(7)
$CH_2CH_2SiMe_3$	002(1)[b]	24.9(2)
$CH_2CH_2CH_2CH_3$	3.55(4)	20.77(7)
CH_2CH_2Ph	1.67(3)	21.19(8)
CH_2CH_2Ph-*p*-NMe_2	42(1)[c]	19.40(8)
CH_2CH_2Ph-*p*-CF_3	0.11(1)[d]	22.71(9)
CH_2CH_2Ph-*p*-CH_3	3.26(6)	20.82(8)

[a]Rate constants and free energies of activation listed are for 280 K. Errors in $\Delta G^{\ddagger}$ represent one standard deviation estimated from the uncertainties in k_1(280) and the temperature.

[b]Extrapolated from k_1 and $\Delta G^{\ddagger}$ measured at 298 K assuming $\Delta S^{\ddagger}$ = -11 eu.

[c]Extrapolated from k_1 and $\Delta G^{\ddagger}$ measured at 265 K assuming $\Delta S^{\ddagger}$ = -11 eu.

[d]Extrapolated from k_1 and $\Delta G^{\ddagger}$ measured at 295 K assuming $\Delta S^{\ddagger}$ = -11 eu.

Table V. Rate Constants for β-Hydrogen Elimination of Cp^*_2ScR Complexes.

R	T(K)	$k_1(sec^{-1})$
CH_2CH_3	275	$5.29(7) \times 10^{-5}$
	280	$9.4(3) \times 10^{-5}$
	284	$2.18(3) \times 10^{-5}$
	290	$3.98(10) \times 10^{-4}$
	296	$6.93(16) \times 10^{-4}$
$CH_2CH_2CH_3$	265	$7.9(2) \times 10^{-5}$
	270	$1.72(4) \times 10^{-4}$
	275	$3.01(2) \times 10^{-4}$
$CH_2CH_2CH_2CH_3$	270	$1.21(2) \times 10^{-4}$
	275	$1.99(2) \times 10^{-4}$
	280	$3.55(4) \times 10^{-4}$
	285	$7.6(3) \times 10^{-4}$
$CH_2CH_2SiMe_3$	298	$\approx 5.3(8) \times 10^{-6}$
CH_2CH_2Ph	270	$5.14(9) \times 10^{-5}$
	275	$6.5(2) \times 10^{-5}$
	280	$1.67(3) \times 10^{-4}$
	285	$3.16(6) \times 10^{-4}$
	290	$5.23(10) \times 10^{-4}$
CH_2CH_2Ph-*p*-CH_3	270	$1.00(4) \times 10^{-4}$
	280	$3.26(6) \times 10^{-4}$
	290	$1.04(2) \times 10^{-3}$
CH_2CH_2Ph-*p*-NMe_2	265	$3.74(5) \times 10^{-6}$
CH_2CH_2Ph-*p*-CF_3	295	$1.32(4) \times 10^{-4}$
	300	$2.26(4) \times 10^{-4}$
	305	$5.66(16) \times 10^{-4}$

EXPERIMENTAL SECTION

General Considerations.

All air sensitive manipulations were carried out using glove box or high vacuum line techniques. Solvents were dried over $LiAlH_4$ or sodium benzophenone ketyl and stored over titanocene. Benzene-d_6, toluene-d_8 and cyclohexane-d_{12} were dried over activated 4Å molecular sieves and stored over titanocene.

Argon, nitrogen, hydrogen and deuterium were purified over MnO on vermiculite and activated molecular sieves. Ethylene (Matheson), propylene (Matheson), 1-butene (Matheson), vinyl fluoride (SCM Chemicals) and butadiene (Matheson) were purified by three cycles of freeze-pump-thaw at −196 °C and then vacuum transferred at 25 °C.

Styrene (Aldrich) and *para*-Methylstyrene (Alfa) were used without further purification. *para*-Trifluoromethylstyrene was prepared by the literature method[34] except that the secondary alcohol, *p*-CF_3-$C_6H_4CH(OH)CH_3$ was formed by the reaction of CH_3MgBr and *p*-$CF_3C_6H_4CHO$ (Aldrich) in diethyl ether. *para*-Dimethylaminostyrene was prepared by the reaction of *p*-NMe_2-C_6H_4CHO and CH_2PPh_3 in diethyl ether. *para*-Trifluoromethylstyrene and *para*-dimethylaminostyrene were purified by vacuum distillation and characterized by ^1H NMR prior to use.

The literature procedure[35] for the synthesis of methylenecyclopropane was followed. Methylenecyclobutane (Aldrich), methylenecyclopentane (Phaltz and Bauer), methylenecyclohexane (Aldrich), 1,4-pentadiene (Aldrich) and 1,5-hexadiene (Aldrich) were dried over activated 4Å molecular sieves and then vacuum transferred and stored in greaseless solvent containers. ^{13}C-C_1-methylenecyclopentane and ^{13}C-C_1-methylenecyclobutane were prepared according to the literature method[36] using ^{13}C-C_1-methylenetriphenylphosphorane. Cp_2Fe, used as an internal standard for NMR tube kinetic experiments, was sublimed twice before use.

Ethyl vinyl ether (Aldrich) was dried over activated 4Å molecular sieves prior to use. Vinyl diphenylphosphine (Strem) was purchased in a sealed ampoule and was used without further purification.

NMR spectra were recorded on Varian EM-390 (^{1}H, 90 MHz), JEOL FX90Q (^{1}H, 89.56 MHz; ^{13}C, 22.50 MHz) and JEOL GX400Q (^{1}H, 399.78 MHz; ^{13}C, 100.38 MHz) spectrometers. Infrared spectra were recorded on a Beckman 4240 spectrometer and reported in cm^{-1}. All elemental analyses were conducted by L. Henling of the Caltech Analytical Laboratory.

The synthesis of $Cp^*_2ScCH_3$, $Cp^*_2ScCH_2CH_3$, $Cp^*_2ScCH_2CH_2CH_3$ and $Cp^*_2Sc(THF)H$ have been previously reported.[5b,5c]

NMR Tube Reactions.

Many of the reactions described in this chapter were carried out in sealed NMR tubes. Approximately 25 mg of the starting material and 0.5 ml deuterated solvent were loaded into a sealable NMR tube in the glove box. The tube was attached to either a 180° needle valve or calibrated gas volume, or fitted with a glass stopper. Volatile reagents were condensed into the evacuated tube at –196°C. All tubes were sealed at –196°C and allowed to warm to room temperature in a fume hood. For NMR tube reactions which involved generation of the Cp^*_2ScH, the NMR tube was fused via a short piece of soft glass directly onto a 24/40" joint with a Kontes quick release valve attached.

For reactions monitored at low temperatures, the sealed tubes, prepared as above, were stored in a dry ice/acetone bath or liquid nitrogen until use. The NMR tube was then loaded into the NMR probe, which was precooled to the desired temperature with a reference tube.

$Cp^*_2ScCH_2CH_2C_6H_5$ (6). $Cp^*_2ScCH_3$ (0.660g, 2 mmol) was placed in a heavy walled glass vessel. Petroleum ether (*ca.* 15 ml) was condensed onto the solid and the resulting solution was cooled to -196°C. Hydrogen (1 atm) was admitted to the vessel. The solution was then stirred at room temperature for 20 minutes. Volatiles were removed from the bomb at -78°C. With the reaction vessel still at -78°C, degassed styrene (0.23 ml, 2 mmol) was added via syringe under an argon flush. Yellow precipitate immediately formed. Warming to room temperature effected dissolution of all the yellow solid. The solution was transferred to a frit assembly in the glove box. Concentration of the petroleum ether and cooling to -78°C afforded light yellow crystals of $Cp^*_2ScCH_2CH_2C_6H_5$, which were isolated by cold filtration (0.470g, 56%).

Anal. Calcd. for $C_{28}H_{39}Sc$: C, 79.96; H, 9.35. Found: C, 78.75; H, 9.24.

$Cp^*_2ScCH_2CH_2C_6H_4$-*p*-CH_3 (7). The same procedure was used as described above, except that *p*-CH_3-styrene (0.28 ml, 2.1 mmol) was added to the petroleum ether solution of $[Cp^*_2ScH]_x$ generated from hydrogenation of 0.695g (2.1 mmol) of $Cp^*_2ScCH_3$. Concentration and cooling of the resulting solution yielded yellow crystals of $Cp^*_2ScCH_2CH_2C_6H_4$-*p*-CH_3 (0.380g, 42%).

Anal. Calcd. for $C_{29}H_{41}Sc$: C, 80.15; H, 9.51. Found: C, 79.90; H, 9.46.

$Cp^*_2ScCH_2CH_2C_6H_4$-*p*-CF_3 (8). $Cp^*_2ScCH_3$ (0.595g 1.8 mmol) and *p*-CF_3-$C_6H_4CHCH_2$ (0.32, 1.84 mmol) were used as described above to produce $Cp^*_2ScCH_2CH_2C_6H_4$-*p*-CF_3 (0.31g, 36%), which was isolated by cold filtration.

Anal. Calcd. for $C_{29}H_{38}F_3Sc$: C, 71.29; H, 7.84. Found: C, 71.11; H, 7.83.

$Cp^*_2ScCH_2CH_2C_6H_4$-*p*-NMe_2 (9). $Cp^*_2ScCH_3$ (0.495 g, 1.5 mmol) and *p*-NMe_2-$C_6H_4CHCH_2$ (.22 g, 1.5 mmol) were used as described above to produce $Cp^*_2ScCH_2CH_2C_6H_4$-*p*-NMe_2 (0.317g, 46%) as a crystalline yellow solid.

Anal. Calcd. for $C_{30}H_{44}NSc$: C, 77.72; H, 9.57; N, 3.02. Found: C, 77.09; H, 9.37; N, 3.49.

$Cp^*_2ScCH_2CHDC_6H_5$ (6-β-d_1). Deuterium (1 atm) was added to a petroleum ether solution (*ca.* 15 ml) of $Cp^*_2ScCH_3$ (0.440g, 1.3 mmol) in a heavy walled reaction vessel. After stirring the solution at room temperature for 20 minutes and removing the volatiles at -78°C, styrene (0.15 ml, 1.3 mmol) was added via syringe under an argon counterflow. The resulting solution was transferred to a frit assembly, which upon concentrating and cooling afforded yellow crystalline $Cp^*_2ScCH_2CHDC_6H_5$ (0.245g, 45%).

Anal. Calcd. for $C_{28}H_{37}DSc$: C, 79.78; H, 9.32. Found: C, 78.91; H, 9.25.

$Cp^*_2ScCH_2CH_2SiMe_3$ (5). $Cp^*_2ScCH_3$ (0.82 g, 2.5 mmol) was loaded into a heavy walled glass vessel. Petroleum ether (*ca.* 10 ml) was condensed onto the solid. Hydrogenation of the solution was carried out as described previously. Under an argon counterflow, vinyl trimethylsilane (0.43 ml, 2.75 mmol) was syringed into the cooled (-78°C) reaction vessel. After warming to room temperature the solution was transferred to a round bottomed flask attached to a frit assembly. Repeated attempts to obtain crystals from slow cooling of a petroleum ether solution were unsuccessful. Removal of all volatiles yielded a bright yellow powder (0.53 g, 1.27 mmol, 51% yield). The solid was considered pure by ^1H NMR (>95%).

$Cp^*_2ScCH_2CH_2CH_2CH_3$ (4). A petroleum ether solution of $Cp^*_2ScCH_3$ (0.414 g, 1.3 mmol) was hydrogenated as above. 1-Butene was condensed into the cooled heavy walled reaction vessel (−196°C) from a calibrated gas volume. The resulting solution was transferred to a frit assembly. As above, repeated attempts to obtain crystals were unsuccessful. A pale yellow powder (0.165 g, 34% yield) was obtained upon removal of all volatiles. The purity of the compound was checked by ^1H NMR (>95%).

$Cp^*_2Sc(\eta^3\text{-}C_4H_7)$ (12). Butadiene (*ca.* 12 mmol) was condensed onto a petroleum ether solution (15 ml) of $Cp^*_2Sc(THF)H$ (0.540g, 1.4mmol). The reaction mixture was stirred for 5 hours at room temperature. Concentration of the solution and cooling to −78°C produced a light orange solid, $Cp^*_2Sc(\eta^3\text{-}C_4H_7)$, which was isolated by cold filtration (0.310g, 60%).

Anal Calcd.for $C_{24}H_{37}Sc$: C, 77.79; H, 10.06. Found: C, 77.15; H, 9.91.

$Cp^*_2ScCH_2CH_2CH_2CH_2CH_2ScCp^*_2$ (15). Hydrogenation of a petroleum ether solution of $Cp^*_2ScCH_3$ (1.0 g, 3.0 mmol) was carried out as described previously. Methylenecyclobutane (3.3 mmol) was condensed from a calibrated gas volume into the reaction vessel at −196°C. The solution was warmed to room temperature and transferred to a frit assembly. Concentration and cooling of the solution afforded light yellow crystals of **6** (0.76 g, 72%).

Anal Calcd.for $C_{45}H_{70}Sc_2$: C, 77.11; H, 10.07. Found: C, 76.90; H, 9.89.

$Cp^*_2ScCH_2\overline{CHCH_2CH_2CH_2CH_2}$ (16). $Cp^*_2ScCH_3$ (0.583 g, 1.77 mmol) was dissolved in *ca.* 15 ml petroleum ether in a heavy walled reaction vessel. Hydrogenation of the solution was carried

out as described previously. Methylenecyclopentane (1.8 mmol, 1.02 equivalents) was condensed into the glass bomb at –196°C from a calibrated gas volume. The solution was allowed to warm to room temperature; it was then stirred for an additional 30 minutes. In the glove box the solution was transferred to a round bottomed flask attached to a frit assembly. Concentration of the petroleum ether solution afforded bright yellow crystals of **6**, which were isolated by cold filtration (0.280 g, 39.7% yield).

Anal Calcd.for $C_{26}H_{41}Sc$: C, 78.35; H, 10.37. Found: C, 77.91; H, 9.77.

$Cp^*_2ScCH=C=CH_2$ (18). $Cp^*_2ScCH_3$ (0.600 g, 1.8 mmol) was loaded into a heavy walled glass vessel. Petroleum ether (*ca.* 15ml) was condensed onto the solid. Allene, purified by two freeze-pump-thaw cycles at –196°C, was condensed into the vessel at –196°C (4.2 mmol, 2.3 equivalents). The reaction was warmed to room temperature and then stirred at 80°C for one hour. The reaction solution was cooled and transferred to a frit assembly. Concentration of the solution and cooling produced a bright yellow waxy solid which was isolated by cold filtration (0.262 g, 41 % yield).

Anal Calcd.for $C_{26}H_{41}Sc$: C, 77.93; H, 9.38. Found: C, 77.72; H, 9.30.

IR (C_6D_6, CaF_2 solution cells): 3140(w), 2960(m), 2900(s), 2860(m), 2720(w), 1896(s).

$Cp^*_2ScPPh_2$ (23). Hydrogenation of a petroleum ether solution of $Cp^*_2ScCH_3$ (0.5 g, 1.5 mmol) was carried out as described previously. Under an argon counterflow, vinyl diphenylphosphine (0.33 g, 1.6 mmol) was syringed into the cooled reaction vessel (-78°C). Upon warming to room temperature, the reaction mixture turned from pale yellow to deep blue in about 15 minutes. The solution was transferred to a round bottomed flask attached to a frit assembly. Attempts to obtain

a solid from this reaction were unsuccessful; removal of all volatiles afforded a dark purple oil which was pure by ^{1}H NMR (>90 %).

Kinetics of β-Hydrogen Elimination of $Cp^*_2ScCH_2CH_2R$ Complexes.

Sealed NMR tubes were prepared and experiments were carried out as described above for the reaction of $Cp^*_2ScCH_3$ with 2-butyne. To determine the dependence of the concentration of 2-butyne on the observed rate constant, a series of experiments were carried out with $Cp^*_2ScCH_2CH_2C_6H_5$ and various concentrations of 2-butyne. Plotting the observed rate constants, k_{obs}, obtained from these experiments versus the concentration of added 2-butyne gave a line with slope 1.4×10^{-6} with deviations from the line less than 10%.

After determining that the reaction rate was independent of 2-butyne concentration over the range 0.6-3.0 M, all subsequent kinetic runs were carried out with a butyne concentration in this range. Rate constants were obtained for each complex at several different temperatures. Activation parameters were derived from an Arrhenius Plot as described previously.

Deuterium Kinetic Isotope Effect of β-Hydrogen Elimination.

$Cp^*_2ScCH_2CHDC_6H_5$ (*ca.* 25 mg) was loaded into a sealable NMR tube with 0.5 ml d_8-toluene. A calibrated gas volume was attached to the tube. The solution was degassed at -78°C; butyne (*ca.* 10 equivalents) was condensed in at -196°C. The tube was allowed to stand at room temperature for 5 hours. The ^{1}H NMR spectrum (400 MHz) was recorded; the terminal vinyl resonances for d_0-styrene and d_1-styrene were cut from the spectrum and weighed. The isotope effect (k_H/k_D) was calculated from the ratio of areas of the cut and weighed peaks.

REFERENCES

1. Collman, J. P.; Hegedus, L. S. *Principles and Applications of Organometallic Chemistry*; University Science Books: Mill Valley, California, 1980; p. 292.

2. Experimental studies include: (a) White, J. F.; Whitesides, G. M. *J. Am. Chem. Soc.* **1976**, *98*, 6521. (b) Reger, D. L.; Culbertson, E. C. *J. Am. Chem. Soc.* **1976**, *98*, 2789. (c) Evans, J.; Schwartz, J.; Urquhart, P. W. *J. Organomet. Chem.* **1974**, *81*, C37. (d) Ikariya, T.; Yamamoto, A. *J. Organomet. Chem.* **1976**, *120*, 257. (e) Bruno, J. W.; Kalina, D. G.; Mintz, E. A.; Marks, T. J. *J. Am. Chem. Soc.* **1982**, *104*, 1860. Theoretical studies include: (f) Thorn, D. L.; Hoffmann, R. *J. Am. Chem. Soc.* **1978**, *100*, 2079. (g) Lauher, J. W.; Hoffmann, R. *J. Am. Chem. Soc.* **1976**, *98*, 1729.

3. Whitesides, G. M.; Gaasch, J. F.; Stedronsky, E. R. *J. Am. Chem. Soc.* **1972**, *94*, 5258-5270.

4. Kazlauskas, R. J.; Wrighton, M. S. *J. Am. Chem. Soc.* **1982**, *104*, 6005-6015.

5. (a) Thompson, M. E.; Bercaw, J. E. *Pure Appl. Chem.* **1984**, *56*, 1. (b) Thompson, M. E. Ph. D. California Institute of Technology, **1985**. (c) Thompson, J. E.; Baxter, S. M.; Bulls, A. R.; Burger, B. J.; Nolan, M. C.; Santarsiero, B. D.; Schaefer, W. P.; Bercaw, J. E. *J. Am. Chem. Soc.* **1987**, *109*, 203-219. (d) Chapter II of this thesis.

6. Bruno, J. W.; Marks, T. J.; Morss, L. R. *J. Am. Chem. Soc.* **1983**, *105*, 6824-6832.

7. The IR spectrum of the polymer obtained from the reaction of $Cp^*_2ScCH_3$ and excess ethylene contained bands typical of polyethylene as well as bands characteristic of vinyl groups. Vinyl groups were thought to arise from vinyl groups chain terminating β-hydrogen elimination. See Reference 5b.

8. (a) Schrock, R. R. *Acc. Chem. Res.* **1979**, *12*, 98. (b) Moore, S. S.; Di Cosimo, R.; Sowinski, A. F.; Whitesides, G. M. *J. Am. Chem. Soc.* **1981**, *103*, 948.

9. Watson, P. L.; Roe, D. C. *J. Am. Chem. Soc.* **1982**, *104*, 6471-6473.

10. Flood, T. C.; Statler, J. A. *Organometallics* **1984**, *3*, 1795-1803.

11. Free ethylene is not observed in the β-hydrogen elimination of $Cp^*_2ScCH_2CH_3$. Presumably it is polymerized by $Cp^*_2ScCH_2CH_3$. Upon completion of the reaction, the concentration of $Cp^*_2ScC(CH_3)=CHCH_3$ is greater than 90% of the initial concentration of $Cp^*_2ScCH_2CH_3$, suggesting that the liberated ethylene does not significantly alter the kinetic results.

12. Kochi, J. K. *Organometallic Mechanisms and Catalysis*; Academic Press: New York, New York, 1978, p. 258.

13. Deuterium incorporation in the β position of $Cp^*_2ScCH_2CH_2CH_2CH_3$ was observed in the $^{13}C\{^1H\}$ NMR spectrum (C_6D_6, RT). A 1:1:1 triplet at δ 34.0 (J_{CD} = 18 Hz) (isotopically shifted from the signal for the perprotio complex at δ 34.5) was assigned to the β carbon with one bound deuterium, $Cp^*_2ScCH_2CHDCH_2CH_3$.

14. [Cp^*_2ScH] is generated by hydrogenation of $Cp^*_2ScCH_3$. Characterization and attempts at isolation of the complex are described in Reference 5c.

15. See Table I, Chapter II of this thesis.

16. Lowry, T. H.; Richardson, K. S. *Mechanism and Theory in Organic Chemistry* 2nd ed., Harper and Row, Publishers: New York, New York, 1981, 130-145.

17. Johnson, C. D. *The Hammett Equation*; Cambridge University Press: Cambridge, England, 1973; Chapter 1.

18. (a) McGrady, N. D.; McDade, C.; Bercaw, J. E. In *Organometallic Compounds: Synthesis, Structure, and Theory;* Shapiro, B. L., Ed.; Texas A & M University Press; College Station, TX, 1983, 46-85. (b) Doherty, N. M. Ph. D. Thesis, California Institute of Technology, 1984. (c) Doherty, N. M.; Bercaw, J. E. *J. Am. Chem. Soc.* 1985, *107*, 2670-2682. (d) Chapter I of this Thesis.

19 T. Ikariya; A. Yamamota *J. Organomet. Chem.* 1976, *120*, 257.

20. (a) Grate, J. H.; Schrauzer, G. N. *J. Am. Chem. Soc.* 1979, *101*, 4601. (b) Schrauzer, G. N.; Grate, J. H. *J. Am. Chem. Soc.* 1981, *103*, 541.

21. (a) Miyashita, A.; Yamamoto, T.; Yamamoto, A. *Bull. Chem. Soc. Jpn.* 1977, *50*, 1102. (b) *Ibid.*, 1109.

22. Egger, K. W. *J. Am. Chem. Soc.* 1969, *91*, 2867.

23. (a) Evans, J.; Schwartz, J.; Urquhart, P. W. *J. Organomet. Chem.* 1974, *81*, C37. (b) Ikariya, T.; Yamamoto, A. *J. Organomet. Chem.* 1976, *120*, 257.

24. In principle, the relative ground state energies for two alkyl complexes, $Cp^*_2ScCH_2CH_2R$ and $Cp^*_2ScCH_2CH_2R'$ could be determined by measuring the equilibrium constant for the reaction shown below (assuming the heats of formation of the free olefins are known). See Reference 2c, Chapter 1 for a system wherein this method was used successfully.

$$Cp^*_2ScCH_2CH_2R + CH_2{=}CHR' \overset{K}{\rightleftharpoons} Cp^*_2ScCH_2CH_2R' + CH_2{=}CHR$$

25. Collman, J. P.; Hegedus, L.; Norton, J. R.; Finke, R. G. *Principles and Applications of Organometallic Chemistry*; University Science Books: Mill Valley, California, 1980; p. 166-167.

26. (a) Lehmkuhl, H.; Naydowski, C.; Benn, R.; Rufinska, A.; Schroth, G. *J. Organomet. Chem.* 1983, *246*, C9-912. (b) Noyori, R.; Odagi, T.; Takaya, H. *J. Am. Chem. Soc.* 1970, *92*, 5780-5781. (c) Noyori, R.; Ishigami, T.; Hayashi, N.; Takaya, H. *J. Am. Chem. Soc.* 1973, *95*, 1674-1676. (d) Noyori, R.; Takaya, H. *J. Chem. Soc., Chem. Commun.* 1969, 525. (e) Green, M.; Hughes, R. P. *J. Chem. Soc., Dalton Trans.* 1976, 1880-1889. (f) Phillips, R. L.; Puddephatt, R. J. *J. Chem. Soc., Dalton Trans.* 1976, 1880-1889. (g) Attig, T. G. *Inorg. Chem.* 1978, *17*, 3097-3102. (h) Whitesides, T. H.; Slaven, R. W. *J.*

Organomet. Chem. **1974**, *67*, 99-108. (i) Pinhas, A. R.; Samuelson, A. G.; Risemberg, R.; Arnold, E. V.; Clardy, J.; Carpenter, B. K. *J. Am. Chem. Soc.* **1981**, *103*, 1668-1675.

27. Moss, J. R.; Bercaw, J. E., unpublished results.

28. Cox, J. D.; Pilcher, G. *Thermochemistry of Organic and Organometallic Compounds*, Academic Press, New York, N. Y., 1970.

29. Good, W. D.; Moore, R. T.; Osborn, A. G.; Douslin, D. R. *J. Chem. Thermodyn.* **1974**, *6*, 303.

30. Weast, R. C., Ed., *CRC Handbook of Chemistry and Physics* 62nd ed., CRC Press: Boca Raton, Florida, 1981.

31. Benson, S. W. *Thermochemical Kinetics*, 2nd ed., John Wiley and Sons, New York, New York, 1976.

32. Parkin G.; Bunel, E.; Burger, B. J.; Trimmer, M. S.; Van Asselt, A.; Bercaw, J. E., submitted for publication in *J. Mol. Cat.*

33. Bunel, E.; Bercaw, J. E., unpublished results.

34. Baldwin, J. E.; Kapecki, J. A. *J. Am. Chem. Soc.* **1970**, *92*, 4869-4873.

35. Koster, R.; Arora, S.; Binger, P. *Angew. Chem. Int. Ed. Engl.* **1969**, *8*, 205.

36. Greenwald, R.; Chaykovsky, M.; Corey, E. J. *J. Org. Chem.* **1962**, *28*, 1128.

APPENDIX I

NMR Programs for Ethylene Polymerization Kinetics

Parameters for Stacking Routine AUTO01

```
ACBLK              0
ACQTM          2.045 sec
ACUT               1
ADBIT     16
ADCHN              0
AG1             0.00 deg
AG2             0.00 deg
AG3             0.00 deg
ANGLE              0
B0         -38.05696
B1           0.00000
BA           0.00000
BF              1.00 Hz
CBF            -1.00 Hz
CGF             0.00 Hz
CLANG           90.0 deg
CLFRM              0
CLFRQ         2801.1 Hz
CLMOD              0
CLPNT            128
CLREF           0.00 ppm
CLRSO           21.9 Hz
CLSPC              0
CLSPR             95
CLTO             127
CMSWT              0
CMVAL   200.00 ppm
COMNT C13CONTINUOUS
CONST         0.010 ms
CP0       0.00 deg
CP1       0.00 deg
CT1       0.0 %
CT2      30.0 %
CT3      70.0 %
CT4     100.0 %
CWP            100 %
CWS              0 %
CXE       2779.2170 Hz
CXS        -10.9418 Hz
DATRW              1
DEADT           36.3 us
DELAY           25.0 us
DESFL SAVING
DFILE METH
DUMMY              0
```

```
EXMOD SGBCM
EXPCM SGBCM:Single.pulse.Bilevel.complete.decouplims:Set-IRRPW
EXREF        20.40 ppm
FILTR         8000 Hz
FILTY            0
FINES            0
FINPT    10.00 ppm
FREQU      16025.6 Hz
GF            0.00 Hz
HZPPM            2
IG               7
INDMY            0
INIPT    -1.00 ppm
INIWT           3.0 sec
INTVL          62.4 us
IRATN            0
IRFIN      14000.0 Hz
IRFN2          0.0 Hz
IRFRQ       399.65 MHz
IRNUC 1H
IRPHS          0.0 deg
IRRNS            0
IRRPW           30 us
IRSET        120.00 kHz
IRST2          0.00 kHz
LDANG          90.0 deg
LOOP1            1
LOOP2            1
LOOP3            1
LOOP4            1
MG            1.00
NGAIN            16
NL         0.00000
OBATN            0
OBFIN      14000.0 Hz
OBFN2          0.0 Hz
OBFRQ        100.40 MHz
OBNUC 13C
OBPHS          0.0 deg
OBSET        119.00 kHz
OBST2          0.00 kHz
P0     187.95 deg
P1     -21.00 deg
PD            0.700 sec
PENCH      3
PENDT      1
PENIG      3
PENSC      2
PENUD            1
```

```
PGGAP    5.0 cm
PI1          45.696 ms
PI2        1000.000 ms
PI3          10.000 ms
PLMOD              1
PLTFL GP:
POINT          65536
PREDL         0.2000 ms
PROBE              0
PRTFL TT2:
PS1            100.0 us
PS2            100.0 us
PS3            100.0 us
PS4            100.0 us
PS5            100.0 us
PW1              2.5 us
PW2              6.0 us
PW3             20.0 us
PW4              1.0 us
PW5              1.0 us
RANGE              0
RESOL           0.49 Hz
RGAIN     22
RWFRM              0
RWTO             127
SAMPO          65536
SCANS            147
SELAD              0
SH                 0
SHIGT   -0.3 cm
SHLNG              1
SHMFL 5MMCH
SI              2.00
SKPLT              2
SLEVL   -1.0 cm
SLVNT TOL
SM                 3
SMARK      2
SMODE              0
SOUFL SFILE
SPCL               1
SPEED             15 Hz
SPLNO      1
SPRW           16383
STEPS  10.0 PPM
T1       0.0 %
T2       0.0 %
T3      90.0 %
T4     100.0 %
TCOMP              0
TEMP.   25.0 C
TH           0.00000
TH1          0.00000
TH10         0.00000
TH2          1.00000
TH3          2.00000
```

```
TH5          4.00000
TH6          0.00000
TH7          0.00000
TH8          0.00000
TH9          0.00000
TIMES              1
TLINE              1
TODAT             48
TR             285.7 us
TRATN              0
TRFIN        10300.0 Hz
TRFN2            0.0 Hz
TRFRQ         399.65 MHz
TRNUC 1H
TRPHS            0.0 deg
TRRNS              0
TRRPW             50 us
TRSET         124.00 kHz
TRST2           0.00 kHz
VPFIL AUTO01
WNDMD              0
WP               100 %
WS                 0 %
XADJ     5.0 cm
XE      24038.5000 Hz
XRANG   29.0 cm
XS           0.0000 Hz
XSHIF    0.0 cm
YBIAS    3.0 cm
YRANG   20.0 cm
YSHIF    0.0 cm
YSPAN   15.0 cm
ZEFCL              1
ZEFRW              1
```

SUM.GLG PROGRAM

```
! ENTER DFILE TO BE ADDED
DFILE .ASK
! ENTER THE NUMBER OF SPECTRA TO BE ADDED
RJOBB .ASK
! ENTER THE STARTING DATA#
RJOBC .ASK
LNKFL SUM $ANLY
! TO SAVE DATA WHEN LINK IS FINISHED, MOVE THE SUM FROM
! JCPU FILE "SUM" TO YOUR ATTCHED FILE, CHANGE DFILE AND WTDAT.
```

SUM.LNK PROGRAM

```
01 CHANG/FI=SUM #CAL/CR MG 1 SH 0
02 CHANG/FI=INDIV #CAL/CR MG 1 SH 0
03 TODAT/RJOBB
04 DATA#/RJOBC
A1 .DO TODAT
10 RDDAT
11 CHANG/FI=SUM DTNAM INDIV
12 #ADD
13 CHANG/FI=INDIV
14 DATA# 1+
A2 .CONT
20 .END.
```

APPENDIX II

Synthesis, Characterization and Reactivity of $Cp^*_2Ta(\eta^2\text{-}CH_2O)H$

When $Cp^*_2Ta(CH_2{=}CH_2)Cl$(1), is treated with excess NaOMe in benzene, the expected metathesis product does not form (equation 1). Rather, one equivalent of ethylene (^{1}H NMR) is evolved and compound **2** is produced (equation 2). Whether the olefin is labilized before or after metathesis occurs is not known; no intermediates are observed.

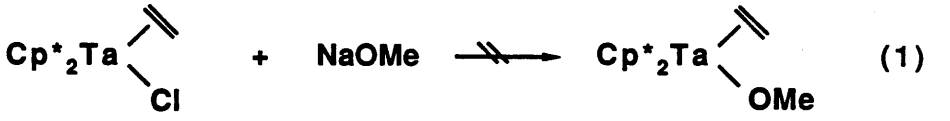

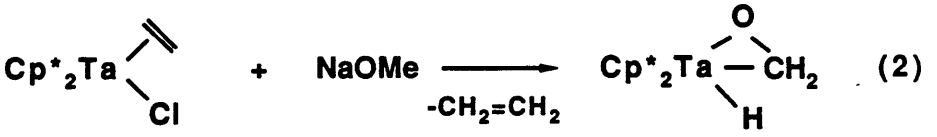

The reaction shown in equation 2 is relatively slow (days) and not practical for preparative scale reactions. In an attempt to produce a complex where the olefin is more labile, the synthesis of the propene analog of **1** was attempted. However, when $Cp^*_2TaCl_2$ is reduced with Na/Hg under excess propene, an orange paramagnetic solid is produced which has not, as yet, been identified (equation 3).

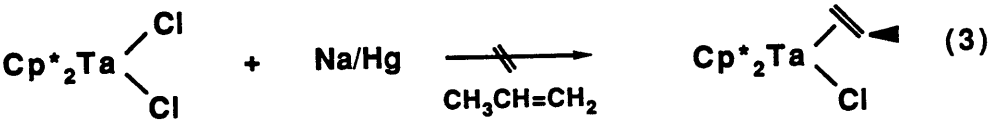

An alternate pathway to produce **2** is to generate the 16e$^-$ [Cp^*_2TaCl] fragment *in situ* in the presence of NaOMe. Indeed, **2** can be prepared as shown below (equation 4).

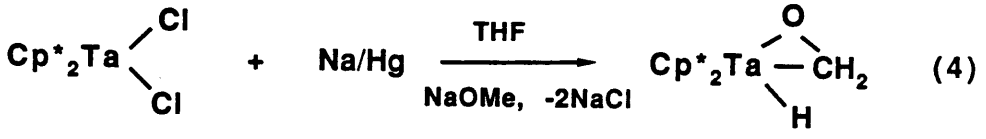

This reaction likely proceeds via initial reduction of the tantalum center, followed by metathesis of the $[Cp^*_2TaCl]$ fragment with NaOMe. β-Hydrogen elimination affords the observed product (see Scheme I).

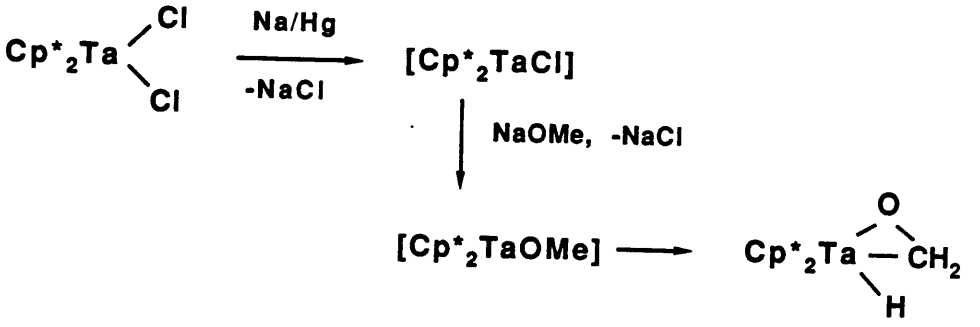

Scheme I. Formation of $Cp^*_2Ta(\eta^2\text{-}CH_2O)H$.

Compound **2** has also been prepared by an independent route shown below in equation 5.[1]

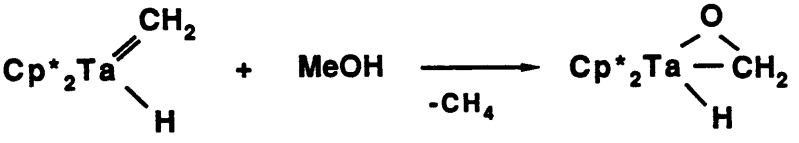

(5)

Variable temperature ^1H NMR of **2** shows that the H_B exchanges with H_A as shown below. Overlapping resonances precluded accurate measurement of the exchange rate; qualitative magnetization transfer is however observed at 60 °C, corresponding to an activation barrier of *ca.* 19(1) kcal/mol for the hydrogen migration.

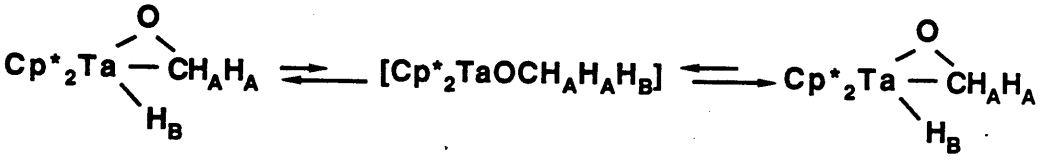

The product of hydrogen migration, [Cp^*_2TaOMe], can be trapped with CO and CNMe, affording $Cp^*_2Ta(L)OMe$ (equation 6 and 7, L = CO (3), CNMe (4), respectively).

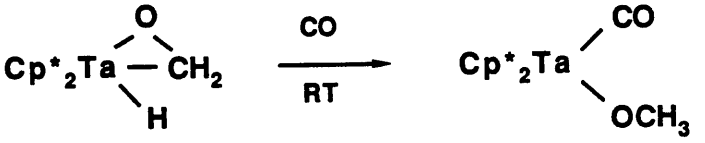

(6)

(7)

Compound **2** shows no reactivity toward H_2 and ethylene[2] even at elevated temperatures. Rather, thermolysis of **2** leads to C-O bond cleavage to form $Cp^*_2Ta(O)Me$, **4**. Formation of **4** follows first order kinetics with $k_{obs}(140°C) = 3.03(3) \times 10^{-6}\ sec^{-1}$ ($\Delta G^{\ddagger}(140°C)$ = 34.9(2) kcal/mol) (equation 8).

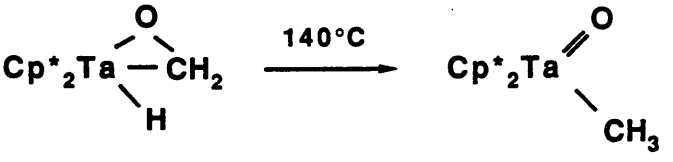

(8)

An inverse kinetic deuterium isotope effect of 0.46(3) (140°C) for the thermolysis of $Cp^*_2Ta(OCD_2)D$ supports a step-wise mechanism (rather than concerted C-O bond breaking and C-H formation) for this transformation, involving a pre-equilibrium of **2** and [$Cp^*_2Ta(OCY_3)$] (Y = H, D), since a shift in the pre-equilibrium toward [$Cp^*_2TaOCY_3$, Y = H, D] is expected for 2-d_3.

The rearrangement of **2** to **4** appears to be irreversible; there is no reaction when **4** is heated to 140°C in the presence of a trapping ligand such as CO (equation 9).

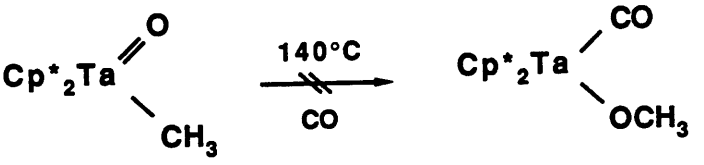

(9)

A white crystal of **2**, suitable for x-ray diffraction, was grown from a slowly cooled petroleum ether solution (–78°C). The molecular structure of $Cp^*_2Ta(\eta^2\text{-}OCH_2)H$ is shown in Figure I; a skeletal view of the tantalum coordination sphere with notable bond lengths and angles is shown in Figure II. The Cp^* ligands are coordinated in the conventional η^5 fashion; the Ta-C and C-C bond lengths (Table V) are similar to those reported for other Group V pentamethylcyclopentadienyl complexes.[3] The crystal structure confirms the isomeric assignment as O-*exo*.

The C-O bond length of 1.398(2) is within the range reported for other η^2-formaldehyde complexes.[4] Although the hydride was not located with any certainty in the structure, we believe, from the NMR data, that the hydride is bonded in a traditional terminal fashion and is not involved in any "agostic" interaction with the formaldehyde carbon.

Attempts to extend the synthetic methodology described above toward the preparation of other tantalum aldehyde hydride complexes have not successful. Reduction of $Cp^*_2TaCl_2$ in the presence of other alkali metal alkoxides (NaOEt, NaOPh, NaOiPr) resulted in the formation of a complex mixture of products. Addition of one equivalent of ethanol or benzyl alcohol to $Cp^*_2Ta(=CH_2)H$ led to impure products; excess ethanol or benzyl alcohol yielded products which were consistent with $Cp^*_2Ta(OR)_2H$, R = Et, CH_2Ph, respectively. These reactions were not pursued.

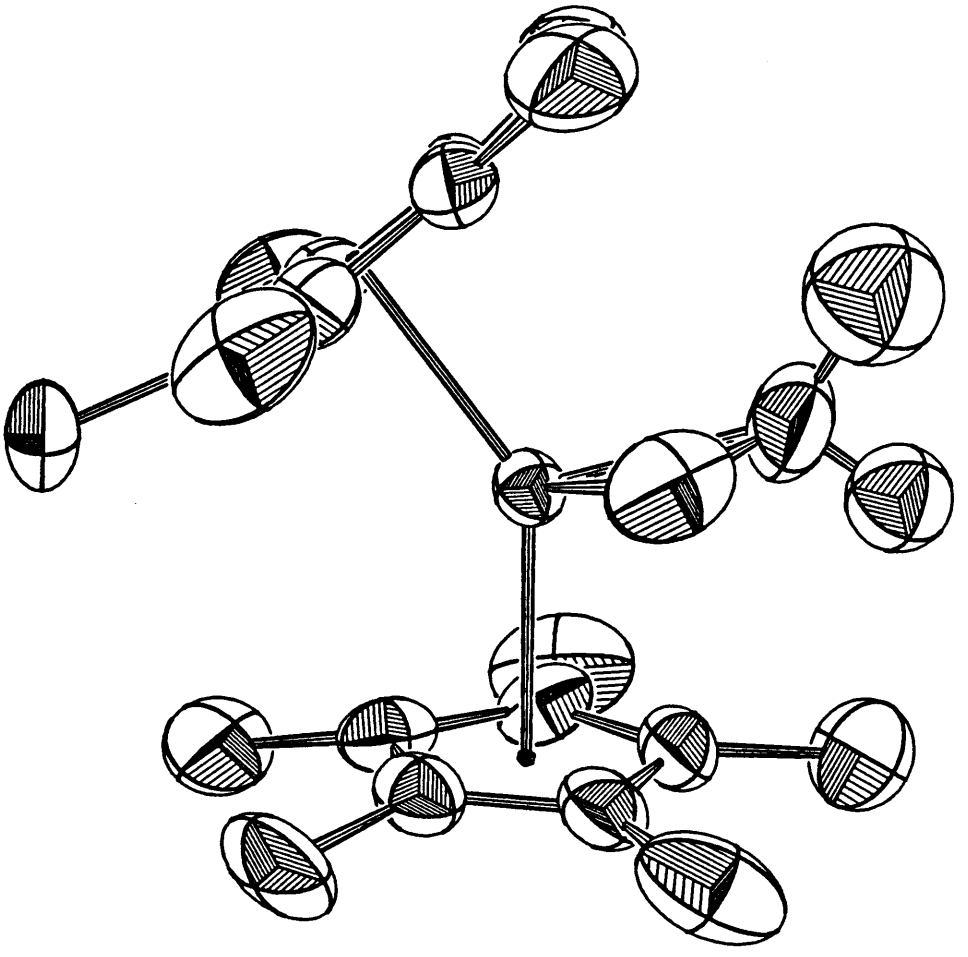

Figure I. Molecular Structure of $Cp^*_2Ta(\eta^2\text{-}CH_2O)H$.

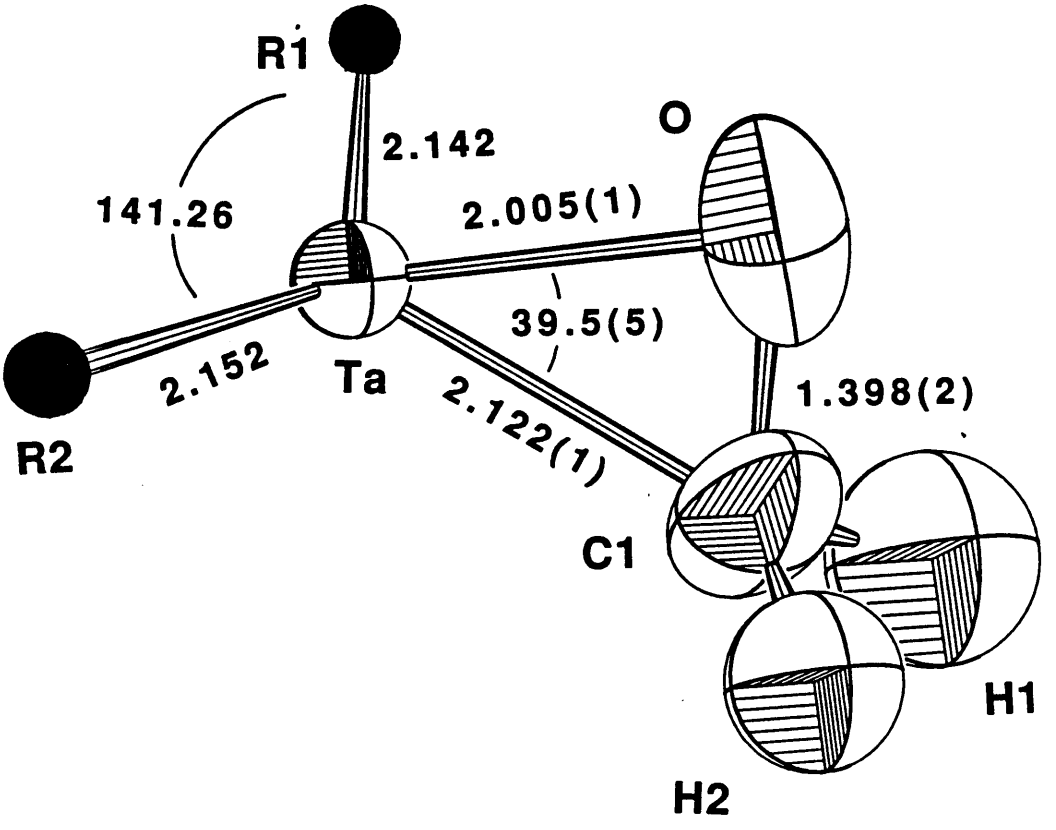

Figure II. Skeletal View of $Cp^*_2Ta(\eta^2\text{-}CH_2O)H$.[a]

[a]Bond distances are in Å. Bond angles are in degrees.

Table I. ^{1}H NMR Data for Cp^*_2Ta Complexes.[a]

Compound	Assignment	δ (ppm)	Coupling (Hz)
$Cp^*_2Ta(CH_2{=}CH_2)Cl$ (1)	$[C_5(CH_3)_5]$	1.55 s	
	CH_2CH_2	0.76 m	AA'BB'
$Cp^*_2Ta(\eta^2\text{-}CH_2O)H$ (2)	$[C_5(CH_3)_5]$	1.74 s	
	CH_2O	2.31 d	$^3J_{HH}$ = 2.4
	Ta-*H*	1.89 br s	
$Cp^*_2Ta(CO)OCH_3$ (3)	$[C_5(CH_3)_5]$	1.70 s	
	OCH_3	3.92 s	
$Cp^*_2Ta(CNCH_3)OCH_3$ (4)	$[C_5(CH_3)_5]$	1.77 s	
	OCH_3	4.07 s	
	$CNCH_3$	3.37 s	
$Cp^*_2Ta(O)CH_3$ (5)	$[C_5(CH_3)_5]$	1.77 s	
	CH_3	0.25 s	
$Cp^*_2Ta(CO)Cl$ (6)	$[C_5(CH_3)_5]$	1.68 s	
$Cp^*_2Ta(CH_2{=}CH_2)I$ (7)	$[C_5(CH_3)_5]$	1.64 s	
	CH_2CH_2	0.36 t	J_{HH} =11
	CH_2CH_2	1.24 t	J_{HH} = 11

[a] ^{1}H (90 and 400 MHz) NMR spectra were taken in benzene-d_6 at ambient temperature, unless otherwise stated. Chemical shifts are reported in parts per million (δ) from tetramethylsilane added as an internal reference or to residual protons in the solvent. Coupling constants are reported in hertz.

Table II. ^{13}C NMR Data for Cp^*_2Ta Complexes.[a]

Compound	Assignment	δ (ppm)	Coupling (Hz)
$Cp^*_2Ta(CH_2{=}CH_2)Cl$ (1)	$[C_5(CH_3)_5]$	108.85 s	
	$[C_5(CH_3)_5]$	11.14 q	J_{CH} = 127
	CH_2CH_2	44.15 t	J_{CH} = 152
	CH_2CH_2	39.90 t	J_{CH} = 152
$Cp^*_2Ta(\eta^2\text{-}CH_2O)H$ (2)	$[C_5(CH_3)_5]$	107.96 s	
	$[C_5(CH_3)_5]$	11.44 q	J_{CH} = 125
	CH_2O	60.14 td	J_{CH} = 159,7
$Cp^*_2Ta(CO)OCH_3$ (3)	$[C_5(CH_3)_5]$	104.35 s	
	$[C_5(CH_3)_5]$	10.60 q	J_{CH} = 126
	CO	274.28 s[b]	
	OCH_3	70.05 q	J_{CH} = 134
$Cp^*_2Ta(CNCH_3)OCH_3$ (4)	$[C_5(CH_3)_5]$	107.35 s	
	$[C_5(CH_3)_5]$	10.94 q	J_{CH} = 126
	$CNCH_3$	(not found)	
	OCH_3	74.30 q	J_{CH} = 134
$Cp^*_2Ta(O)CH_3$ (5)	$[C_5(CH_3)_5]$	115.26 s	
	$[C_5(CH_3)_5]$	11.65 q	J_{CH} = 126
	CH_3	20.34 q	J_{CH} = 122
$Cp^*_2Ta(CO)Cl$ (6)	$[C_5(CH_3)_5]$	103.72 s	
	$[C_5(CH_3)_5]$	11.03 q	J_{CH} = 127
	CO	262.76 s	
$Cp^*_2Ta(CH_2{=}CH_2)I$ (7)	$[C_5(CH_3)_5]$	107.44 s	
	$[C_5(CH_3)_5]$	12.00 q	J_{CH} = 126
	CH_2CH_2	40.31 t	J_{CH} = 150
	CH_2CH_2	33.30 t	J_{CH} = 147

[a] ^{13}C (100.25 MHz) NMR spectra were taken in benzene-d_6 at ambient temperature, unless otherwise stated. Chemical shifts are reported in parts per million (δ) from tetramethylsilane

referenced from solvent signal. Coupling constants ($J_{^{13}C-^{1}H}$) were obtained from a gated (^{1}H NOE enhanced) spectrum and are reported in hertz.

[b]Chemical shift obtained from spectrum of isotopically enriched sample.

Table III. Summary of Crystal Data for $Cp^*_2Ta(CH_2O)H$ (2).

formula: $C_{21}H_{33}TaO$	f.wt. 482.4
Space group $P2_1/n$	T = 21 °C
z = 4	V = 1961(1)Å^3
a = 9.918(7)	
b = 14.190(4)	
c = 14.028(3)	
β = 96.53(4) °	
λ MoKα = 0.71073 Å	
Scan Range 1.0° above Kα_1, 1.0° below Kα_2	
Reflections +h, ±k, ±l	
Collected 3979 reflections	
Averaged 3442 reflections	
(3193 $I > 0$, 2684 $I > 3\sigma_I$)	

Table IV. Final Parameters[a]

	x	y	z	U_{eq}[b]
Ta	10388(3)	23061(3)	27010(2)	328(1)
O	-3891(80)	24369(60)	15768(51)	736(22)
C	4729(152)	32090(89)	15166(87)	758(40)
C11	-5681(94)	20600(63)	38630(64)	459(23)
C12	7100(91)	22136(75)	44038(61)	488(24)
C13	11249(88)	31418(75)	42360(66)	472(23)
C14	1065(111)	35701(63)	36336(65)	524(26)
C15	-9691(94)	28980(71)	34070(63)	498(24)
C11M	-14475(124)	12208(85)	38804(90)	831(35)
C12M	13283(131)	15767(94)	51806(70)	845(40)
C13M	22924(133)	36103(100)	47509(90)	946(40)
C14M	748(148)	45942(80)	33791(96)	956(45)
C15M	-22823(103)	30928(109)	28507(76)	830(36)
C21	30963(89)	13466(63)	29162(59)	435(22)
C22	20457(93)	7056(60)	29282(63)	429(22)
C23	12506(102)	7483(61)	19963(66)	496(25)
C24	19461(105)	13560(66)	14427(63)	504(25)
C25	30453(90)	17326(62)	20014(64)	435(22)
C21M	42458(109)	14886(93)	36936(85)	808(36)
C22M	18566(133)	-617(76)	36344(83)	799(37)
C23M	559(117)	1632(84)	16852(94)	864(38)

C24M	15305(133)	14887(97)	3853(74)	874(39)
C25M	40801(116)	23201(81)	15979(99)	778(33)

[a] x, y, z x 10^5; U_{eq} x 10^4

[b] $U_{eq} = 1/3\ \Sigma_i\Sigma_j U_{ij}(a_i^* a_j^*) a_i \cdot a_j$; $\sigma U_{eq} = 6^{-1/2} <\sigma U_{ii}/U_{ii}> U_{eq}$

Table V. Distances and Angles

Atom	Atom	Dist. (Å)
Ta	C1	2.122(1)
	O	2.005(1)
	C11	2.431(9)
	C12	2.451(10)
	C13	2.451(10)
	C14	2.462(10)
	C15	2.470(9)
	C21	2.443(9)
	C22	2.487(9)
	C23	2.440(9)
	C24	2.471(10)
	C25	2.456(9)
	R1	2,142
	R2	2.152
C1	O	1.398(2)
	H1	1.004(125)
	H2	0.983(97)
O	H1	2.075(124)
O	H2	2.005(96)
C11	C12	1.418(13)
	C15	1.387(13)

Atom	Atom	Atom	Angle
C1	Ta	O	39.48(42)
C11	C12	C13	108.35(82)
C12	C13	C14	107.85(85)
C13	C14	C15	108.39(84)
C14	C15	C11	107.45(82)
C15	C11	C12	107.88(81)
C21	C22	C23	107.13(77)
C22	C23	C24	105.98(76)
C23	C24	C25	109.46(83)
C24	C25	C21	108.40(80)
R1	Ta	R2	141.26

	C11M	1.478(15)
C12	C13	1.408(13)
	C12M	1.493(15)
C13	C14	1.382(14)
	C13M	1.454(16)
C14	C15	1.439(14)
	C14M	1.495(16)
C15	C15M	1.466(15)
C21	C22	1.385(12)
	C25	1.391(12)
	C21M	1.499(15)
C22	C23	1.449(13)
	C22M	1.498(15)
C23	C24	1.394(13)
	C23M	1.472(15)
C24	C25	1.376(13)
	C24M	1.506(16)
C25	C25M	1.483(15)

R1 and R2 are the centroid coordinates of C11 through C15 and C21 through C25 Cp* rings respectively.

Table VI. Atom Coordinates (x 10^4) of Hydrogen Atoms.

	x	y	z
H1	822(100)	3345(91)	886(88)
H2	17(94)	3821(72)	1558(66)
H111	-1498	1076	4564
H112	-2335	1389	3615
H113	-1236	615	3600
H121	2290	1500	5140
H122	1222	1809	5800
H123	939	951	5121
H131	2440	3510	5370
H132	2298	4266	4659
H133	3148	3368	4524
H141	-420	4920	3720
H142	-349	4685	2704
H143	948	4858	3411
H151	-2120	3632	2454
H152	-2602	2548	2462
H153	-2958	3256	3239
H211	3957	1212	4259
H212	4428	2128	3818
H213	5064	1187	3526
H221	2525	66	4164

H222	2038	-656	3427
H223	964	-39	3854
H231	-710	540	1410
H232	-245	-191	2219
H233	242	-302	1213
H241	630	1520	230
H242	1928	1019	18
H243	1917	2101	176
H251	4410	2780	2020
H252	3720	2630	1016
H253	4845	1949	1457

Table VII. Gaussian Amplitudes (x 10^4).

	U_{11}	U_{22}	U_{33}	U_{12}	U_{13}	U_{23}
	377(2)	306(2)	301(2)	-22(2)	36(1)	-1(2)
O	701(5)	974(67)	499(42)	223(46)	-82(37)	-123(41)
C1	1219(115)	449(75)	612(75)	263(79)	136(76)	29(60)
C11	527(57)	418(60)	452(52)	-77(44)	146(45)	-63(42)
C12	418(52)	696(75)	351(47)	146(52)	53(40)	-31(48)
C13	373(51)	504(61)	532(57)	27(48)	15(44)	-146(50)
C14	815(74)	332(53)	471(55)	6(53)	275(54)	-18(43)
C15	466(54)	651(77)	392(49)	68(50)	113(42)	153(46)
C11M	867(89)	703(83)	1007(92)	-301(70)	475(77)	12(70)
C12M	1206(105)	1007(99)	347(56)	403(84)	195(64)	127(58)
C13M	917(4)	1054(108)	863(91)	-266(83)	88(75)	-524(82)
C14M	1413(122)	433(70)	1117(106)	89(77)	561(97)	-37(68)
C15M	521(64)	1360(109)	608(71)	261(69)	57(54)	-14(72)
C21	437(52)	450(55)	409(51)	40(45)	14(43)	-75(42)
C22	506(55)	316(49)	466(53)	79(44)	66(44)	39(40)
C23	715(67)	293(50)	498(55)	-83(47)	144(51)	-205(43)
C24	719(69)	408(56)	403(51)	86(51)	146(50)	-36(43)
C25	439(53)	381(56)	496(54)	-54(44)	95(44)	54(43)
C21M	518(66)	1035(101)	836(83)	122(67)	-71(67)	-234(74)
C22M	1218(103)	407(63)	819(81)	160(68)	325(76)	197(58)
C23M	746(81)	632(80)	1205(108)	-140(66)	70(77)	-435(77)
C24M	1180(105)	1015(101)	433(62)	343(85)	119(67)	-105(62)
C25M	660(73)	619(71)	1129(101)	-80(63)	425(71)	1(72)

EXPERIMENTAL SECTION

General Considerations.

All air sensitive manipulations were carried out using glove box or high vacuum line techniques. Solvents were dried over $LiAlH_4$ or sodium benzophenone ketyl and stored over titanocene. Benzene-d_6 and toluene-d_8 were dried over activated 4 Å molecular sieves and stored over titanocene.

Argon and nitrogen were purified over MnO on vermiculite and activated molecular sieves. Ethylene (Matheson) and propene (Matheson) were purified by three cycles of freeze-pump-thaw at -196^0 C and then vacuum transferred at 25^0 C. Carbon monoxide (Matheson) was used directly out of the lecture bottle. Methylisocyanide, prepared by literature methods,[5] was stored over activated 4 Å molecular sieves.

NMR spectra were recorded on Varian EM-390 (^1H, 90 MHz), JEOL FX90Q (^1H, 89.56 MHz; ^{13}C, 22.50 MHz) and JEOL GX400Q (^1H, 399.78 MHz; ^{13}C, 100.38 MHz) spectrometers. Infrared spectra were recorded on a Beckman 4240 spectrometer and reported in cm^{-1}. All elemental analyses were conducted by L. Henling of the Caltech Analytical Laboratory.

$Cp^*_2Ta(CH_2{=}CH_2)Cl$ (1). $Cp^*_2TaCl_2$ (8.5 g, 0.016 mol) and 1% Na/Hg (58g, 0.025 mol) were loaded into a large glass bomb with 70 ml THF. Ethylene (4 atm) was condensed into the glass bomb at −196° C. The reaction mixture was warmed to room temperature and sloshed for six days. The reaction was deemed complete when solid $Cp^*_2TaCl_2$ was no longer visible (starting material is relatively insoluble in THF). Excess ethylene was removed. The orange solution was decanted away from the amalgam and filtered through a fine porosity frit to remove any trace amounts of amalgam. The filtrate was transferred to a frit assembly. THF was removed to afford a

yellow-orange residue which upon recrystallization from a mixture of petroleum ether/toluene resulted in 6.5 g of a gold solid (1) (79%).

IR (Nujol): 2720, 1260, 1163, 1128, 1024, 940, 850, 798, 719, 591, 390.

Anal. Calcd. for $C_{22}H_{34}ClTa$: C, 51.32; H, 6.66. Found: C, 50.59; H, 6.39.

$Cp^*_2Ta(CH_2O)H$ (2). A large thick walled glass vessel was charged with $Cp^*_2TaCl_2$ (2.0 g, 3.8 mmol), 1% Na/Hg (13.2 g, 5.7 mmol) and excess $NaOCH_3$ (2.0 g, 35 mmol). THF (*ca.* 25 ml) was added to the vessel, which was then sloshed at room temperature for 24 hours. The pale yellow solution was decanted away from the amalgam and filtered through a pad of celite to remove any trace amounts of amalgam. The celite pad was subsequently washed extensively with toluene. The filtrate was then transferred to a frit assembly. Removal of all volatiles left a pale yellow residue which, upon recrystallization from cold petroleum ether, afforded 1.2 g of white crystalline **2** (68 %).

Anal. Calcd. for $C_{21}H_{33}OTa$: C, 52.28; H, 6.89. Found: C, 52.11; H, 6.80.

$Cp^*_2Ta(CD_2O)D$ (2-d_3). The same procedure was used as described above for **2** except that $Cp^*_2TaCl_2$ (2.0 g, 3.8 mmol) was reduced by 1% Na/Hg (13.2 g, 5.7 mmol) in the presence of $NaOCD_3$ (2.0 g, 35 mmol). Recrystallization from petroleum ether afforded 1.07 g of white crystalline **2-d_3** (58 %).

Anal. Calcd. for $C_{21}H_{30}D_3OTa$: C, 51.95; H, 6.85. Found: C, 51.98; H, 6.70.

$Cp^*_2Ta(CO)OCH_3$ (3). A solution of $Cp^*_2Ta(CH_2O)H$ (81 mg, .17 mmol) in petroleum ether (*ca.* 10 ml) was stirred in a thick walled glass vessel under an atmosphere of carbon monoxide. Within minutes, the solution changed from clear to emerald green. After 30 minutes, excess CO was removed and the solution was concentrated to *ca.* 4 ml. The solution was transferred to a schlenk flask and cooled slowly (24 hours) to -80^0 C to afford emerald green crystals of $Cp^*_2Ta(CO)OCH_3$, (67 mg, .13 mmol, 77%).

IR (C_6D_6, CaF_2):1835 ν(CO)

Anal Calcd. for $C_{22}H_{33}O_2Ta$: C,51.76; H,6.47. Found: C, 52.26; H,6.53.

Kinetic Measurement of the Rearrangement of $Cp^*_2Ta(CH_2O)H$ (2, 2-d_3) to $Cp^*_2Ta(O)CH_3$ (5, 5-d_3).

The rearrangement process (See equation 10) was monitored by ^1H NMR. Sealed NMR tubes of **2, 2-d_3** were prepared by dissolving approximately 25 mg of **2, 2-d_3** in 0.5 ml toluene-d_8. Ferrocene was added as an internal standard. NMR tubes were sealed under 4 atm N_2 to prevent the toluene from refluxing. Samples were heated in constant temperature oil baths ($\pm 1^0$ C). Spectra (EM390, 90 MHz) were recorded at appropriate time intervals by removing the sample from the oil bath and cooling it to room temperature. The decay of the Cp^* peak height of **2** was measured relative to the ferrocene added as an internal standard.

The first order rate constants (k_H, k_D) were obtained from the slope of the plots of ln([**2**]/[Cp_2Fe]) vs. time.

Structure Determination for $Cp^*_2Ta(CH_2O)H$ (2).

A white crystal of $Cp^*_2Ta(CH_2O)H$, grown by the slow cooling of a petroleum ether solution to -80^0 C, was mounted in a glass capillary under a nitrogen atmosphere. Unit cell parameters were obtained by least squares refinement of twenty-five centered reflections (22 < 2θ <25): a = 9.918(7), b = 14.190(4), c = 14.028(3); α,γ = 90°, β = 96.53(4)°. The systematic absences led to the unambiguous assignment of the space group $P2_1/n$ (h0l: h + l = odd; 0k0: k = odd). Data were collected on a CAD4 diffractometer with graphite monochromator and Mo radiation (λ = 0.7107 A). Intensity data were corrected for a 6% linear decay, as indicated by the three check reflections. No absorption corrections were applied. A summary of the data collection information is given in Table III.

The coordinates of the tantalum atom were derived from the Patterson map; subsequent Fourier and difference Fourier maps revealed the remaining atoms in the molecule. Several cycles of full-matrix least squares refinement with anisotropic Gaussian amplitudes for all non-hydrogen atoms and isotropic thermal parameters for the formaldehyde hydrogens resulted in R = $\{SW|Fo|-|Fc/k|W/|Fo|\}$ = 0.0517 (3193 reflns with I>0) and GOF = $\{SW(Fo_2 - Fc_2/k))_2/n_O - n_p)\}^{1/2}$ = 2.82, where n_O is the number of reflections and n_p is the number of parameters (3442 reflections). The parameters for the Cp^* hydrogens H111-H253 were not refined. The final difference Fourier showed symmetric pairs of peaks near the Ta atom, indicative of residual absorption. The final values for the atom coordinates and Gaussian amplitudes are given in Table IV and V; Table VI lists the final hydrogen atom coordinates and B's; bond lengths and angles are located in Table VII.

REFERENCES

1. Van Asselt, A.; Burger, B. J.; Gibson, V. C.; Bercaw, J. E., *J. Am. Chem. Soc.* **1986**, *108*, 5347.

2. This lack of reactivity contrasts with that observed by Green and co-workers for the related compound, $W(PMe_4)H_2(\eta^2\text{-}CH_2O)$. See: Green, M. L. H.; Parkin, G.; Moynihan, K. J.; Prout, K. *J. Chem. Soc., Chem. Commun.* **1984**, 1540.

3. See Chapter 1, Reference 13.

4. Buhro, W. E.; Georgiou, S.; Fernandez, J. M.; Patton, A. T.; Strouse, C. E.; Gladysz, J. A. *Organometallics* **1986**, *5*, 956-965 and references therein.

5. Ugi, I.; Fetzer, U.; Enolzer, U.; Knupfer, H.; Offermann, K. *Angew. Chem. Int. Ed. Engl.* **1965**, *4*, 472.